Summer 8-2016

Correlation of Polymer Performance and Hansen Solubility Parameters

Daniel Jobse Mania
University of Southern Mississippi

CORRELATION OF POLYMER PERFORMANCE

AND HANSEN SOLUBILITY PARAMETERS

by

Daniel Jobse Mania

A Thesis
Submitted to the Graduate School
and the School of Polymers and High Performance Materials
at The University of Southern Mississippi
in Partial Fulfillment of the Requirements
for the Degree of Master of Science

Approved:

_____
Dr. James W. Rawlins, Committee Chair
Associate Professor, Polymers and High Performance Materials

_____
Dr. Jeffrey S. Wiggins, Committee Member
Associate Professor, Polymers and High Performance Materials

_____
Dr. Sarah E. Morgan, Committee Member
Professor, Polymers and High Performance Materials

_____
Dr. Karen S. Coats
Dean of the Graduate School

August 2016

Published by the Graduate School

ABSTRACT

CORRELATION OF POLYMER PERFORMANCE

AND HANSEN SOLUBILITY PARAMETERS

by Daniel Jobse Mania

August 2016

Ready-to-use (RTU) grout is becoming more important to the finish and remodeling construction industry. Market research shows it to be a fast-growing product that not only is creating its own space but also is beginning to supplant existing technology.

The original intent of this research was to investigate formulation parameters and how they affect grout performance. It was learned that particle size and oil absorption (OA) value are important filler properties that affect performance as much as adequate packing density and optimal pigment volume concentration (PVC) without going beyond critical PVC (CPVC).

Polymer architecture was also determined to be extremely important, but difficult to predict. Properties such as tensile strength and elongation can be adequately modeled by polymer T_g, however, T_g alone is not a good predictor of hydrophobicity or stain repellency performance.

This conundrum led to research into Hansen solubility parameters (HSP) and whether these could be used as performance predictive tools. Since HSP of polymers cannot be directly measured, Group Contribution Theory (GCT) had to be employed to estimate polymer HSP.

It was determined that HSP is not as good of a performance predictor for physical strength properties, like tensile strength, as polymer T_g: but HSP does have utility for relative performance prediction of wet state properties such as hydrophobicity, stain repellency, or solvent resistance. It was further discovered that HSP may be useful with predicting relative performance of wet state properties such as wet tensile strength and elongation.

ACKNOWLEDGMENTS

I would like to thank and acknowledge the following list of the people. The list is in alphabetical order. I have included their work affiliation and some general information about how they aided me with this project:

- Amanda Andrews – Wacker Chemical Corporation – Silicone Division – Formulating discussions.
- Dr. Michael Austerberry – Wacker Chemical Corporation – Silicone Division – Proof reading and writing suggestions.
- Nick Babicky – Wacker Chemical Corporation – Set up testing protocols and provided training for universal testing device.
- Steven Bechtel – Wacker Chemical Corporation – Polymers Division – Formulating Discussions.
- Michele Bruck – Chemir Analytical – Help with TGA test method to determine $CaCO_3$ concentration in commercial samples.
- Dr. Bret Calhoun – The University of Southern Mississippi (USM) – Was instrumental in helping me get through USM, including helping me prepare for my Thesis defense and graduation.
- Rick Coffey – Wacker Chemical Corporation – Silicones Division – Sample preparation and testing.
- John Collins – Wacker Chemical Corporation – Silicones Division – Instrumentation training and help.
- Tim Corbin – Wacker Chemical Corporation – Obtained samples and material information.

- Ben Creech – Wacker Chemical Corporation – Silicones Division – Supplied marketing information.
- Mr. Dilhan Fernando – The University of Southern Mississippi – DSC analysis and some interpretation.
- James Greene – Wacker Chemical Corporation – Silicones Division – Served as my corporate sponsor for the project and aided in many data and formulation discussions.
- Aaron Hart – J Rettenmaier USA – Supplied cellulose fibers and technical information.
- Dr. Dietmar Haslbeck – Wacker Chemical Corporation – Performed and analyzed Pyrolysis/GC-MS work which aided in qualitative monomer composition of polymers.
- Jerry Havens – Wacker Chemical Corporation – Silicones Division – Formulation and data discussion, as well as some testing help.
- Ken Herman – Wacker Chemical Corporation – Polymers Division – Aided in sample material procurement.
- Evie Hollerbach – Wacker Chemical Corporation – Fine Chemicals Division – Supplied initial commercial marketing data which served as impetus for research.
- Dr. Robert Y. Lochhead – The University of Southern Mississippi – For supplying polymer solubility and group contribution theory information and literature.
- Patrick Kelly – Wacker Chemical Corporation – Polymers Division – MFFT data collection and analysis.

- Lucas Madison – Wacker Chemical Corporation – Silicones Division – Sample preparation and testing.
- Stephan Marrack – Wacker Chemical Corporation – Silicones Division – Performed flexural strength testing.
- Mr. Sharathkumar Mendon – The University of Southern Mississippi – Reviewing, editing and suggestions for written drafts.
- Laurent Morineaux – Wacker Chemical Corporation – Silicones Division – For being the Business Team Director that "forced" me into pursuing my Master's degree…without which my degree, this document and all the knowledge I have gained would not be possible.
- Dr. Sarah E. Morgan – The University of Southern Mississippi – In addition to serving on my Thesis Committee she aided with discussions about physical property testing and data analysis.
- Jose Murillo – Omya Corporation – Supplied calcium carbonate fillers and technical information.
- Steve Napier – Michigan Manufacturing Technology Center – Aided with DOE setup and data analysis.
- Diana Omecinsky – Wacker Chemical Corporation – NMR analysis and interpretation of polymer spectra.
- Dr. James W. Rawlins – The University of Southern Mississippi (USM) – For being my guide and mentor throughout my graduate school time at USM. For being my Thesis Advisor, including formulating, data analysis, writing, research and literature discussions.

- Chris Reeves – Wacker Chemical Corporation – FT-ATR, NMR analysis and interpretation of polymer spectra.
- Bernie Rickard – Wacker Chemical Corporation – TGA analysis of grouts and analytical testing of grouts and polymers.
- Kathy Rosar – Wacker Chemical Corporation – Polymers Division – Helped with MFFT bar work with polymers for formulating.
- Steve Ross – Wacker Chemical Corporation – Prepared samples for NMR analysis.
- Pat Rossiello – Dow-Wolf – Supplied many raw materials, some polymer samples and technical information.
- Roland Ruan – Wacker Chemical Corporation – Analytical analysis of grouts and polymers.
- Dr. Uwe Scheim – Wacker Chemical Corporation – Silicones Division – Reviewed data and some technical writing and offered formulation and data testing advice.
- Brenda M. Spears-Mania – Wife (CEO of Family Unit) – Editing writing.
- Ira Stone – Minifibers Inc. – Supplied samples and information for polymeric fibers.
- Donald Stephens – Wacker Chemical Corporation – Sample production and testing.
- George Tessier – Wacker Chemical Corporation – Polymers Division – Formulating discussions.

- Karen Thoms – Wacker Chemical Corporation – Analytical analysis of grouts and polymers.
- Carlos Toledo – Ashland Chemical Corporation – Reviewed early phases of work and offered formulating and performance suggestions.
- Erica Vera – Wacker Chemical Corporation – Silicones Division – Prepared and tested samples.
- Barry Weeks – Wacker Chemical Corporation – Analytical analysis of grouts and polymers.
- Dr. Jeffrey Wiggins – The University of Southern Mississippi – For serving on my Thesis Committee and helping me to become a better writer.
- Adam Zubke – Wacker Chemical Corporation – Obtained samples and material.

DEDICATION

I want to thank my best friend, wife, and the love of my life, Brenda, and my inspiration, my daughter, Ashley, for their support and understanding while I worked on this project and classes to earn my Master's degree.

I would also like to thank Wacker Chemical Corporation, especially everyone in the SC Business Unit, for their support, including financial, without which I would not have been able to earn this degree.

TABLE OF CONTENTS

LIST OF TABLES

LIST OF ILLUSTRATIONS

LIST OF ABBREVIATIONS

2-EHA	2-Ethyl Hexyl Acrylate
1K	One Component
2K	Two Component
AA	Acrylic Acid
AN	Acrylonitrile
ANSI	American National Standards Institute
ASTM	American Standard Test Methods
BA	Butyl Acrylate
BMA	Butyl Methacrylate
C^{13}-NMR	Carbon-13 Nuclear Magnetic Resonance
CED	Cohesive Energy Density
CoV	Coefficient of Variation
cP	*Centipoise*
CPVC	Critical Pigment Volume Concentration
CTIOA	Ceramic Tile Institute of America
DOE	Design of Experiment
DSC	Differential Scanning Calorimetry
EVA	Ethylene-Vinyl Acetate
FT-ATR	Fourier Transform Attenuated Total Reflectance
GCT	Group Contribution Theory
H^{1}-NMR	Proton Nuclear Magnetic Resonance

HSP	Hansen Solubility Parameter
MAA	Methacrylic Acid
MFFT	Minimum Film Forming Temperature
mm	Millimeter
MMA	Methyl Methacrylate
MMSA	Methods Materials Standards Association
MPa	Mega Pascals
OA	Oil Absorption Value
OSR	Oil-based Stain Repellency
PCC	Pearson Correlation Coefficient
PPh	Propylene Glycol Phenyl Ether
psi	Pounds per Square Inch
PUD	Poly Urethane Dispersion
PVA	Poly Vinyl Acetate
PVC	Pigment Volume Concentration
R_o	Radius of Interaction
R_a	Hansen Distance between two materials
RED	Relative Energy Difference
RTU	Ready To Use
T_g	Glass Transition Temperature
TGA	Thermal Gravimetric Analysis
TSR	Total Stain Repellency
μm	Micro Meter

UTS	Ultimate Tensile Strength
VA	Vinyl Acrylic
WA	Work of Adhesion
WSR	Water-based Stain Repellency

CHAPTER I - INTRODUCTION

The use of tiling materials as surface modifiers and decoration are becoming increasingly more important and prevalent. These materials are typically adhered to either a supporting or structural substrate to protect it from environmental attack as well as for aesthetic reasons. This type of construction has been around for thousands of years.

Grouts are used to fill in gaps in building and construction materials. Tile grouts are used to fill in the gaps between tiles and stones used as surfacing materials[1]. The tile grouting material is used to create a more uniform and aesthetically pleasing surface while also protecting the substrate from environmental exposure. Tile grouts have been used for as long as tiling has been in use[2].

Grout usage has increased at a rate equaling the growth of the tile industry. For each ten units of tile adhesive used, approximately one unit of grout is needed. This represents a very large commercial opportunity for business. Part of the impetus for this current research was to aid the expansion of business opportunities into the grout market through technical expertise.

Tile grouts come in a variety of types that are divided by price-point, end-use application and performance expectations. Commercially, cement grouts are the most prevalent. They have good physical properties, are easy to apply and cleanup, and are very economical. However, they suffer from poor stain repellency, lack of hydrophobicity, poor color control, efflorescence, and have to be mixed on-site, which can lead to performance variations.

Cement grouts can be modified with liquid additives to improve both stain repellency and hydrophobicity[3], but must be mixed on-site, which can lead to performance variation. Additionally, these materials can often exacerbate efflorescence problems, while still not delivering a high degree of stain repellency.

At the top end of the spectrum of grouting materials are the 2K polymeric systems, mostly epoxy grouts. Epoxy grouts have good physical properties, excellent stain repellency and hydrophobicity, do not show efflorescence, and do not have color issues. However, they are expensive, often difficult to clean-up, can contain harmful chemical moieties, and also need to be mixed on-site.

The last main type of grout is 1K, water-based, pre-mixed polymeric grouts that are often referred to as ready-to-use (RTU) grouts. RTU grouts are typically based on acrylic emulsion polymers but can be made using other technologies such as polyurethane dispersions (PUD's) and water-based epoxy resins.

RTU grouts do not need to be mixed on-site, thus only the material that is needed for a job is used, and the remainder is saved for future use. They have good stain repellency, are easy to apply and cleanup, have good color qualities and do not show efflorescence. However, they lack good physical strength and are typically not very hydrophobic. The cost point is somewhere between cements (low end) and 2K epoxy (high end), which varying mainly by the polymer used.

Wacker Chemical Corporation initiated a marketing project to determine the growth potential of RTU grouts as a means to determine whether research effort needs to be invested into this emerging market[4]. The marketing project established that the

growth rate of this technology and current status of product performance warranted technical research and development activity.

Figure 1 shows the performance versus cost of the main grout types available commercially. The bubble size indicates the relative size of each grout type in total sales dollars[5]. The performance data was based on evaluation of the basic grout technologies, while the costs were normalized to a per gallon cost at local big-box construction stores. Current market trends, as observed from trade shows, show increases use of RTU grout with performance characteristics that approach those of 2K epoxy grouts. Changes in the grout market are driving RTU grout technology to its technological limits[6].

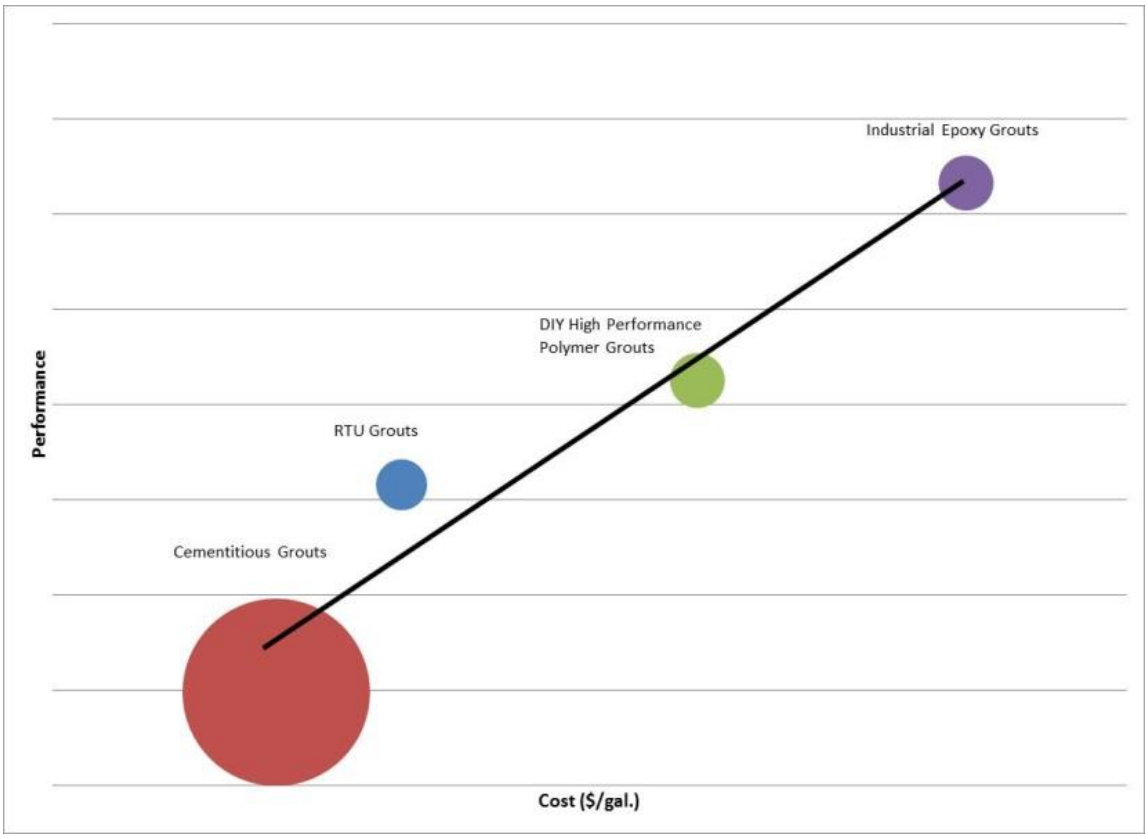

Figure 1. Performance versus cost of grout technologies with 2007 relative market size shown with the bubble diameter[5].

The original goal of this project was to develop a firm understanding of the formulation principles of RTU water-based grouts to push this technology to its performance limit. Specifically, the objectives were to combine the ease of cleanup, no need for on-site mixing, and superior stain repellency while mitigating the deficiencies of lack of physical strength, durability, and hydrophobicity so that these grouts can be used in application areas previously only accessible to either cement or 2K polymeric systems.

Multiple driving factors aided this research in its initial stages. The aforementioned internal marketing project motivated the manufacturers to drive RTU grout technology performance towards 2K polymer performance. A subsequent grout market performance survey established the strengths and weakness of each grout type and the lack of strength, durability, and hydrophobicity of RTU grouts[7]. At this point, a project was set up to determine how the formulation parameters such as pigment volume concentration (PVC), filler type, solids, polymer type, and filler content, affected RTU grout performance.

The ultimate goal of this project was to determine best practice formulation techniques to drive RTU grout performance as close to 2K polymer grout performance as possible. Secondary goals were to aid with the development of polymers and/or additives that could help improve RTU grout performance while optimizing formulation parameters. This second goal is of commercial importance to Wacker and will not be detailed within the context of this research.

As the main focus of this research was directed toward learning how to formulate a RTU grout, the effects of each formulation parameters upon the RTU grout

performance had to be established. Since this project was so complicated and potentially over-reaching it was completed in several phases of work:

I. Pre-formulation Research

II. Broad Implication Initial Formulation Strategy

III. Narrowed Strategy

IV. Effect of Filler

V. Starting Point Formulation

Phase I utilized a rudimentary starting point formulation derived from the analytical values of the commercial products and prior art knowledge. This phase laid out the framework for the raw materials that would be used. Some test samples were made to determine the limits of use of some raw materials. For example, the formulation contained a cellulose ether thickener to increase viscosity and exert rheological control. It was noted that very high viscosity grade (> 20,000 cP) cellulose ether resulted in too stiff of a final RTU grout. The dispersant level for each filler was determined via a dispersant demand test method.

Phase II was presented at the 40th International Waterborne, High-Solids and Powder Coating Symposium in 2013[7]. However the glass transition temperature (T_g) of the hard polymer was erroneously reported as 50°C in the original publication. To determine broad T_g implications, one hard and one soft emulsion polymer were chosen as extreme ends of the T_g range. The primary focus of Phase II was to determine the main effects of the raw materials. As such, this phase utilized a Taguchi DOE to elucidate main effects from:

- Filler oil absorption (OA) value
- Filler particle size
- Filler hardness
- Pigment volume concentration (PVC)
- Presence or absence of fiber
- Fiber length:
    - Long (6 mm)
    - Short (3 mm)
- Fiber concentration
- Polymer T_g:
    - Hard (63°C)
    - Soft (10°C)

Taguchi DOE's focuses only upon the main effects and can be augmented by prior art knowledge to remove experiments that are known to offer no useful information[7]. Factorial DOE's take into account as many conceivable interactions as possible. The experimentalist may decide to limit the number of interactions studied with the DOE, but this will also limit the amount of main effects data that is generated[8]. Taguchi DOE was used because the experiments were limited to 36, with replicates, instead of using a Factorial DOE that would have required 720 experiments, without replicates, to achieve similar results. Most importantly, using Taguchi DOE resulted in significant time savings since it took nearly one hour to produce each sample.

Using the data from Phase II, it was determined that formulating with as high PVC as possible, but below the critical PVC (CPVC) was very important for low

shrinkage and strength properties. Fiber incorporation was found to improve the tensile strength. Fiber concentration needed to be < 0.5% by weight of the total formulation and using a shorter fiber resulted in grout that did not appear hairy upon cure. Filler content was a little ambiguous, but the general trend pointed towards the use of larger particle size fillers with low OA values. Filler hardness did not appear to contribute to variation in properties. Finally, performance properties improved (with the exception of elongation), upon using a harder polymer with high T_g. Table 1 gives a rough formulating guide generated after analyzing the data from Phase II.

Phase II still did not answer conclusively what type of fiber was optimal, and neither did it address the filler content very well. It appeared that high T_g polymers were better for water-uptake, stain repellency, surface hardness, ultimate tensile strength (UTS), and Young's modulus. However, since two points do not make a trend the polymer T_g question needed to be explored further.

Table 1

Rough Formulation Guidelines for RTU Grout

Formulation Parameter	**Advantage**
High T_g polymers	Water-uptake prevention, Stain repellency (overall, but specifically water-based staining agents), Surface hardness, UTS and Young's modulus
Low T_g polymers	Ease-of-cleanup, Stain repellency (versus oil-based staining agents), Elongation
Higher PVC	Lower shrinkage, Less cracking, Surface hardness, Ease-of-cleanup
Lower PVC	Lap-shear adhesion, Elongation

Table 1 (continued).

Small particle size fillers	Water-uptake prevention, Application properties, Surface hardness, UTS
Large particle size fillers	Stain repellency, Shrinkage, Cracking, Lap-shear adhesion, Young's modulus
High OA value fillers	Water-uptake prevention, Surface hardness, Application properties, Elongation, UTS
Low OA value fillers	Lower shrinkage, Less cracking, Lap-shear adhesion
Presence of fibers	Less shrinkage and cracking (although they can be deleterious to water uptake prevention and application properties if not optimally used)

Phase III of the project utilized information learned from Phase II, and was presented at the 41st International Waterborne, High-Solids and Powdering Coatings Symposium in 2014[9]. The goal of this phase was to gain a better understanding of the main effects of the raw materials used and evaluate a slightly broader range of polymer T_g's with the objective of deriving a good starting point formulation for further testing of specific raw materials.

A Taguchi DOE was again employed to realize the main effects and to minimize the time of the total experiment. The following parameters were investigated:

- Polymer – Four different T_g's:
  - 10 °C, 17 °C, 39 °C and 63 °C
  - These were reported as 12 °C, 17 °C, 33 °C and 61 °C in the original work
- Filler content – (eight different fillers):

    - Particle sizes ranging from 6.0 to 21.0 μm
    - OA values ranging from 6.5 to 29.0 gm/100 g of linseed oil
    - Two Moh's hardness values:
        - 4 (silicates)
        - 7 (calcium carbonates)
- Fiber content – four choices:
    - None
    - Polyethylene
    - Nylon
    - Cellulose

Phase III validated the results of the earlier work regarding high PVC, and the role of filler properties, in that the fillers with larger particle sizes and lower OA's performed better with respect to water uptake, hardness and strength properties. This promoted the investigation of the impact of a Fuller Curve[10], which is used in the concrete industry to give better packing density with fillers and aggregate.

In some cases, fibers imparted a slight advantage, particularly with nylon fibers. For this reason nylon fibers (3 mm in length) were added at 0.5% by weight for all subsequent work with RTU grouts.

Polymer T_g showed fairly strong correlations with some performance properties. Tensile strength, elongation, dry hardness and oil stain repellency all exhibited strong correlations with polymer T_g. However, some properties exhibited odd jumps in performance, most of which occurred with polymer D which contained both long and

short chain monomers. This behavior, again, led us to question the nature of the correlation between polymer T_g and performance.

Phase III still left unanswered questions about the specific effect of polymer T_g and the data was not sufficient to generate a good starting point formulation.

Phase IV results have not been published as yet. This phase focused upon using the information derived from the previous three phases, in combination with information from the commercial survey and prior art knowledge to produce a workable starting point formulation. This phase of the project focused upon using the following inputs:

- 3mm nylon fiber at 0.5% concentration by weight
- Filler combination to maximize packing according to a Fuller Curve[10]
    - 87% by weight, average particle size 21 μm – calcium carbonate
    - 12% by weight 14 μm particle size – silicate
    - 1% by weight 6 μm particle size – calcium carbonate
- Sample D as the polymer of choice due to balance of properties
- PVC
    - 75% of theoretical CPVC
    - 85% of theoretical CPVC

The filler system was chosen since the filler hardness did not appear to have as much impact as the filler amount, which is better controlled by OA value. Additionally, the filler packing was determined to be more important than the filler type. As such, the ratio reflects the best mathematical volumetric space filling with the fillers investigated.

Polymer D was chosen because it had a very good balance of most properties. More importantly, due to the near balance of long and short chain pendant groups in the polymer backbone it has some of the best hydrophobic and stain repellent properties.

It has been noted several times that higher PVC resulted in better overall performance. Using the finalized formulation parameters PVC was evaluated one last time to determine its effect on performance properties. This information was then used to set the PVC level for all subsequent work with RTU grouts.

Phase V was the last phase of research for this thesis. All the previous phases utilized some form of a DOE to determine the main effects and interactions to derive information on how to formulate RTU grouts and to develop a good starting point formulation.

This phase used that information and evaluated ten different emulsion polymers in the starting formulation. All the emulsions are commercially available but will not be specifically named. The emulsions T_g's ranged from -6 °C to 63 °C, and comprised of three all acrylic, two styrenated-acrylic, one vinyl-acrylic, two ethylene-vinyl acetate (EVA), one EVA modified with a hydrophobic long-chain acetate monomer and a poly(vinyl acetate) latex. Overall, these polymers were comprised of eleven monomers offering a broad range of pendant backbone chemistry.

The original goal of Phase V was to determine the effects of polymer T_g upon RTU grout performance. The section titled "Performance versus Polymer T_g (K)" of this document details the results of that work. Only dry elongation and dry flexural strength were found to be affected (in a statistically relevant manner) by T_g. With increasing T_g, dry elongation decreased, while dry flexural strength increased. Wet and dry UTS, wet

and dry surface hardness (by Shore D Durometer), and Young's modulus showed some degree of correlation with polymer T_g. On the other hand, wet elongation, dry and wet adhesion, shrinkage, water-absorption, and stain repellency (total, oil-based and water-based) showed little to no correlation with polymer T_g.

Two main pieces of information from this phase led to a discussion about Hansen solubility parameters (HSP) and its potential correlation with polymer T_g. First was, the simple fact that many properties did not seem to correlate very well with T_g. Secondly, Polymer D, with a balance of long and short chain pendant groups appeared to almost always be an outlier in performance. For example, in water absorption, stain repellency, tensile strength, hardness, adhesion, and flexural strength, it performed better than would be expected based solely upon its T_g. The performance of Polymer D (with a middling T_g) was nearly always more in line with either end of the T_g spectrum, depending upon which end of that spectrum showed better performance.

Since T_g did not end up being a very good predictor for performance the existing data was evaluated to determine if a correlation existed between grout performance and polymer solubility parameters. HSP are widely accepted in the coatings industry and were used in this study.

It is not possible to analytically determine HSP of polymers since they do not have heats of vaporization. As such, group contribution theory was employed to determine the total HSP from the component HSP values, specifically δ_H for hydrogen bonding, δ_P for polarity and δ_D for dispersion or Van der Waals forces. Van Krevelyns' method and chemical group values were used to determine the calculated HSP for each monomer and then the polymer.

At this stage comes the actual prospectus of research. All of the available data an information will be utilized to determine if a link exist between polymer HSP and performance of RTU grout? If so, does a correlation exist between total HSP or one or all of its component values?

When doing any formulating work it is often helpful if some material choices can be made utilizing performance predictions based upon some raw material characteristic such as polymer T_g or HSP. The utility of this work will be determined by the ability to be able to utilize HSP to determine any performance parameter such as stain repellency. If the hypothesis of using HSP to predict stain repellency can be rendered useful, this could become a very powerful formulating tool for a plethora of applications that involve ease-of-clean, stain repellency and dirt pick-up resistance properties.

CHAPTER II – METHODS AND MATERIALS

Methods

Evaluation of the materials used in this research consisted of two distinct types of methodologies. One type of evaluation included analytical wet chemical and instrumental analysis of commercial grouting materials and the emulsion polymers used for producing the test samples. The second type of analysis determined performance properties of the grouting materials. The test methods and materials section is divided between methods for materials analysis (e.g., solids, differential scanning calorimetry (DSC), and nuclear magnetic imaging (NMR) spectroscopy), and methods for evaluating the grout performance properties (e.g., tensile testing, water absorption and adhesion).

Analysis of Materials Methodology.

These analysis methods were used to determine physical properties and composition of polymers for performance comparison as well as to aid in setting up the specific formulation constants for both commercial and test grout formulations. The commercial grouts were analyzed to give a frame-work for setting up the initial test formulations.

Analytical Test Methods

Table 2

Analytical Test Methods.

Property	**Test Method**
Solids content by weight (%)	ASTM D 2369[11]
Solids content by volume (%)	ASTM D 2697[12]
Water content by weight (%)	ASTM D 4017[13]
Solvent content by weight (%)	By subtraction

Table 2 (continued).

Pigment content by weight (%)	ASTM D 3723[14]
Pigment content by weight (%)	Thermal gravimetric analysis (TGA)
Calcium carbonate content by weight (%)	TGA
Solid polymer content by weight (%)	By subtraction
Density (lbs./gal.)	ASTM D 1475[15]
Polymer (T_g)	DSC
Minimum Film Forming Temperature (MFFT)	MFFT Bar
Monomer composition	Pyrolysis-GC-MS FT-NMR (^1H, ^{13}C) FT-IR Fox equation (using T_g by DSC)

Table 3

Analytical Equipment.

Test	**Equipment Description**	**Conditions**
TGA	Perkin-Elmer TGA 7	N_2 purge @ 20 mL/min, 20 °C to 900 °C @ 20 °C/min.
DSC	Mettler-Toledo DSC 1 Star	N_2 purge @ 150 mL/min., Equilibrate @ -10 °C for 20 min., Heat @ 5 °C/min. to 100 °C
Fourier Transform (FT)-NMR (FT-NMR ^1H & ^{13}C) spectroscopy	Bruker Avance II 400 MHz 5 mm BBFO Probe B-ACS 60 sample changer	30° pulses with 5 s relaxation delays with 128 scans

Table 3 (continued).

FT-Attenuated Total Reflectance (ATR) Spectroscopy	Thermo-Nicolet 6700 Single Bounce Diamond ATR DTGS – TEC Detector	Room temperature scanned 128 scans @ 4 cm^{-1} resolution
Pyrolysis-Gas Chromatography Mass Spectrometry (Pyrolysis-GC-MS)	Pyrolysis probe – Modell Pyrola 2000, platinum ribbon	2 sec. @ 590 °C then 2 sec. @ 1000 °C
	GC – HP 5890 Series II	1:30 split injection ratio, He transport gas @ 1.0 mL/min., Oven parameters: 65 °C – 1 min., Ramp @ 10 °C/min. from 65 °C to 150 °C, Ramp @ 20 °C/min from 150 °C to 250 °C,
	MS – HP 5972 Quadupole Mass Spectrometer	Column – HP 5 Ultra Inert (60 m x 0.25 mm ID)
MFFT-Bar	Rhopoint MFFT Bar 90	3 mil films by 0.75 inch width, temperature range from – 10 °C to 90 °C
Muffle Furnace	ThermoLyne 1300 Furnace	Initial Temperature: 110 °C for 1 hour Ramp from 110 °C to 500 °C at 6.5 °C/min. Hold at 500 °C for 4 hours
Karl Fisher Titrator	Metrohm 836 Titrando 805 Dosimat 801 Stirrer Platinum Electrode	Solvent: Methanol Titrant: Comp 5 by Aqua Star

The determination of the solids range by weight and volume of the commercial grouts aided in setting the starting point solids content for the formulated grouts. The polymer content of the commercial grouts helped establish the potential pigment volume concentration (PVC) of formulated samples. The water content of the commercial grouts aided in establishing the relative amount of polymer, assuming that emulsion polymers used had a solids content of 50% by weight. The solvent content established the presence and quantity of other additives such as coalescing solvents, e.g., higher amount of coalescing solvent is associated with higher polymer T_g.

The pigment/filler content was further analyzed by TGA to determine if there were any carbonaceous materials (calcium carbonate) in the commercial grouts. This is important since most calcium carbonate fillers have lower OA values, thus allowing for more filler to be incorporated and facilitate higher PVC.

Commercial RTU Grout Evaluation

Ten commercial ready-to-use (RTU) grouts were purchased and analyzed according to the methods listed in the Methods and Materials section of this thesis in order to: establish base-line performance standards as goals for formulated grouts and to determine a range of basic formulating guidelines to aid with starting point formulation development. Additionally, the average performance of RTU grouts was compared to other grout technologies in an attempt to understand where this technology fits within the grout market.

Table 4 shows the average values for the physical parameters or formulation constants of the commercial samples.

Table 4

Commercial Grout Formulation Parameter Average Data

Property	Value
Solids Content Weight (%)	84.1
Solids Content Volume (%)	86.7
Water Content Weight (%)	15.2
Solvent Content Weight (%)	0.7
Filler/Pigment Content Weight (%) – by ash content	71.9
Calcium Carbonate Content of Total Filler by Weight (%) - by TGA	78.3*
Solid Polymer Content Weight (%)	12.1
Density (lbs./gal.)	14.1

* Note – This was the average content of calcium carbonate within the total filler content for samples that contained calcium carbonate.

Figures 2 – 11 are the Thermo-Gravimetric Analysis (TGA) analyses of the 10 commercial grout samples. These were done to first get an estimate of the filler and polymer solids within each formulation, as well as to determine the amount of calcium carbonate filler was present (if any). Figure 12 is a TGA scan of calcium carbonate alone as a reference.

Figure 12 shows that the carbonate starts to degrade a little below 700°C. Based upon this fact it appears that seven of the commercial grouts have calcium carbonate as part of the filler material. The grouts that contain calcium carbonate are: A, C, D, E, F, G and J. Using the fact that 44.7% of the mass of the reference calcium carbonate was burned off the amounts of calcium carbonate in the grouts can be estimated. Table 5 shows the estimated amount of calcium carbonate present in each sample. This data

indicates that the average amount of filler in any given water-based RTU grout is 77.5% by weight, with approximately 43.5% of that being calcium carbonate for a total calcium carbonate filler load of 33.7 % of the formulation by weight.

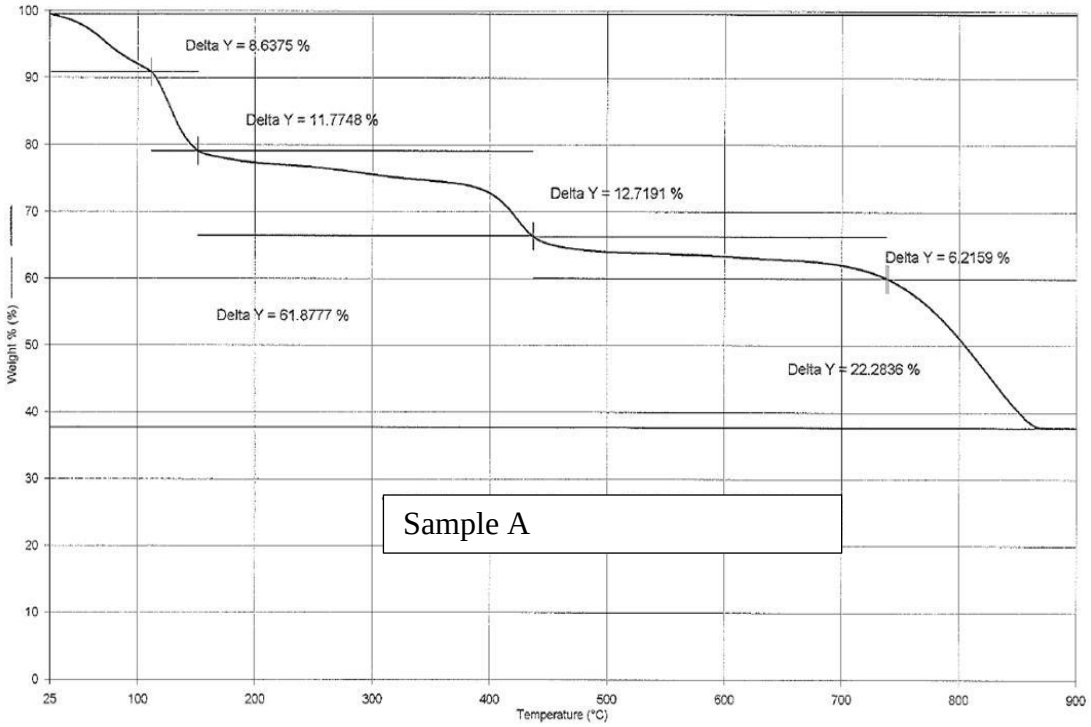

Figure 2. TGA Thermal Curve of Commercial RTU Grout Sample A.

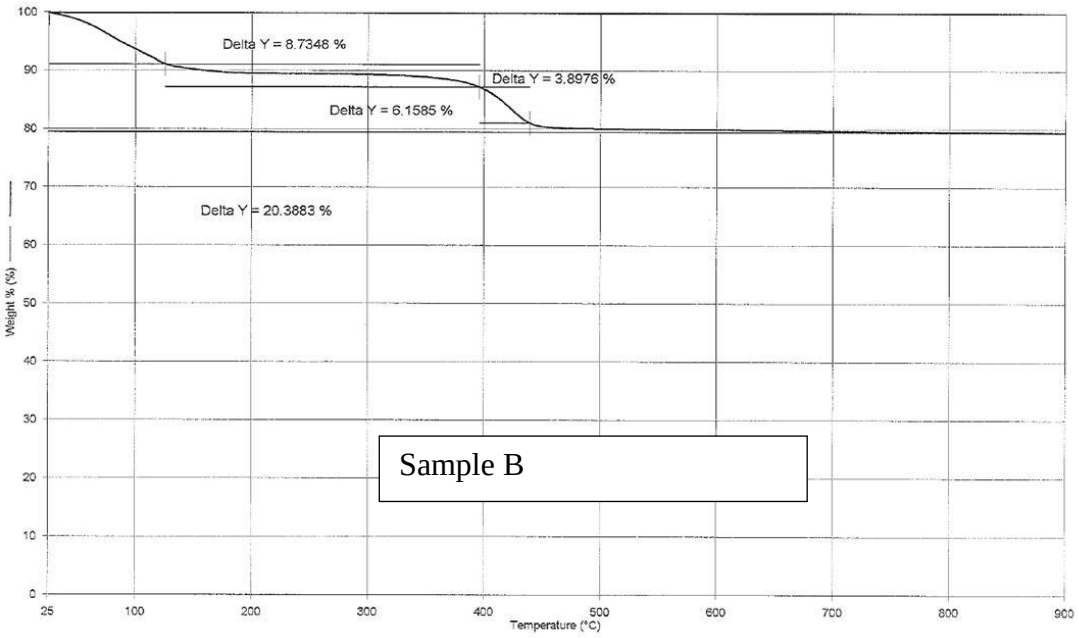

Figure 3. TGA Thermal Curve of Commercial RTU Grout Sample B.

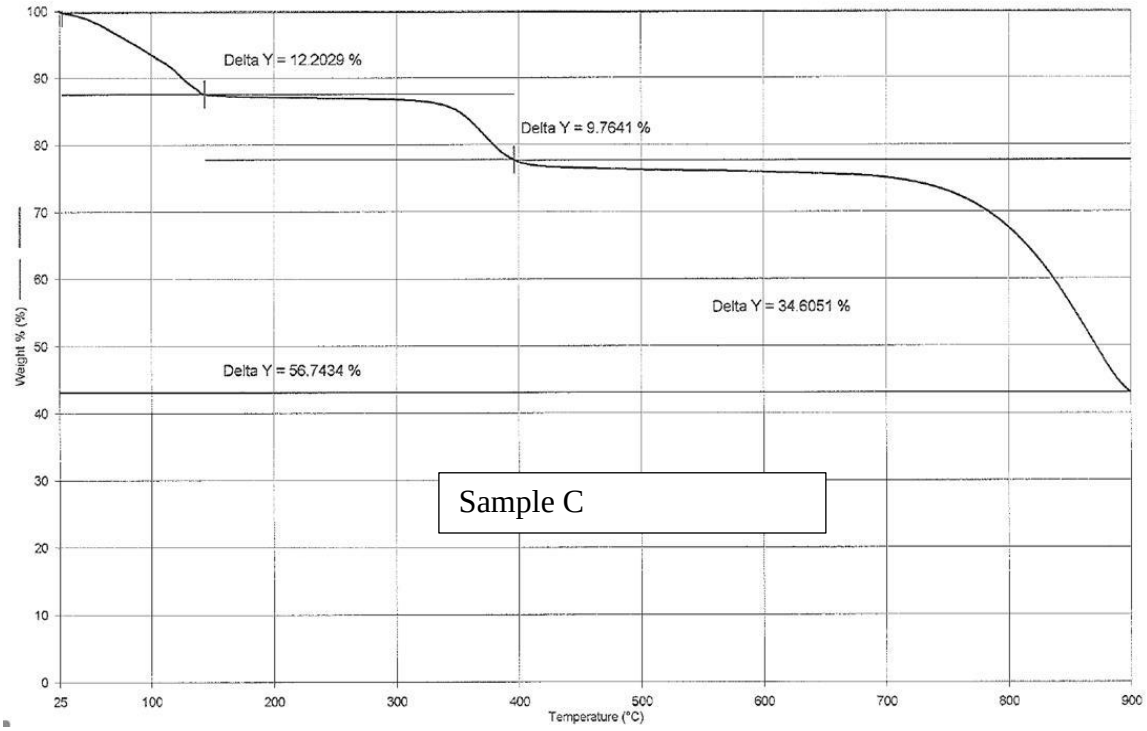

Figure 4. TGA Thermal Curve of Commercial RTU Grout Sample C.

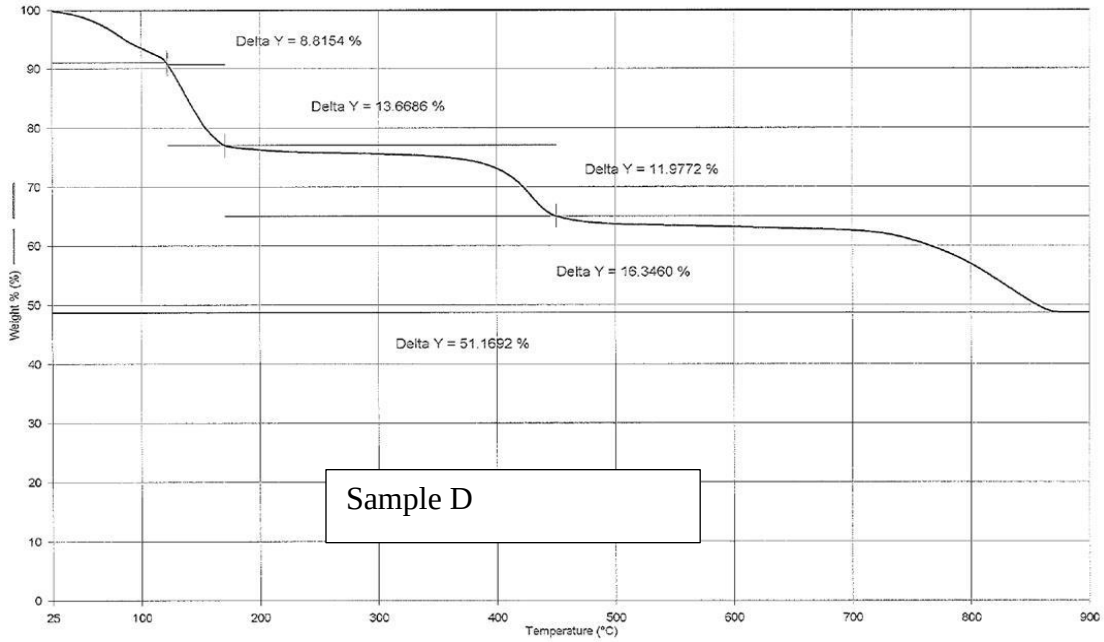

Figure 5. TGA Thermal Curve of Commercial RTU Grout Sample D.

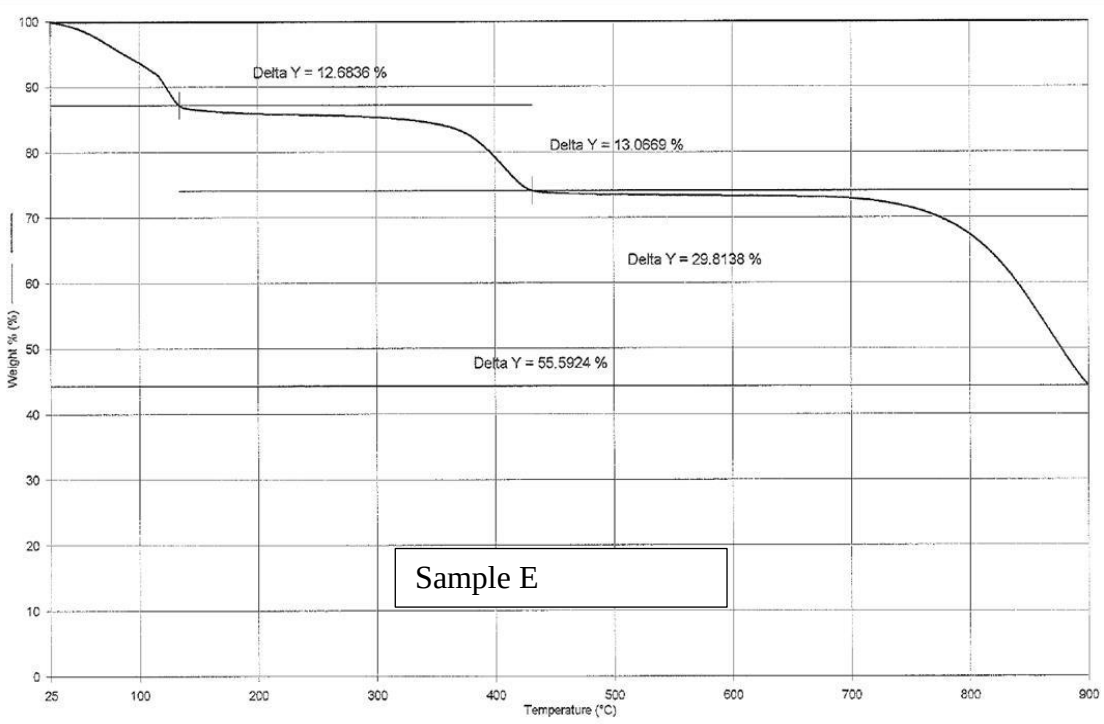

Figure 6. TGA Thermal Curve of Commercial RTU Grout Sample E.

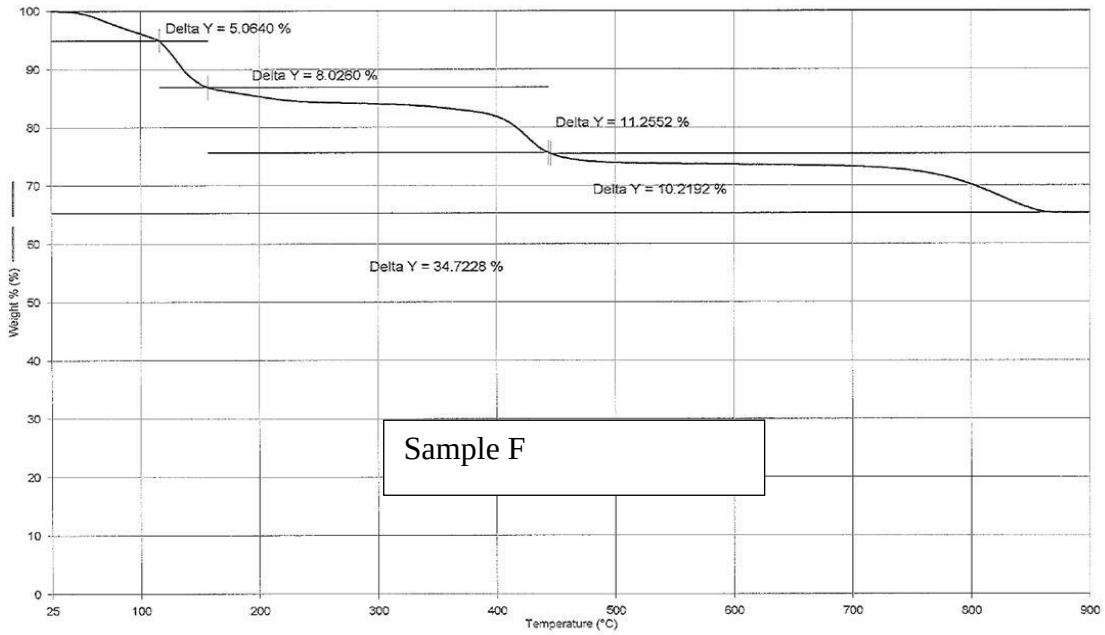

Figure 7. TGA Thermal Curve of Commercial RTU Grout Sample F.

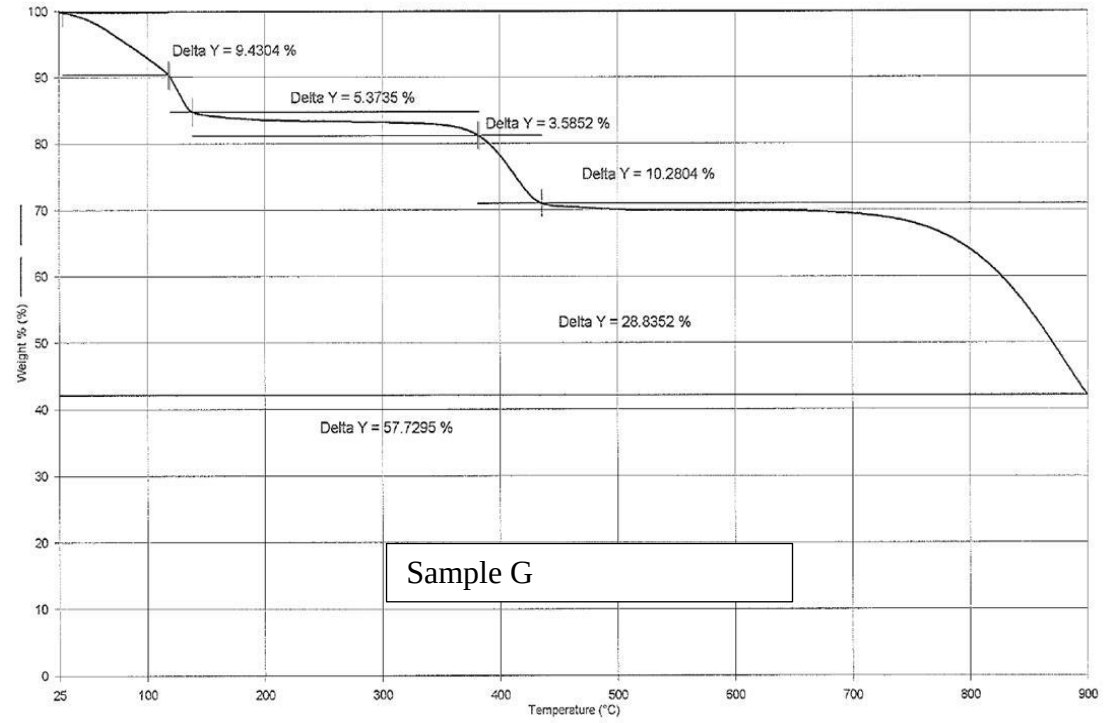

Figure 8. TGA Thermal Curve of Commercial RTU Grout Sample G.

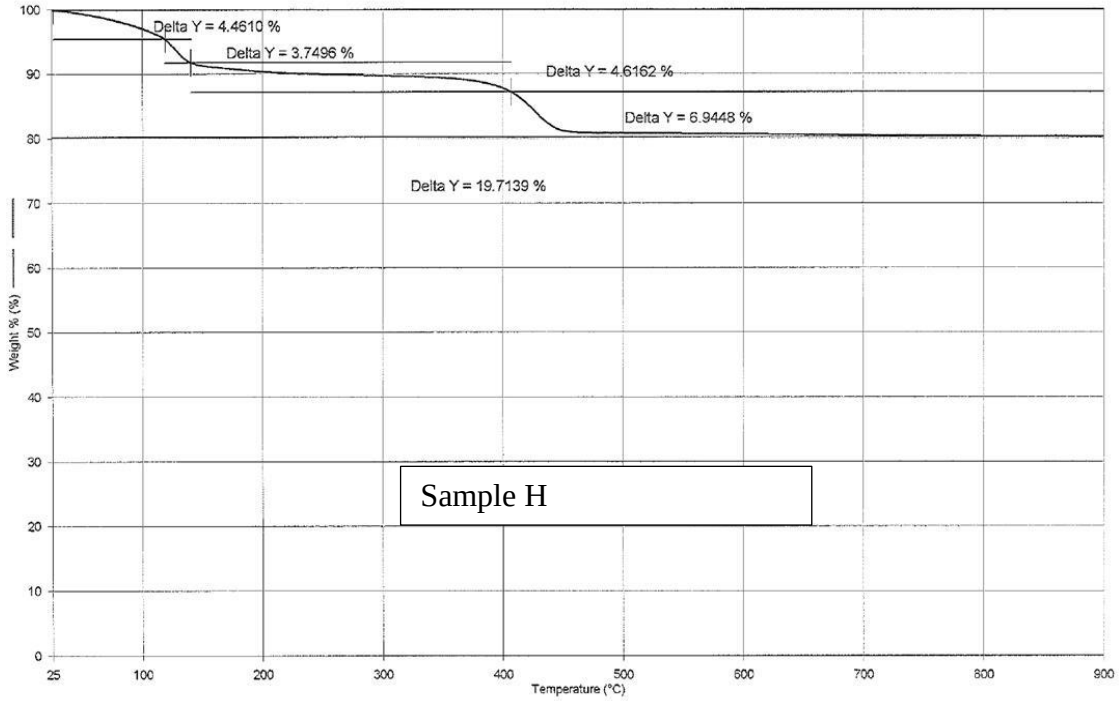

Figure 9. TGA Thermal Curve of Commercial RTU Grout Sample H.

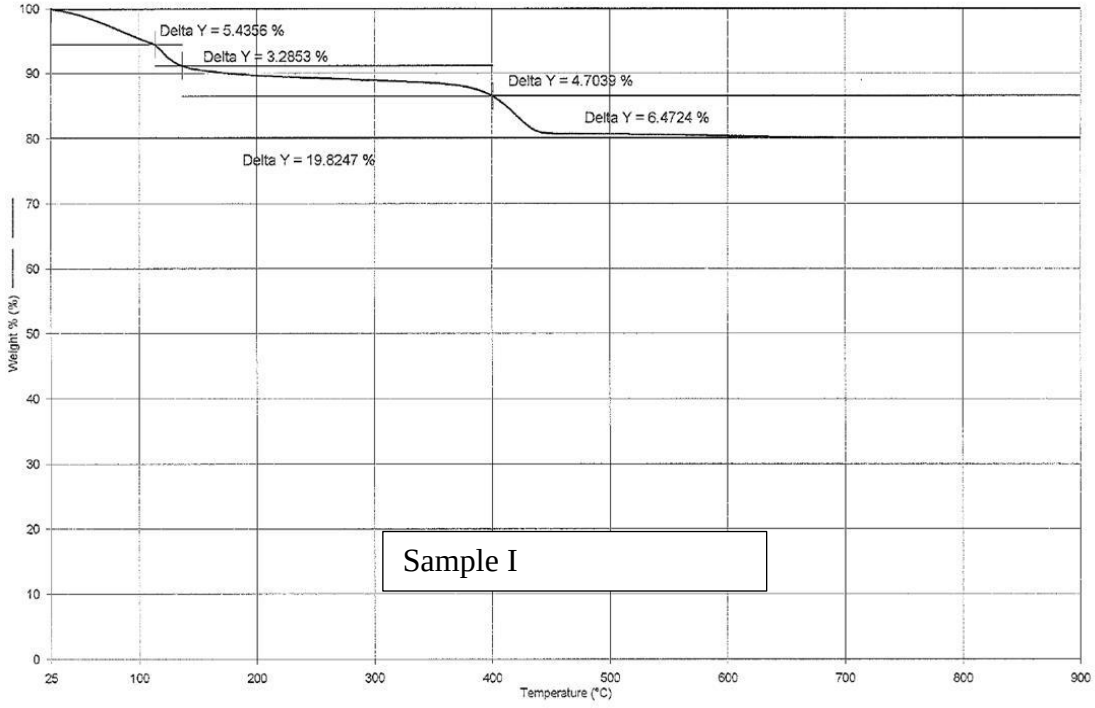

Figure 10. TGA Thermal Curve of Commercial RTU Grout Sample I.

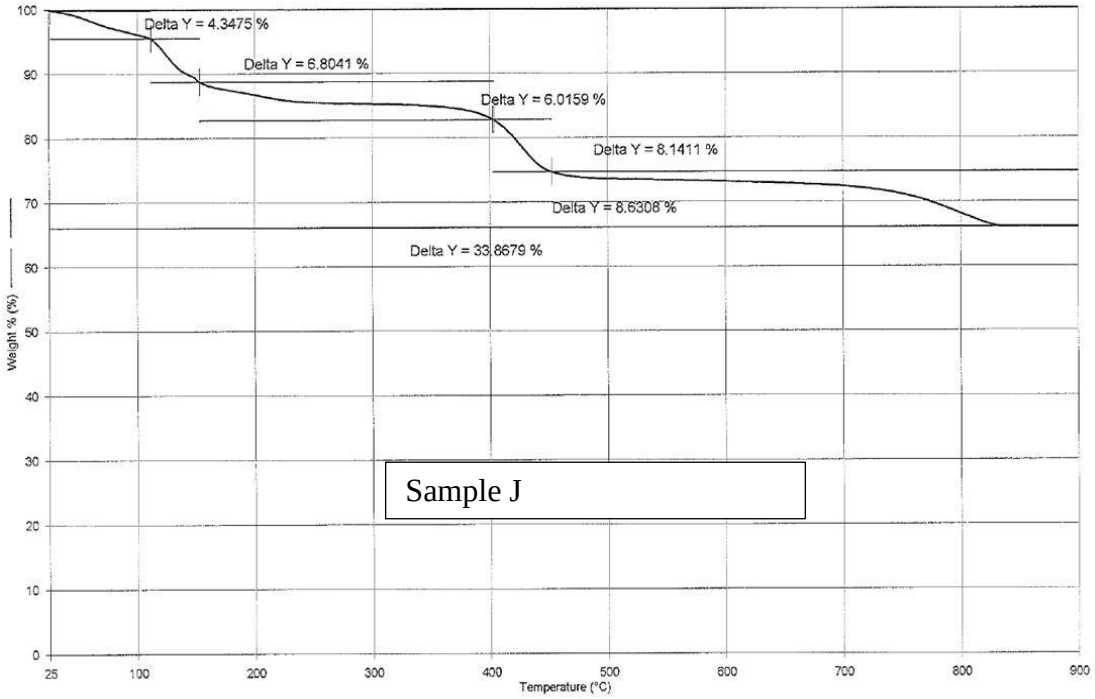

Figure 11. TGA Thermal Curve of Commercial RTU Grout Sample J.

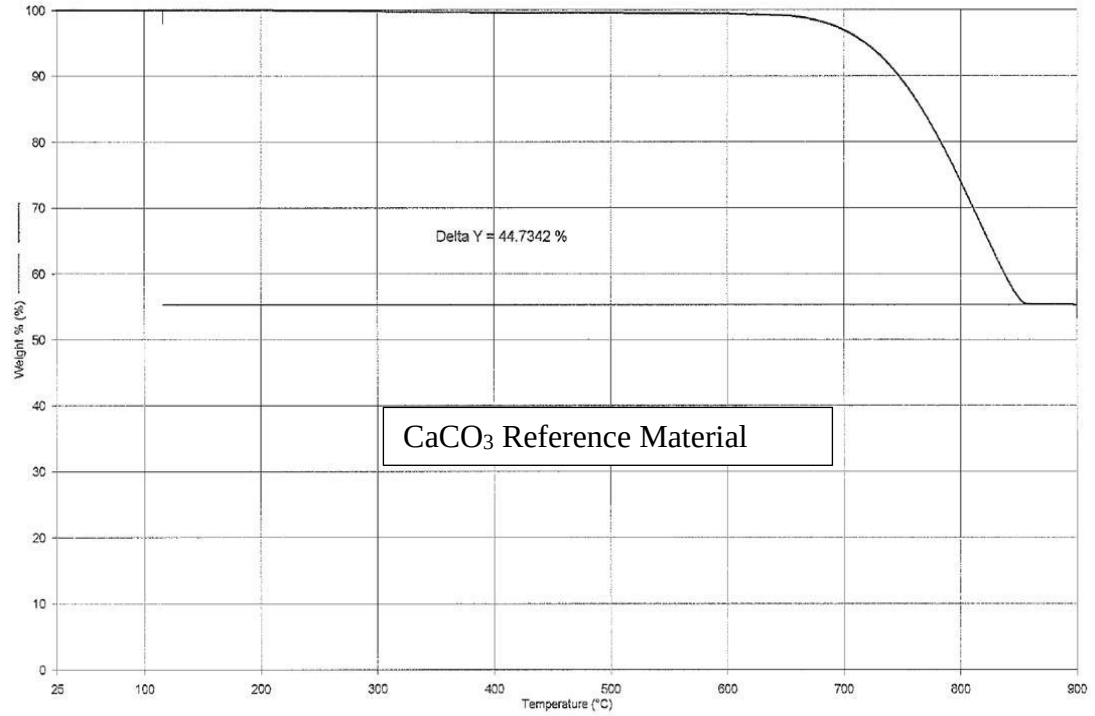

Figure 12. TGA Thermal Curve of Calcium Carbonate Reference Material.

The filler content was also measured by ashing in a muffle furnace for 4-hours at 500°C. The average filler content by the ashing method was determined to be 71.9% by weight. This is a little lower than the one determined by TGA. However, it does verify the relatively high filler content by weight of these materials. The difference in value can be attributed to several factors; 1 – greater precision with TGA, 2 – calculation errors with respect to $CaCO_3$ content and 3 – indeterminate loss of waters of hydration and/or carbonates with the ashing method.

Table 5

Commercial RTU Grout Average Performance Data

Sample	**Total Mass (%) Filler Retained**	**Mass (%) Carbonate Lost**	**Mass (%) Calcium Carbonate**	**Mass (%) Other Fillers**	**Mass (%) Total Fillers**
A	38.1	22.3	49.9	15.8	65.7
B	79.6	0.0	0.0	79.6	79.6
C	43.3	34.6	77.4	8.7	86.1
D	48.8	16.3	36.5	32.5	69.0
E	44.4	29.8	66.7	14.6	81.3
F	65.3	10.2	22.8	55.1	77.9
G	42.3	28.8	64.4	13.5	77.9
H	80.3	0.0	0.0	80.3	80.3
I	80.2	0.0	0.0	80.2	80.2
J	66.1	8.6	19.2	57.5	76.7
Average	NA	NA	33.7	43.8	77.5
Minimum	NA	NA	0.0	8.7	65.7
Maximum	NA	NA	77.4	80.3	86.1

Utilizing all of the available analytical information the following base-line formulating parameter guidelines (rough guidelines) were used for future formulation work:

- Solids content by weight = 85%
- Filler content by weight = 75%
- Calcium carbonate filler = 60%
- Other filler = 15%
- Solid binder content by weight = 12%
- Water content by weight = 15%

The commercial samples were also used to develop base-line average performance for a RTU grout. Table 17 shows the average values, standard deviations, and ranges of performance for the commercial survey. It is rather apparent that there is a wide range of performance for this market. These values were used to compare and contrast the performance of the formulated samples.

Table 6

Commercial RTU Grout Average Performance Data

Property	**Average Value**	**Standard Deviation**	**Range (min – max)**
Hardness	32	17	6 – 61
Volume Shrinkage (%)	13.3	10.6	2.4 – 39.7
Lap-Shear Adhesion (MPa)	0.42	0.25	0.13 – 0.80
Total Cracking (1 – 10)	9.0	0.7	7.8 – 10.0
Stain Repellency (0 – 40)	8.6	3.3	4.0 – 13.5
Water Uptake (%)	33.0	37.2	10.3 – 98.2

Table 6 (continued).

Tensile (UTS – MPa)	1.47	0.79	0.43 – 2.73
Tensile (Elongation - %)	11.0	6.3	1.6 – 26.4
Tensile (Young's Modulus – MPa)	1.80	1.79	0.34 – 5.45
Ease-of-clean-up (1 – 10)	9.5	0.7	8.0 – 10.0
Application (1 – 10)	9.2	1.9	4.0 – 10.0

One property of concern that sticks out is the water uptake percentage. The average sample increased in mass by 33% in water weight. The minimum was just above 10% with a maximum of over 98%. The establishment of these base-line values was done so that the formulation parameters could be explored so that these performance parameters could be improved.

Performance Evaluation Methodology

These methods were used for multiple purposes. The first use determined base-line performance of the commercial grout to set performance standards for the formulated grouts. The next use of the performance data was for formulation development. Several stages of formulation development were completed to optimize the physical properties, specifically high PVC, high pigment to binder ratio, high solids, and low water content. The formulations were then evaluated to optimize the filler and fiber content for type, concentration, OA value and particle size. Lastly, the performance evaluation methods were used to determine any correlation between polymer T_g and HSP with grout performance.

Performance Test Methods

Unlike cementitious or epoxy grouts, RTU grouts do not have established performance specifications. There is a working MMSA committee developing specifications and test methods for use, but this is in the early stages of development. A testing protocol was designed utilizing current ANSI standards for cementitious and epoxy grouts, as well as some MMSA proposed test methods. Table 4 lists the properties investigated and the associated methods used.

Table 7

Physical property evaluation test methods.

Property	**Method**
Shrinkage	Developmental
Tensile properties (modulus, UTS, elongation)	Developmental
Lap-shear adhesion	Developmental
Water-uptake (absorption)	Developmental
Stain testing	CTIOA 72 – modified[16]
Hardness	ASTM D 2240[17] - Shore D – Durometer
Cracking	Subjective from application panels
Flexural strength	Developmental

Volume Shrinkage. ASTM C 531[18] is used to measure linear shrinkage in cementitious and epoxy grouts, however, there is no method to measure linear shrinkage for RTU grouts. As such, a developmental method was employed that used shrinkage measurement principles for joint compounds. Figure 13 is a picture of the ¼ inch thick metal mold with a six inch long and ¼ inch wide groove and rounded at the ends that

were used to simulate a grout line. The mold was secured to a coated Leneta card and pre-weighed. Grout was applied into the groove forming a grout line and was scraped smooth with the plane face of the metal mold. The grout was weighed and allowed to dry/cure for 24 hours. More grout was applied to the existing grout line and again scraped smooth. The grout reweighed and the percent shrinkage was determined by dividing the second grout weight into the first.

Figure 13. Shrinkage Mold.

Tensile Properties. Since there is no test method to determine the tensile properties of these products, information was gleaned from multiple sources including Kinloch's *Adhesion and Adhesives*[19], Koleske's *Paint and Coatings Testing Manua*[20], ASTM C 307[21], ASTM D 412[22], ASTM D 2370[23], ASTM D 3182[24] and ASTM D 4708[25] to develop a test method. Rubber molds were created in the shape of the ASTM D 412 standard rubber dog bones for use in tension testing of rubber materials (4.5 inch length, with 1.5 inch being 0.25 inch wide between two one inch by one inch tabs, with a thickness of 0.1 inch in Figure 14). The thickness of each sample was measured using a Mitutoyo digital micrometer. The sample materials were applied with a metal spatula and scraped smooth into the molds. The samples were dried for three days, removed, and

placed face down to dry for four more days prior to testing. Air compressed alligator grips with a 2-inch gauge length were used to hold the samples. Figure 15 shows a representative test sample loaded in the machine for testing. The samples were pre-loaded with 0.2 lbs.-force and pulled at a rate of 2.5 inch/min. until they broke. UTS and elongation were recorded and the Young's modulus was calculated from the initial slopes of the curves for each sample.

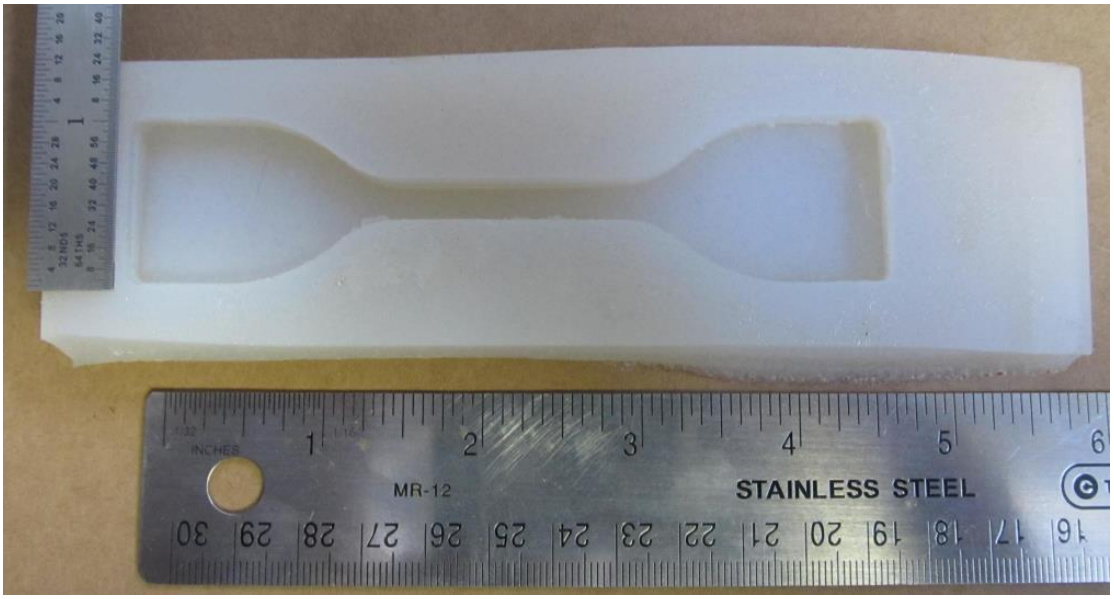

Figure 14. Tensile Mold.

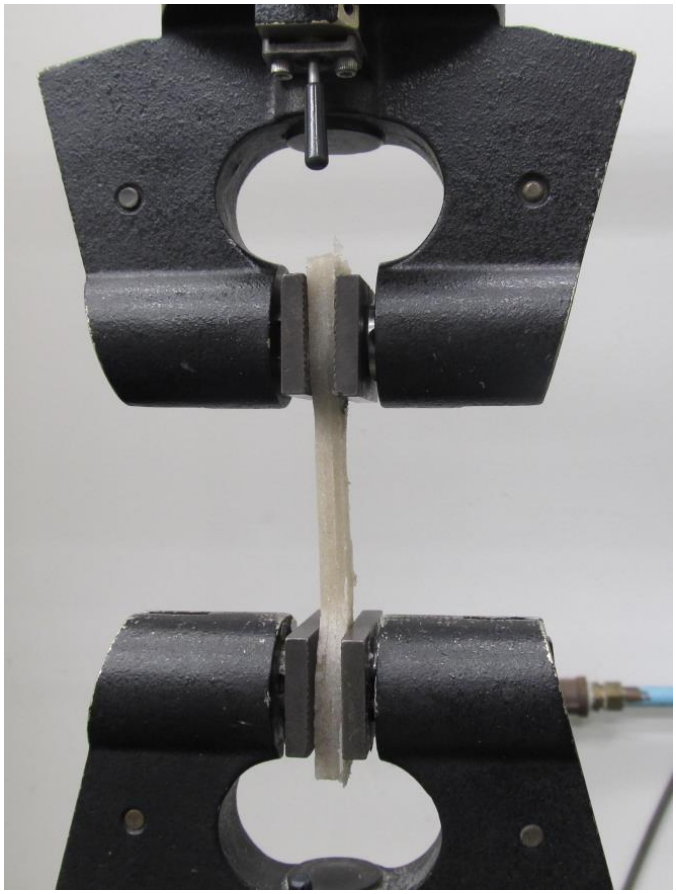

Figure 15. Tensile test jig and reference sample.

Lap Shear Adhesion. Since there is no test method to determine the tensile properties of RTU grouts, information was gleaned from multiple sources including Kinloch's *Adhesion and Adhesives*[19], Koleske's *Paint and Coatings Testing Manual*[20], ASTM D 1002[26], ASTM D 3163[27], ASTM D 3983[28] and ANSI A118.1.5[29] to develop a suitable test method. Grout material was applied on both surfaces of marble tiles measuring 2 inch x five inch x 0.5 inches using a back-butter technique. The tiles were squeezed together using 0.125 inch wide spacers which were removed after the tiles were set on a tray with an appropriately sized riser on one side. The riser allowed both ends of

the tile to be supported without causing any strain on the adhered joint. The joint length was approximately one inch. Figures 16 shows the entire set-up including the spacers, tools used and the platform for drying the samples, representative samples from side and top view, and the instrument sample setup. The samples were allowed to dry for seven days. The joint area was then measured and tested in tension by using bolt tightened alligator grips to hold each end. The gauge width was approximately four inches. A pre-load of 0.2 lbs.-force was used and the samples were pulled at a rate of 0.05 in./min. until failure.

Figure 16. Lap shear tools, sample and test jig with reference sample.

Water Absorption. A tiled board was created using a gypsum board measuring 12 inch x 12 inch x 0.75 inches, and adhering 16 vitreous tiles measuring two inch x two inch x 0.25 inches with a mastic tile adhesive in a square grid pattern. The grid was made with 0.25 inch spacing between the tiles. This board was allowed to dry for several days. A reverse rubber mold (Figure 17) was created from one of these boards to afford the production of square samples with the same dimensions at the vitreous tiles above. Three replicates of each sample were produced. The samples were allowed to cure for three days and then removed from the mold and allowed to cure for an additional four days face down. The samples were then weighed and placed in a water bath on stainless steel

wire racks. The final water uptake value was listed as the increase from dry to the 1440-min. (24-hr) time interval.

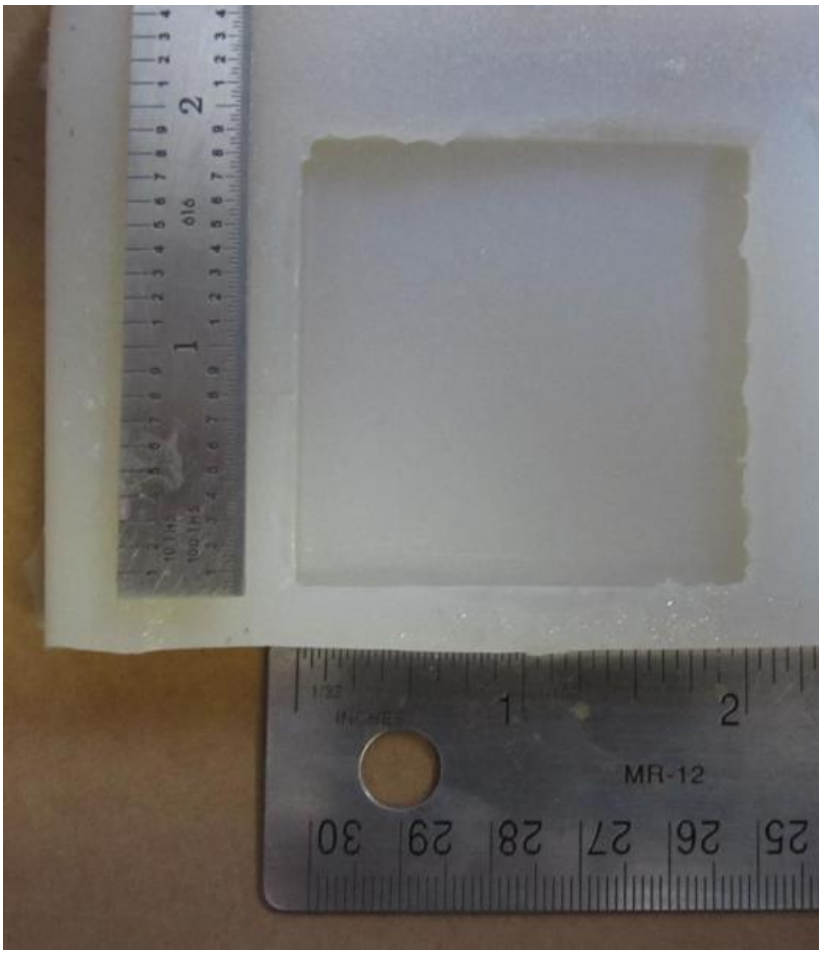

Figure 17. Mold for water-absorption samples.

Stain Testing. Stain repellency testing was evaluated using two similar methods. Both methods require the grout to be applied onto an appropriate substrate and cured/dried for seven days prior to stain repellency testing. In one method the grout is applied to a pre-prepared tile board. Figure 18 shows the tile board was prepared by using 12 inch x 12 inch x ½ inch thick drywall boards and applying two inch x two inch x ¼ inch vitreous tiles to the boards. A ready-to-use or mastic tile adhesive was used, with ¼ inch grout lines (using ¼ inch grout spacers) to adhere the tiles to the board. The

boards were allowed to dry/cure for at least 24 hours prior to applying the grout. The other method involves filling a four inch wide x ¼ inch thick plastic jar lid with grout. Both methods require the grout to be worked smooth during application.

Once the grout had cured/dried for seven days staining agents are applied to the grout surface and allowed to reside for four hours prior to cleaning. The staining agents that were chosen are typically used in testing many stain repellent materials (i.e. tile and grout sealers, cementitious grouts, garage floor coatings, etc.):

- Skydrol – An aeronautic hydraulic fluid, purple in color. The base chemistry is phosphate ester and is considered by many in the concrete sealer industry as one of the most pervasive staining agents
- Brake Fluid – A hydraulic fluid consisting of a mixture of glycol ethers, mineral oils and silicone oils.
- Motor Oil – Mixed chain length hydrocarbons
- Vinegar – White wine vinegar, approximately 5% acetic acid
- Vegetable Oil – Wesson® brand soya oil
- Red Wine – Fermented grapes
- Ketchup – Tomato puree with vinegar and other additives
- Mustard – Mustard seed, vinegar, yellow dye and other additives
- Soy Sauce – Kikkoman® brand, containing wheat and soy bean fermentation by-products in a high salt (mostly sodium chloride) concentration
- Coffee – Coffee bean (tannins) extract with water
- Coca-cola® – Carbonated sugar, water and acid mixture with additives

- Water – de-ionized and reverse osmosis used to determine beading characteristics and true hydrophobicity

The cleaning process was the same for both types of sample substrates (tile board or disk). First the panels were rinsed under flowing lukewarm water and rubbed lightly to remove dry and loose debris. The panels were then uniformly sprayed with Formula® 409 cleaner (ten squirts for tile boards – four squirts for disks). The cleaner was allowed to sit for fifteen seconds to allow the cleansing chemicals some time to take action. The surfaces were both rubbed, gently, with a damp, soft sponge in a controlled and repeatable manner (back and forth five times for each grout line – back and forth five times each along perpendicular directions for the disk). The panels were then rinsed again under running lukewarm water for 15 seconds and set aside to dry for 24 hours prior to rating the stain repellency performance. The drying/waiting time is consistent with recommendations of the CTIOA-T7216 Field Report for stain repellency testing of tile sealers. The stains are then each rated on a zero (no stain) to four (completely stained – none removed) subjective scale. The stain ratings were then summed for complete stain repellency.

The tile board method was preferred since it has been shown that tile boards allow for accurate stain repellency testing for cementitious grouting materials[30]. This is because any stain repelling chemicals that may be incorporated need to migrate to the grout surface to prevent stains. It has been shown that higher application forces are required to facilitate the movement of the stain repellent materials to the grout surface[30]. Tile board application forces are nearly 18 times higher than the forces required to apply grout within a disk. However, it has not been shown whether this same phenomena

occurs with RTU grouts, as such, the MMSA has adopted a grout disk method for stain repellency testing. Although, they also utilize a colorimeter to measure the stain intensity, this was not done in this study since no colorimeter can accurately measure color on a cupped grout line.

It has been repeatedly noted by the author that the subjective rating of tile boards is repeatable as long as a control panel is always tested with each test set. The repeatability improves when the same people rates the samples for stain repellency rating. Additionally, it has been shown that while ultimate scores may differ between operators rating the same samples, the rank order of ratings remains the same between operators.

Figure 18. Ungrouted panel, grouted panel, grouted and stained panel.

Cracking. The grouted panels were rated for two types of cracking (edge and center). Edge cracking occurs where the grout cracked near the tile edges and pulled away from the tile. Center cracking occurs in the bulk of the grout material. Grouted panels were subjectively rated on the same 1.0 to 10.0 scale as the application properties and were rated by the same experienced grout applicators.

Flexural Strength. There is no agreed upon method to evaluate flexural strength of RTU grouts. As such, several ASTM methods were referenced for ideas to build this method. ASTM C531[18] is used to prepare cementitious and epoxy grouts for linear

shrinkage and these prisms are then tested for flexural strength according to ASTM C 580[31]. However, RTU grouts will not dry and cure properly at such high thicknesses. ASTM D 4476[32] is used to evaluate fiber reinforced pultruded plastic rods for flexural strength, but RTU grouts cannot be pultruded into such bars. However, these test methods all gave insight into the design of a specialty mold to be used to produce RTU grout samples for flexural strength testing.

Teflon® rectangular molds were prepared as sown in Figure 19. The mold space is 10 mm x four mm x 80 mm within the block. Small extraneous holes in the corners of the mold facilitate sample removal. The samples were prepared by adding grout to the molds and scraping off the excess. The samples were allowed to dry for two days, carefully removed from the molds, and allowed to dry for an additional 12 hours prior to testing.

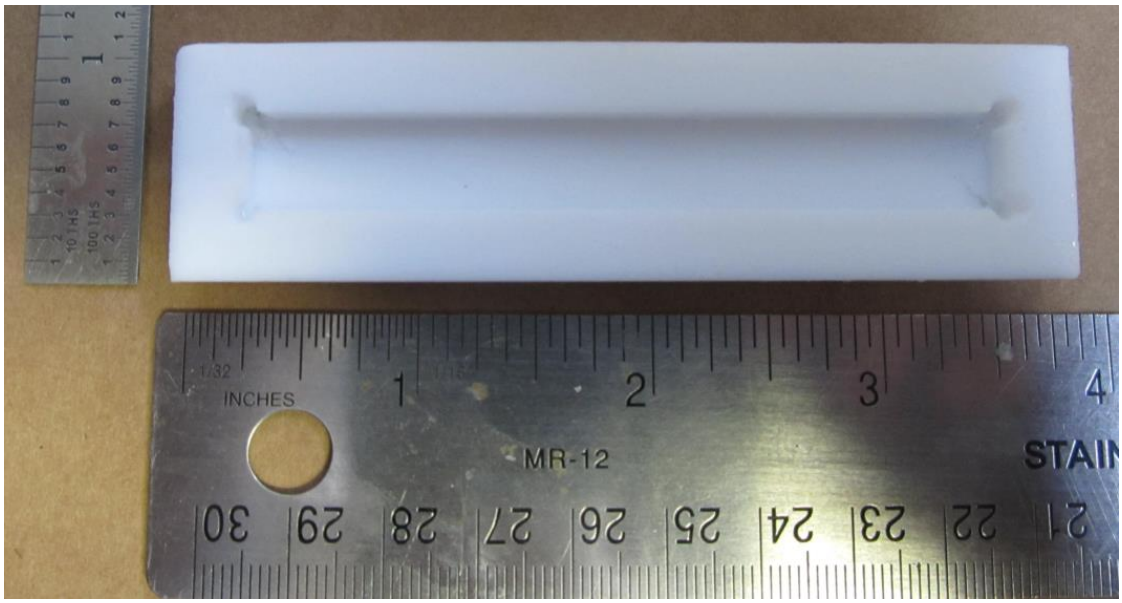

Figure 19. Flexural strength mold.

Flexural strength was evaluated using a three-point bend apparatus in compression mode, with the force applied from the top (Figure 20). The gauge length for testing was 60 mm under a constant load rate of 0.125 lbs./min.

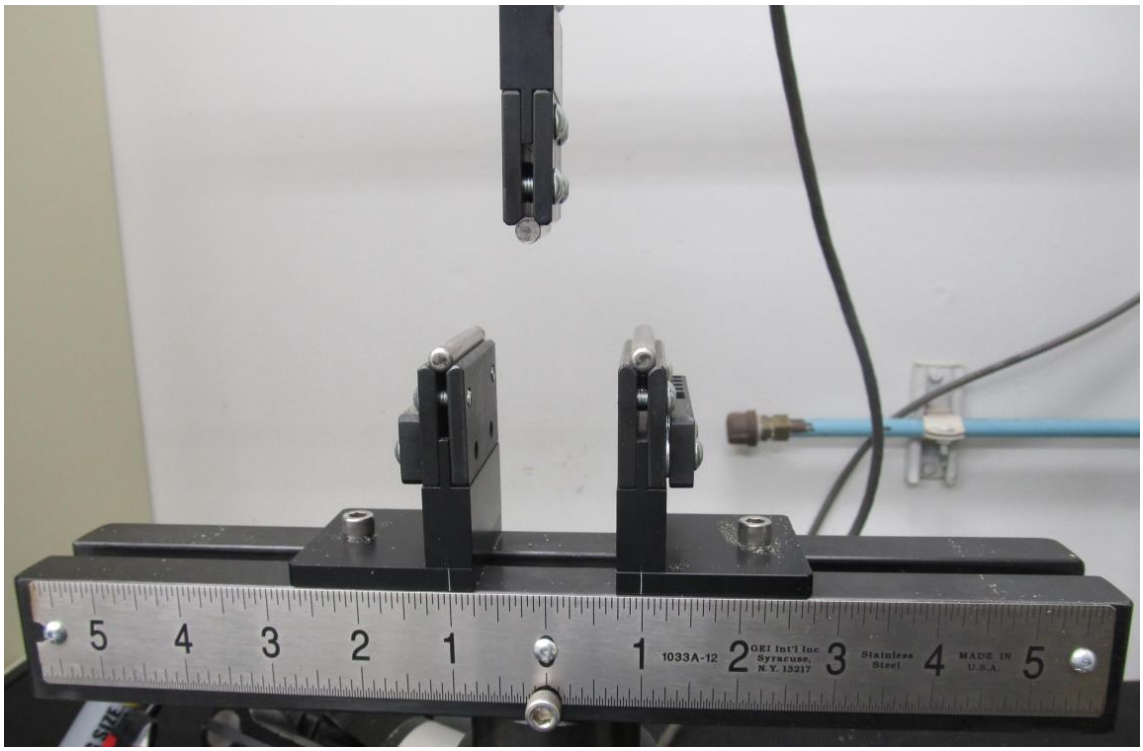

Figure 20. Flexural strength testing jig.

Evaluation Equipment Used

- United SFM-30K Universal Testing Machine – Tensile (using alligator grips) and lap-shear properties (under compression loading)
- Shore D Durometer by Humboldt Manufacturing – Surface hardness
- Hobart 50N (5 quart capacity bowl) – for mixing formulated samples
- Mitutoyo Digital Micrometer – For dimensional measurements for all physical testing

- Zwick MPM (Z010) Universal Testing Machine with a 10 kN load cell – Flexural properties using a TH22-360 Af20 3-point loader

Materials

The materials used in this project were either commercial grouts (purchased online or at local retail outlets) or prepared in our lab. The commercial grouts are note named in this document and are simply denoted as Commercial Grout (A – J).

The raw materials used to formulate the test grouts are listed below: (emulsion polymers and their properties are listed separately):

- Tamol® 681 – Dispersing agent – an ammonium salt of a hydrophobic co-polymer – Dow Chemcial[33]
- Minex® 3 – Medium particle size, high oil absorption value filler – micronized nepheline syenite – median particle size 10.8 μm, oil absorption value 25 g/100 g – Minex[34]
- Snowhite® 21 PT – Large particle size, medium oil absorption value filler – dry ground calcium carbonate – median particle size 21.0 μm, oil absorption value 11 g/ 100 g – Omya[35]
- Omyacarb® 6 PT – Small particle size, low oil absorption value filler – dry ground calcium carbonate – median particle size 6.0 μm, oil absorption value 6 g / 100 g – Omya[36]
- Nylon Fibers – Nylon mixed luster – 3 mm length, 31 μm diameter, 97 aspect ratio, 0.6 kPa tensile strength – MiniFibers[37]
- Mineral spirits (Odorless) – Defoamer

- Walocel® MW 15000 PFV – aqueous phase thickener – fine particle size cellulose either, 15000 cP viscosity grade (2% solution), delayed solubility – DowWolf[38]
- Rozone® 2000 – fungicide/algaecide, formaldehyde free – Dow Chemical[39]
- Kathon® LX 1/5% - Biocide (in-can preservative) – Dow Chemical[40]
- 3M™ Novec™ Fluorosurfactant FC 4432 – Surface application cleaning aid, viscosity reducer – fluoro-surfactant (C4 technology) – 3M[41]
- Ammonium Hydroxide (28%) – pH adjustment
- Dowanol® PPh – Coalescing agent – propylene glycol phenyl ether – Dow Chemical[42]
- Acrysol® RM 825 – non-ionic urethane-based, rheology modifier – Dow Chemical[43]

The polymers (A – L) were supplied by Wacker Chemical Corporation and Dow Chemical, and are not identified in this document. Please note that some letters are skipped because in earlier research, these polymers were determined to be very similar to other polymers, however, we kept the naming convention to maintain the integrity of all of the work done (whether reported externally or not).

The premise of this paper is to evaluate polymer performance by both the glass transition temperature (T_g) and by HSP. To accomplish these two analyses, the polymers need to be completely analyzed so that the monomer compositions can be elucidated.

Ten polymers were used in this study. All of them chain-growth polymers polymerized via a double/vinyl bond. This type of polymer was chosen because this is the type of polymer used in most commercial RTU grouts. Additionally, all of the

polymers used in this study have the same carbon-carbon backbone with pendant groups on every other carbon atom. The different T_g's and polymer performance for these ten polymers is derived from the varying pendant groups associated with the monomers used to produce these polymers.

The following basic methods used are listed below with a brief description of the expected data that can be extracted from that particular test.

- Differential Scanning Calorimetry (DSC) – Used to determine the T_g of the polymer.
- Fourier Transform – Attenuated Total Reflectance Infra-Red Spectroscopy (FT-ATR) – Used to determine the main functional groups present on the polymer.
- Pyrolysis/Gas Chromatography (GC)/Mass Spectral Analysis (MS) – Used to determine qualitative monomer composition. Chain-growth polymers, especially vinyl polymerized polymers lend themselves very well to qualitative monomer analysis by this method due to the fact that they exhibit retropolymerization[44], which will degrade at least part of the polymer into the component monomers.
- Nuclear Magnetic Spectroscopy (NMR), H^1 and in some cases C^{13} – Used to determine specific monomer quantities by integration and quantifying one specific peak for a monomer that is not present in other monomers.
- Minimum Film Forming Temperature (MFFT) Bar – Used to determine the crack point, knife point of the neat polymer and to determine the optimal amount of propylene glycol phenyl ether (PPh) coalescing solvent to formulate

the grouts to form a film at 50°F (10°C). This is the lowest recommended temperature of application for the commercial RTU grouts.

- Fox Equation – To utilize all of the above collected information to determine final monomer composition.
- Thermal Gravimetric Analysis (TGA) – This test was performed on dried films. This was done to determine the decomposition profile of the polymer to determine if other non-volatile materials are present.

Fox Equation:

$$1/T_{gP} = [M_1]/T_{gM_1} + [M_2]/T_{gM_2} + \cdots + [M_N]/T_{gM_N} \qquad \text{Equation 1}$$

T_g in Kelvin and concentration in weight percent

Table 9 shows the monomer composition in both weight and mole percent. T_g is the temperature where a polymer transitions from a hard, glassy state to a soft, rubbery state. From a molecular standpoint it is the temperature region where translational motion begins and free volume increases. Given that T_g is actually a temperature range and not a fixed point there is debate on what temperature to report. The inflexion point of the heat flow curve is the point that T_g was reported for purposes of this research.

Table 8

Polymer T_g and monomer composition.

Polymer	**T_g (K)**	**Monomer Composition (mol. %)**
A	336	Styrene (79.3), 2-Ethyl-hexyl acrylate (14.7), Acrylonitrile (5.3), Methacrylic acid (0.7)
B	312	Styrene (83.5), 2-Ethyl-hexyl acrylate (15.8), Methacrylic acid (0.7)

Table 8 (continued).

C	313	Methyl methacrylate (80.3), 2-Ethyl-hexyl acrylate (18.8), Acrylic acid (0.8)
D	290	Methyl methacrylate (53.8), Butyl acrylate (29.9), 2-Ethyl-hexyl acrylate (11.4), Butyl Methacrylate (4.2), Methacrylic acid (0.7)
E	283	Methyl methacrylate (64.0), Butyl acrylate (31.5), Butyl methacrylate (3.9), Methacrylic acid (0.6)
F	296	Vinyl acetate (56.6), Methyl methacrylate (24.3), Butyl acrylate (19.1)
H	267	Ethylene (50.6), Vinyl acetate (49.4)
I	274	Vinyl-acetate (56.6), Ethylene (43.4)
J	309	Vinyl-acetate (100.0)
L	274	Vinyl-acetate(64.0), Ethylene (28.1), VeoVa (7.9)

The following paragraphs show how one example polymer, polymer E, was analyzed to determine the polymer structure and monomer content.

Supplier information indicated that polymer E is a soft acrylate type polymer with a DSC scan, in Figure 21, showing the T_g range to be 280 to 291K (7 to 18°C) with a T_g of 283K (10°C) as evidenced by the inflexion point.

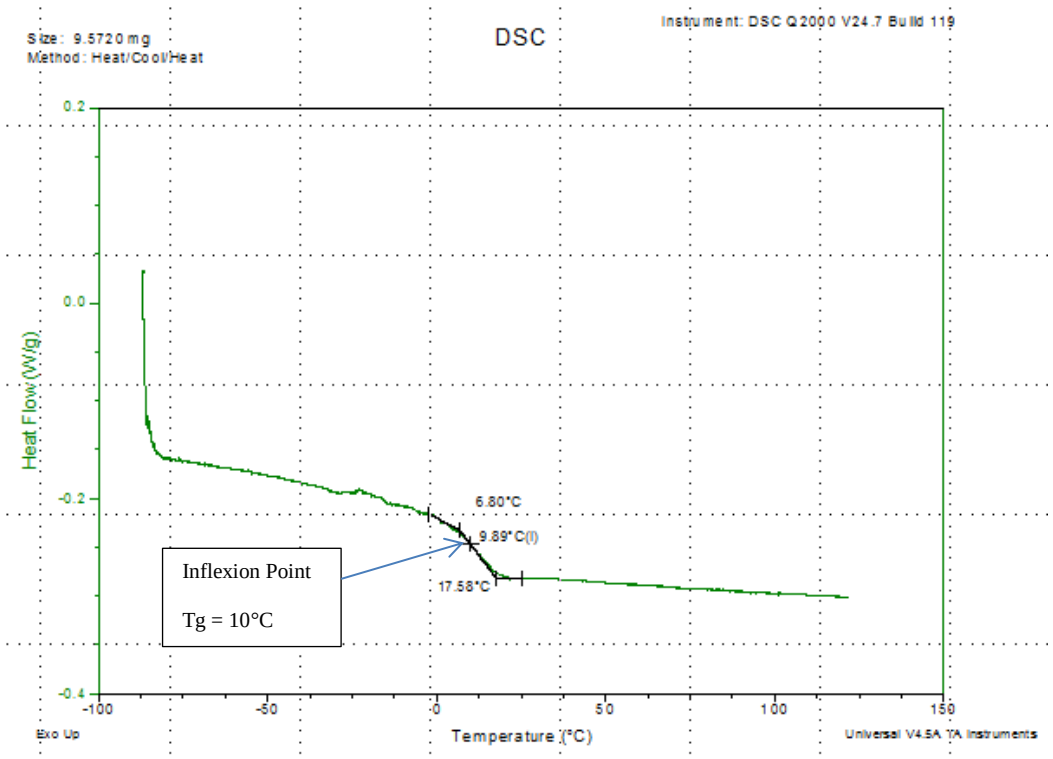

Figure 21. DSC Scan of Polymer E.

No peaks greater than 3000 cm^{-1} indicate a lack of aromatic groups. The peak at 1725 cm^{-1}, a carbonyl, confirms the acrylic nature of the polymer.

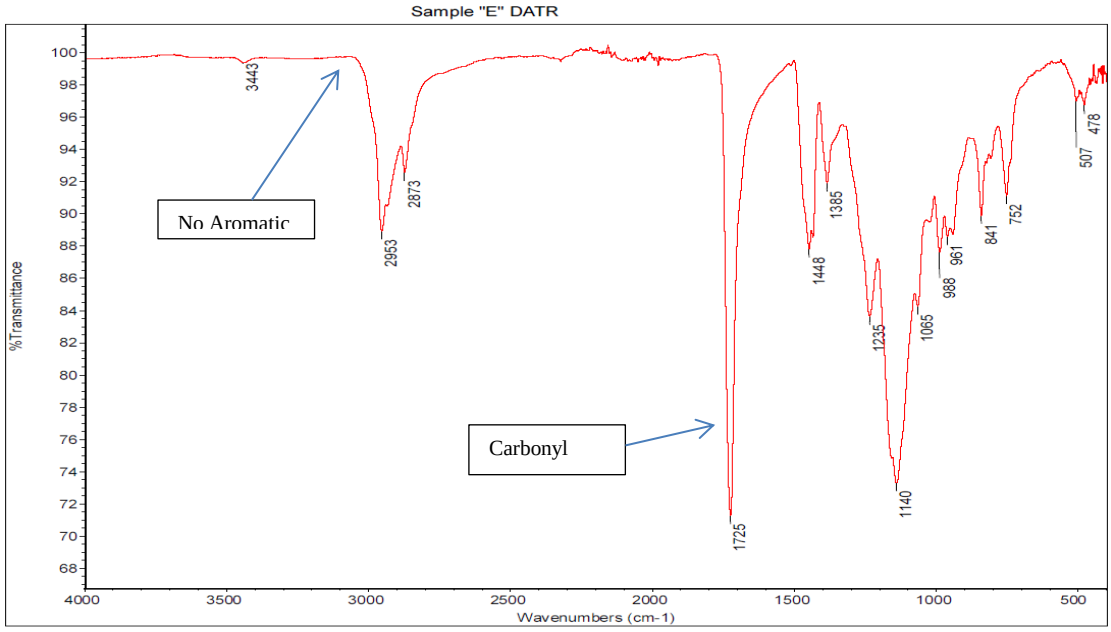

Figure 22. FT-ATR Spectra of Polymer E

Pyrolysis-GC-MS confirms the presence of the specific monomers present by first evaluating each of the peaks in the chromatograph by further evaluation using the total ion chromatograms for each individual peak. Figure 23 shows the pyrolysis-GC chromatograph with each major peak labeled by MS analysis.

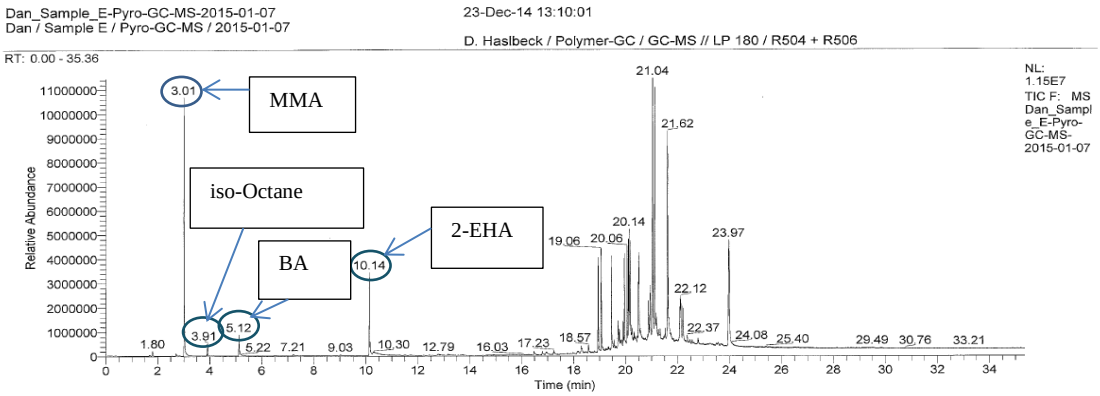

Figure 23. Pyrolysis-GC-MS Chromatograph of Polymer E

The total ion chromatograms, Figure 24, show each peak identified by the time, in minutes, where the peak was identified and then shows which monomer it is by the unique total ion chromatogram.

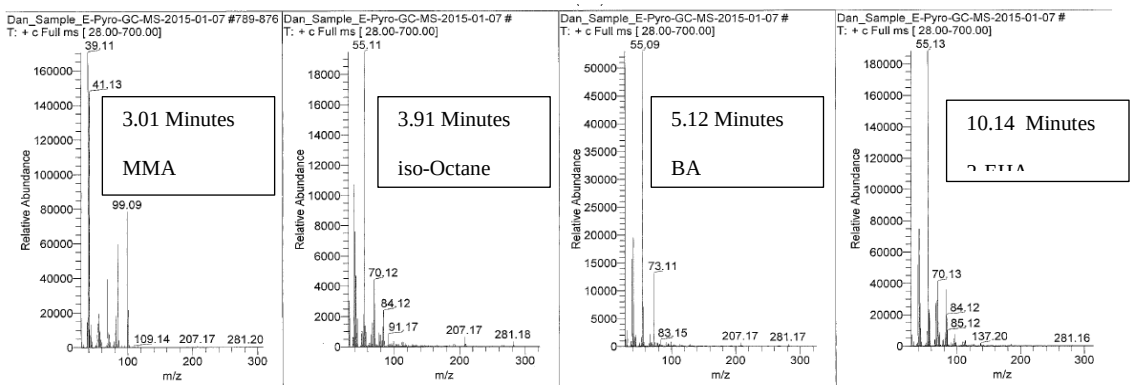

Figure 24. Total Ion Chromatograms of Components of Polymer E.

The H^1-NMR spectra in Figure 25 shows the spectra of a typical acrylic polymer. Each monomer was verified by a Wacker Analytical Chemist to verify the presence of each monomer found by other techniques. However, the exact analysis will be left out of paper as NMR techniques are not the focus of this work. It has been included so that the reader can determine for themselves the accuracy of the monomer composition.

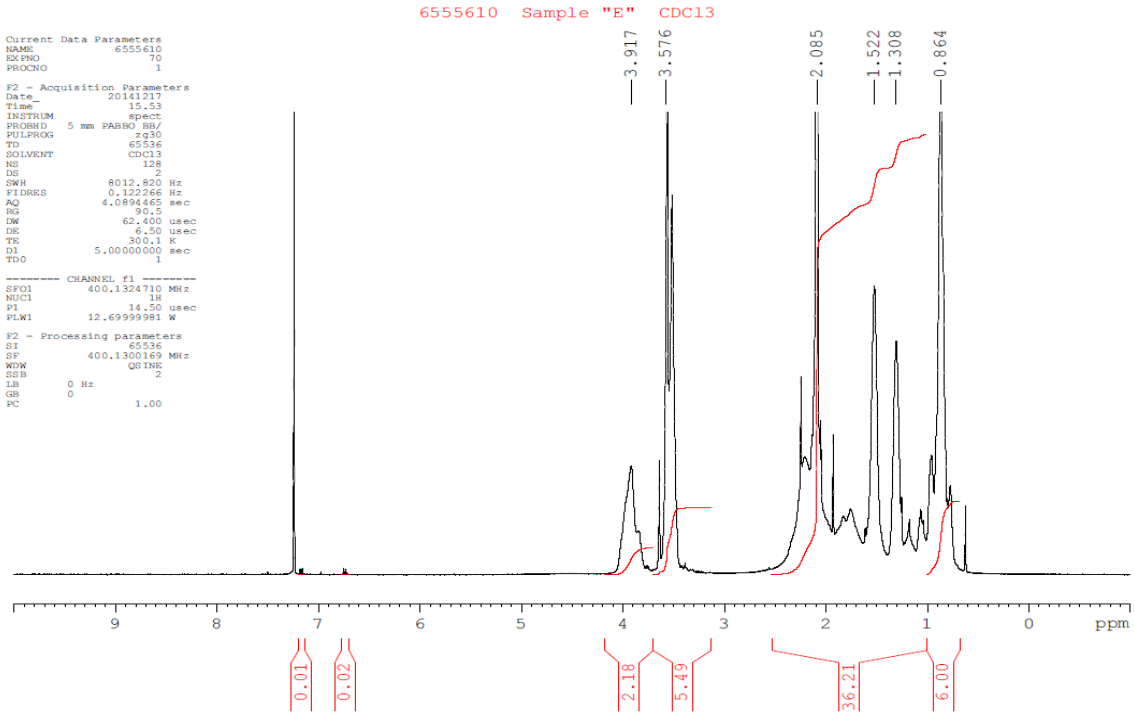

Figure 25. H^1-NMR Spectra of Polymer E.

Figure 26 is a TGA thermal curve for polymer E showing that with a dry film of polymer there are no other materials that volatilize out of the polymer, such as plasticizers.

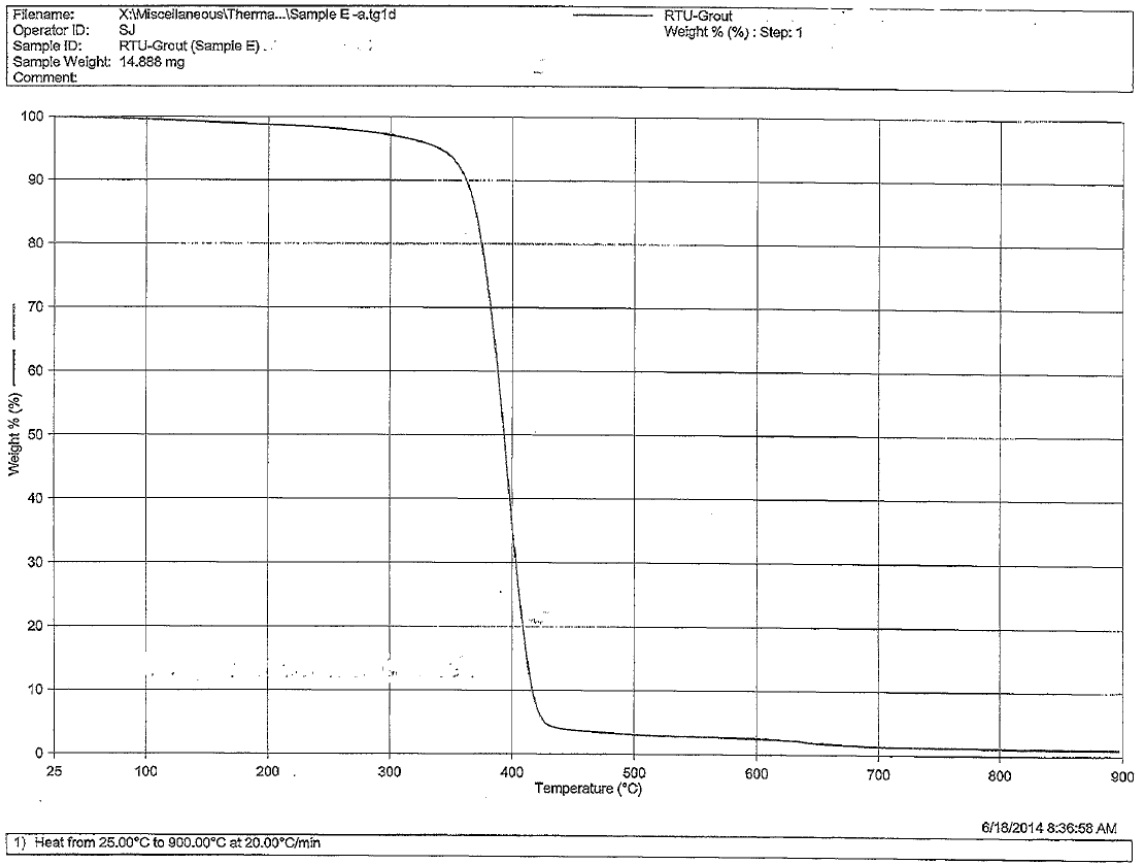

Figure 26. TGA Thermal Curve of Polymer E.

MFFT bar analysis using a concentration ladder of PPh coalescing solvent were used to determine the optimal film forming concentration of coalescent to be added to polymer E to form a film at 283 K (10° C). The crack point for the neat polymer is 285 K (12° C). The crack point is the point where the film shows evident cracking above this temperature line on the MFFT bar. The knife point of polymer E was determined to be 294 K (21° C). The knife point is a more accurate measure of film integrity since it is the point at which no cracking occurs above this temperature thus ensuring a film with true integrity[45]. The knife point is determined by scraping from higher temperatures where the material is a rubbery film until you come to a point on the MFFT bar where the film appears to be clear, but will easily crack apart. Using knife point data the optimal PPh

concentration of 1.3% by weight of total polymer is needed to form a film with integrity at 283 K (10° C). The chart in figure 27 shows the PPh concentration versus knife point temperature.

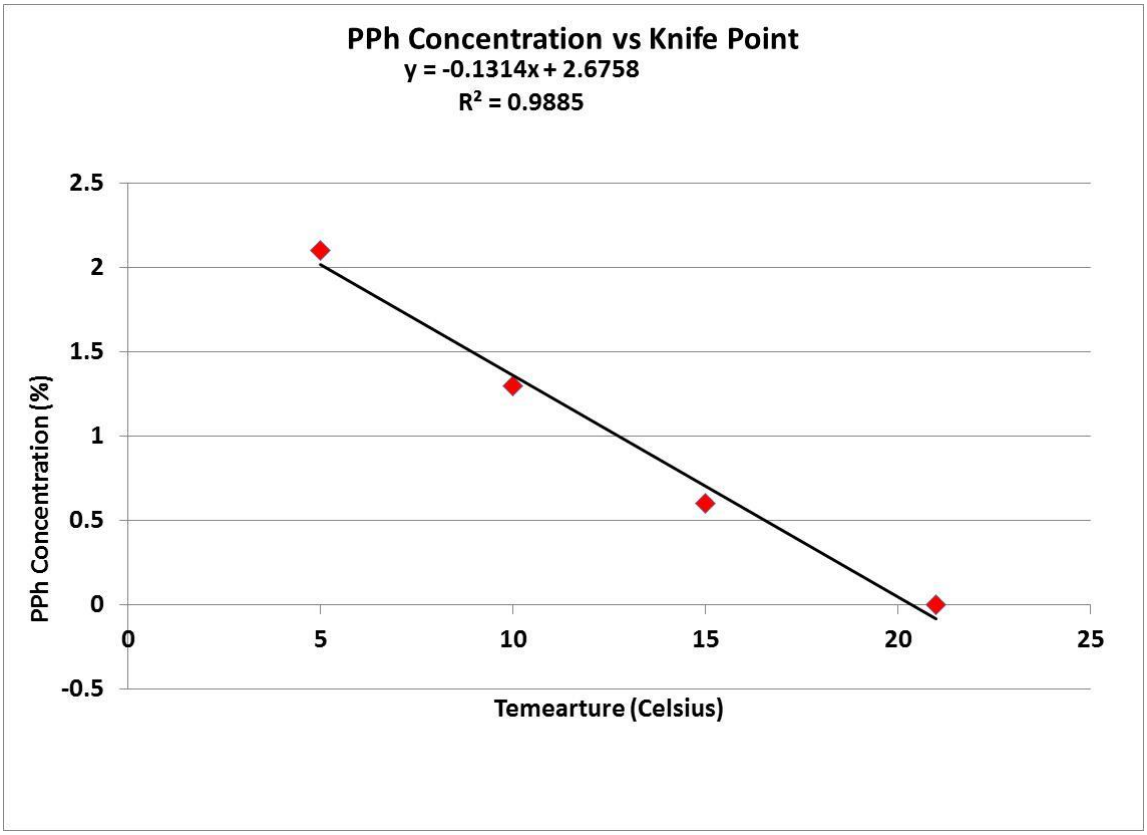

Figure 27. MFFT of Polymer E with PPh by Knifepoint.

Figure 28 shows the structure for polymer E, showing each monomer only once and identifying the molar concentration by letters.

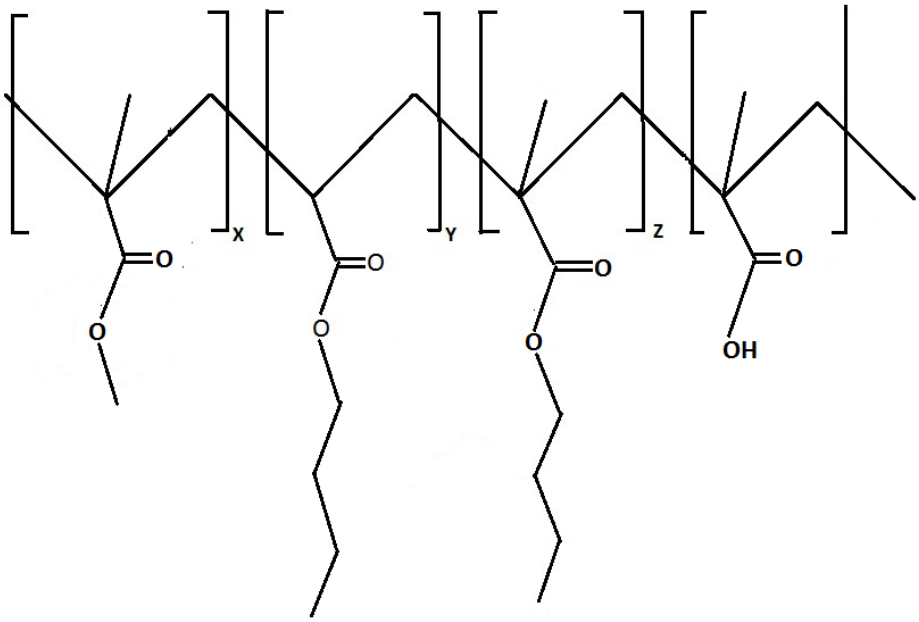

Figure 28. Representative Structure of Polymer E

Table 10 shows the optimal concentration of PPh to be added to each polymer to achieve optimal film formation at 283 K (10° C). Additionally, table 10 also shows the crack point and knife point of each polymer used in this research.

Table 9

MFFT Data for Polymers.

Polymer	**Crack Point (°C)**	**Knife Point (° C)**	**Optimal PPh Concentration (%)**
A	55	63	7.4
B	20	26	5.1
C	22	28	5.4
D	15	20	1.8
E	12	21	1.3

Table 9 (continued).

F	13	27	3.9
H	-12	-4	0.1 (none)
I	-2	4	0.1 (none)
J	30	33	6.7
L	-6	5	0.1 (none)

The following Figures, 29 – 37, show the representative structure of each polymer as determined by the same techniques used to determine the structure for polymer E.

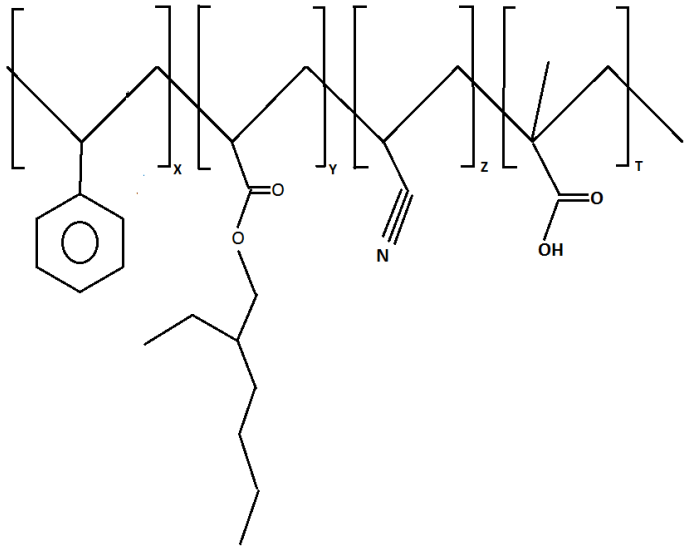

Figure 29. Relative Structure of Polymer A.

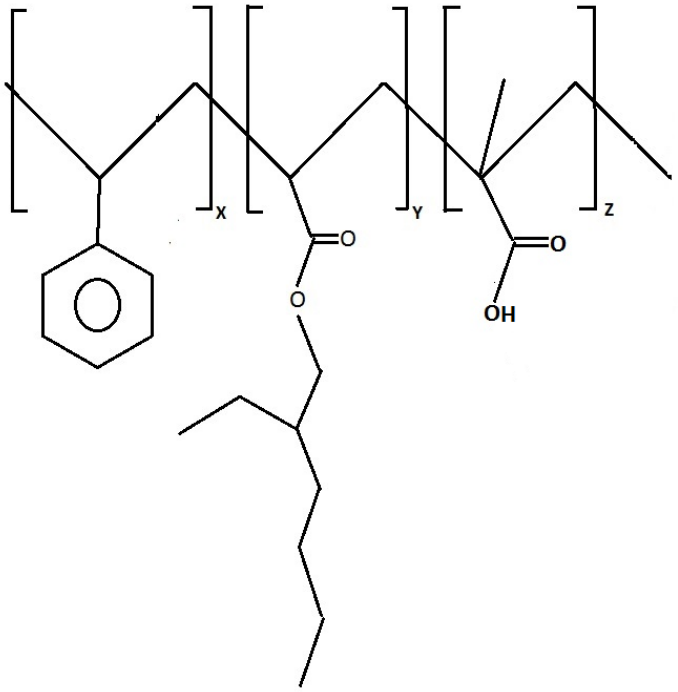

Figure 30. Relative Structure of Polymer B.

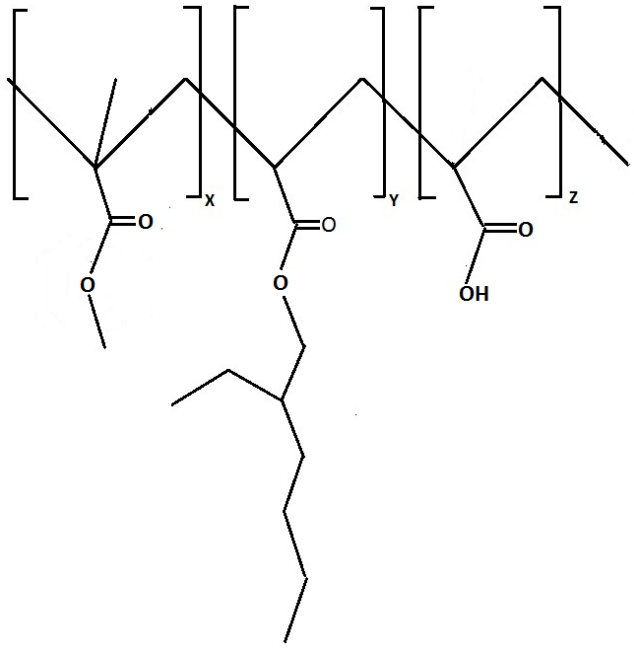

Figure 31. Relative Structure of Polymer C.

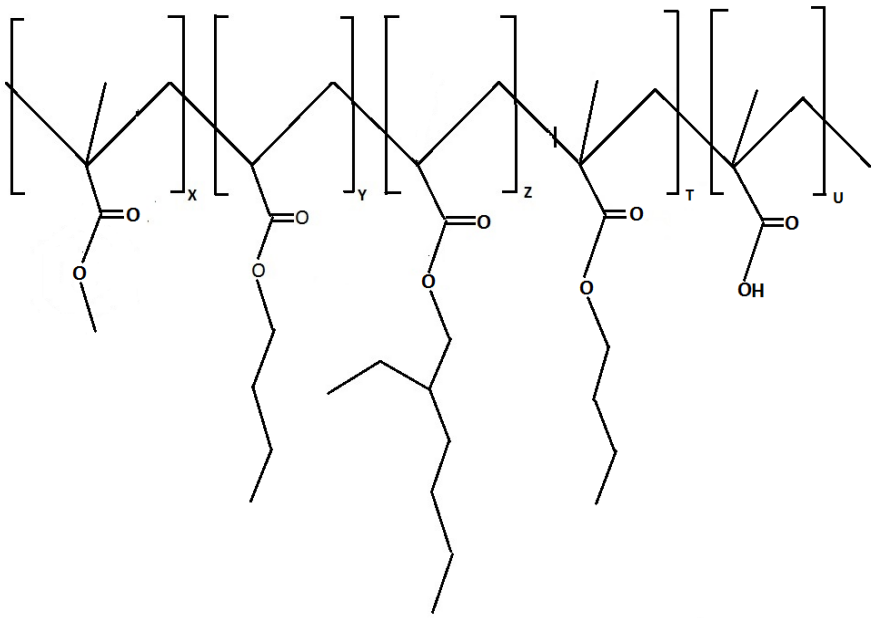

Figure 32. Relative Structure of Polymer D.

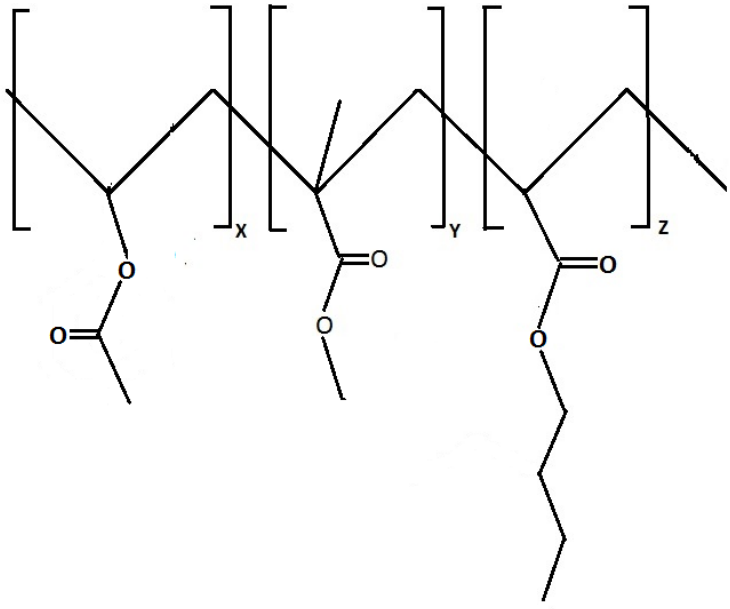

Figure 33. Relative Structure of Polymer F.

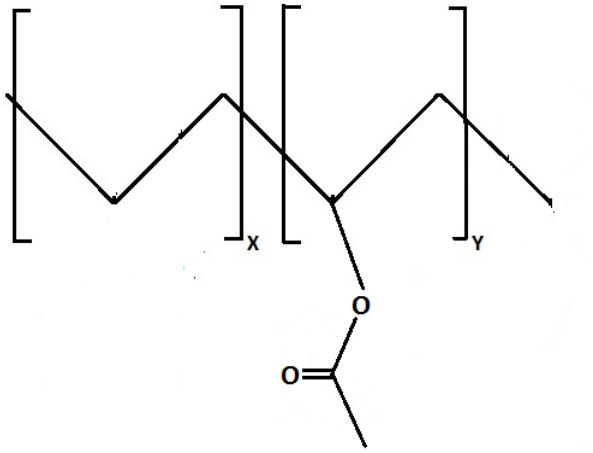

Figure 34. Relative Structure of Polymer H.

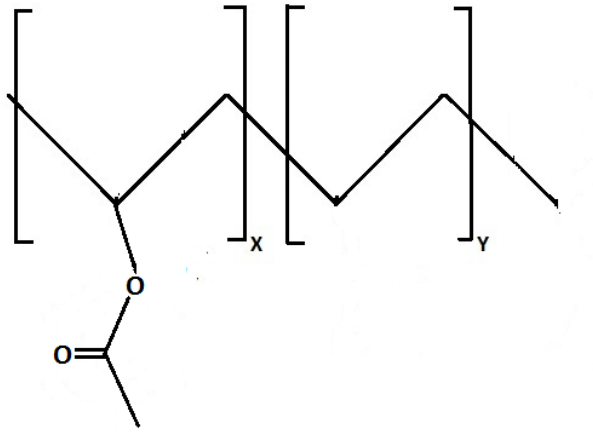

Figure 35. Relative Structure of Polymer I.

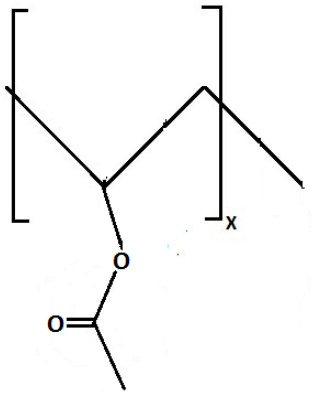

Figure 36. Relative Structure of Polymer J.

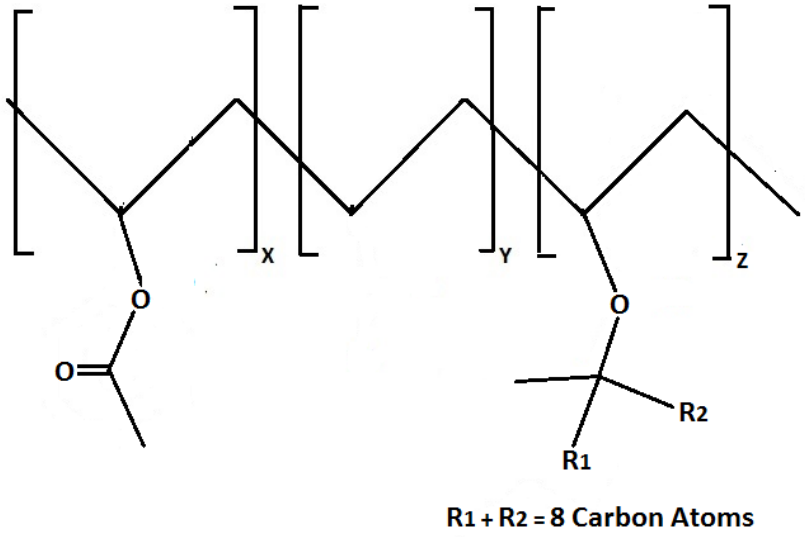

Figure 37. Relative Structure of Polymer L.

For brevity, the remainder of the data that was used to determine polymer structure (H^1-NMR, FT-ATR, DSC and TGA) as well as the charts showing the PPh concentration versus temperature for each of the polymers are listed in the Appendix.

Error Analysis of Test Methods

ASTM E 178-08[46] was used to determine if there were any outlier data points present by utilizing a Dixon calculation. Table 12 shows the data after these calculations

were performed. This table was derived from the original research published and presented at the 40th Annual Waterborne Symposium[7].

Table 10

Test Method Statistical Analysis Data Table

Property	**Mean**	**Standard Deviation**	**Min.**	**Max.**	**CoV**	**+/- Confidence Interval @ 99%**
Non-Volatile (weight %)	91.95	0.34	91.14	92.30	0.004	0.35
Non-Volatile (volume %)	92.34	0.74	91.00	93.52	0.008	0.76
Density (lbs./gal)	14.81	0.07	14.67	14.91	0.005	0.07
Lap Shear (MPa)	0.18	0.13	0.03	0.46	**0.722**	0.13
Tensile Strength (MPa)	0.68	0.43	0.26	1.34	**0.630**	0.44
Elongation (%)	3	2	0	7	**0.670**	2.06
Tensile Modulus (MPa)	4.84	4.95	0.02	11.84	**1.023**	5.09

Table 10 (continued).

Hardness (Shore D)	38.7	5.3	32	48	0.137	5.45
Volume Shrinkage (%)	7.7	0.1	7.5	8.0	0.013	0.10
Water Uptake (%)	6.75	0.33	6.26	7.14	0.049	0.34
Stain Repellency (out of 40)	4.4	1.2	2.5	7.0	**0.273**	1.23
Total Cracking (out of 10)	10.0	0.0	10.0	10.0	0.000	0.00
Ease-of-clean-up (out of 10)	4.6	0.5	3.0	6.0	0.112	0.51
Application (out of 10)	9.5	0.5	9.0	10.0	0.055	0.51

Assuming a coefficient of variation (CoV) below 0.15 would yield a statistically valid test method there are three test methods that appear to be questionable: Lap-shear adhesion, all components of tensile testing (Young's Modulus, UTS and Elongation) and Stain Repellency.

During the evaluation of lap-shear (CoV = 0.722) samples, it was noted many times that the adhesive bond was often stronger than the strength of the tiles. Slippage of the test specimens in the grips would further skew the data. The leads the author to the conclusion that this test method needs to be modified and further studied.

All components of the tensile test had large CoV values: UTS = 0.63, elongation = 0.67 and Modulus = 1.02. These values clearly show far too much variation with the test method. This test method could be improved by making thicker samples since many samples were broken upon loading into the grips of the test equipment.

Stain repellency testing had a CoV value of 0.273. While this value is higher than the acceptable 0.15, this test method is based upon subjective ratings of ten different summative components. Due to the nature of the subjective rating system the author believes this value is acceptable for gross differentiation between samples.

Even though the lap shear adhesion and tensile property test methods have questionable data, the values derived from them will still be used throughout the analysis, although the focus for these two test methods will be on gross differentiation only.

In the previous paper, the CoV were listed for all of the testing done. The adhesion and tensile data had questionable CoV's and as such were not discussed at length in the previous paper. Those test methods were re-visited and modified with the result of lowering the CoV's from an average of 76% to less than 15% each.

Taguchi DOE

Minitab 16 was used to derive a Taguchi Method DOE including 36 samples with replicates. A Taguchi Method was used to reduce the number of experiments thus allowing for as much information as possible to be extracted out of the smallest sample set possible. Cesarone likens the use of the Taguchi Method as a DOE designed by engineers for use by engineers, whereas standard DOE practices such as factorial analyses were designed by researchers for research use[47]. Additionally, Taguchi Method through the use of orthogonal arrays attempts to collect as much information about major

interaction effects, while mostly ignoring minor interaction effects[10]. Standard DOE without replicates would have called for 96 samples, nearly three times for the same by Taguchi including replicates.

Design of Experiment #1

A Taguchi Method DOE was utilized with the following parameters: high versus low T_g polymer, high versus low PVC, small versus large particle size, high versus low OA and fiber content (none, long and short). Table 26 shows the numeric inputs for the DOE from Minitab 16.

Table 11

Input Parameters for Taguchi DOE

Input Parameter	**1**	**2**	**3**
Polymer	T_g = 12°C	T_g = 40°C	NA
PVC	80% of CPVC	85% of CPVC	NA
Filler	PS = 6 micron OA = 8	PS = 6 micron OA = 11	PS = 21 micron OA = 6
Fiber	3 mm	6 mm	None used

It has previously been shown that RTU grout performance is controlled mainly by polymer, filler and fiber content and their respective interactions. Some properties such as surface hardness improve with harder polymers and higher filler content, whereas other properties such as elongation improve with softer polymers and lower filler content. The previous study was conducted using a Taguchi Doe focusing on the extremes of

polymer T_g and only one type of filler and fiber. The current research utilizes four polymers of varying T_g's, as well as multiple fillers and fibers. This paper will focus upon main effects of the RTU grout properties in an attempt to more specifically highlight the best practice formulation techniques.

Design of Experiment #2

A Taguchi Method DOE was utilized with the following parameters: polymer T_g, filler type (calcium based versus silicate based), high versus low PVC, small versus large particle size, high versus low OA and fiber type (Nylon, PE, cellulose or none). Table 27 shows the inputs for the DOE from Minitab 16. Sixteen samples were produced from this DOE.

Table 12

Input Parameters for Taguchi DOE

Input Parameter	**1**	**2**	**3**	**4**
Polymer T_g (°C)	12	17	33	61
PVC	80% of CPVC	85% of CPVC	NA	NA
Filler Type	Calcium	Silicate	NA	NA
Filler Particle Size	Low (min = 3.9 µm)	High (max = 21.0 µm)	NA	NA
Filler OA Value	Low (min = 6.9)	High (max = 29.0)	NA	NA
Fiber	PE	Nylon	Cellulose	None

The key here to the DOE's for the Taguchi Method is that they focus on main effects by allowing the user to input experimental parameters based upon existing knowledge, as opposed to testing each conceivable permutation, of which many results may be either useless and/or misleading.

CHAPTER III - PERFORMANCE VERSUS POLYMER T_g (K)

Prior to any discussion about the specific performance of any material in the formulation, in this case the polymer, a general discussion about the total formulation and the impact that each specific raw material could have upon the final performance.

Grouts were formulated to be as close to the Critical Pigment Volume Concentration (CPVC) as they could be in an effort to maximize performance properties. Patton shows that tensile strength and adhesive strength both increase with PVC and reach a maximum at CPVC[48]. Sudduth showed that maximum tensile strength is achieved at CPVC[49]. Toussaint et.al. showed that as PVC increased there is a dramatic increase in tensile strength, and the stress-strain relationship changed from an elastomeric to a brittle material as PVC approached the CPVC[50]. The basic premise for increase in tensile and adhesive properties (tested under tension) reflect the fact that as a crack propagates through a material energy is dissipated upon coming into contact with filler particles. The greater the number of filler particles, the greater is the energy that is dissipated, thus with increasing PVC, more energy is required to propagate cracks to failure by either tensile break or disruption of adhesive and/or cohesive forces.

Since PVC and CPVC are so critical it is important to know how to estimate and calculate these values theoretically. PVC is expressed as the ratio of volume of filler and pigment materials to the volume of pigment, filler and non-volatile binder (Equation 2):

$$\text{PVC (\%)} = \frac{100 \times (\text{volume of pigment + filler})}{(\text{volume of pigment + filler + non-volatile binder})} \qquad \text{Equation 2}$$

CPVC is estimated by utilizing Equation 3[51], which relies upon oil absorption (OA) values. OA values are derived by determining how much linseed oil is required to just wet the filler or pigment particles. Equation 3 gives the CPVC that a particular system can achieve with some assumptions; the OA values for each filler are an average for that filler given variations in particle size and particle size distribution, ideal packing behavior and similar binding capacity of the system in question being comparable to linseed oil.

$$\text{CPVC (\%)} = \frac{100}{1 + \frac{\rho_P \times OA}{100 \times \rho_L}} \qquad \text{Equation 3}$$

Where:

ρ_P = density of pigment or filler

OA = oil absorption value of pigment or filler

ρ_L = density of linseed oil (0.935)

Equation 3 works for a single pigment or filler. To accommodate multiple fillers, each filler's theoretical CPVC value was calculated and then multiplied by its volume percentage in the filler until the total filler volume as a percentage equaled the total CPVC. Table 16 below shows the results of these calculations.

The volume percentages were chosen based upon estimations of optimal packing density using the particle sizes of fillers and assuming complete space filling. While precise space filling is not possible, these numbers do offer the best available option for optimal filling.

Table 13

CPVC Contribution of Fillers.

Filler	Theoretical CPVC (%)	Filler Volume (%)	Contribution to Total CPVC (%)
Snowhite 21 PT	84.2	85	71.6
Omyacarb 6 PT	75.8	2	1.5
Minex 3	58.9	13	7.6
	Total	100	80.7

Other raw materials used in the grout, such as dispersant, defoamers, and thickeners could potentially affect many performance properties. However, since all of them with the exception of the coalescing solvent and polymer were used in the exact same concentrations, it was assumed that any performance parameters that are affected by these raw materials will be similar across all formulations.

The same coalescing solvent was used in each formulation and was incorporated based upon the amount needed to form a film at 50 °F (10 °C or 283 K), as the polymers were tested using an MFFT-bar. Since the coalescing solvent is used in relatively small concentrations varying from 0.5 to 3.5% by volume, and most of the coalescing solvent will have evaporated by the time the grout was tested, the effect of the coalescing solvent will be negligible to the final properties.

The remaining raw material that would have a prime effect upon the grout performance is the polymer. The main focus of this research is to determine which properties are affected by either polymer T_g, HSP or both.

For most applications, polymers are typically chosen first by the T_g. In general if one wants a hard, tough material a polymer with a high T_g will be chosen. Conversely if one wanted a material to have flexibility or ductile properties a polymer with a lower T_g will be chosen.

Ten polymers were evaluated in this study with the first focus of performance evaluation being polymer T_g. While these polymers may not be exhaustive of chain-growth, vinyl polymers, it is believed this group of polymers is representative of the current state-of-the-art for RTU grout formulation. Table 17 lists the polymer sample designation with the T_g (K) as determined by DSC.

Table 14

Polymer T_g's Used in this Research.

Sample	**T_g (K)**
A	336
B	312
C	313
D	290
E	283
F	296
H	267
I	274
J	309
L	273

There are more numerous studies than is practical to list here referencing performance parameters by T_g. Many of these studies focus upon a very few number of similar polymers with varying ranges (typically small) of T_g. Innumerable polymer

textbooks listing general performance characteristics as a function of T_g, mainly describing harder, brittle, less ductile materials having higher T_g's with more softer, flexible and more ductile materials having lower T_g's. Relevant references relating performance to specific T_g will be discussed as each performance parameter is discussed.

At the beginning of this research, it was thought that polymer T_g would be a good performance predictor for most RTU grout performance properties. It was further hypothesized that polymer T_g would play a crucial role in prediction of physical performance such as tensile strength, flexural strength, and elongation, while HSP may be a more appropriate predicator of stain repellency performance and hydrophobic properties such as water absorption.

Some specific polymer performance issues that should be discussed, however, are side chain effects. The discussion will focus only on side chain effects since all of the polymers used in this study have a C – C backbone. Some are di-substituted as in the case of the methacrylates, while the remainder are mono-substituted.

Obviously any polymer with a di-substituted backbone carbon atom will have less mobility, leading to stiffness and allowing for stress concentrations that could cause brittle failure, low elongation, and potentially lower tensile strengths and adhesive strength. However, depending upon how the strain or force is applied this same stiffness could yield higher compressive strength properties. Conversely, materials with mono-substitution, could have more reptation, thus allowing for dispersal of stress concentrations, higher tensile strengths and adhesive strength, and increased elongation, but could also result in lower yield strengths, leading to lower compressive strength properties.

The length and bulkiness of the side chains themselves will also lead to performance differences. Longer and bulkier the side chain greater is the separation between chains in most cases and can lead to more reptation, but this could be off-set if the side chains are of sufficient length to cause inter chain entanglements. Additionally, polar side groups can increase hydrogen bonding while other groups can lead to increased Van der Waals forces, which could lead to semi-crystalline behaviors or zones, and reduce reptation. Overall, anything that leads to stiffness can increase bulk modulus properties while decreasing ductile properties, and anything that reduces stiffness could decrease bulk modulus properties while increasing ductile properties.

Side-chains could also impact water-absorption and stain repellency. Longer, more hydrophobic groups with less affinity for water should have lower water absorption properties, as well as less affinity for water-based stains such as ketchup, mustard or coffee. This could be off-set by polar groups, which could increase water sensitivity, and increase water absorption and staining by water-based stains.

Longer chain lengths promote higher affinity for organic materials. As they become more hydrophobic, they should become more oleophilic, and thus be more prone to staining with oil based stains such as vegetable oils.

Table 18 lists the correlation coefficients of each evaluated property as a function of T_g (K). Correlation coefficients range from -1.00 to 1.00, with either extreme indicating a perfect correlation. Negative values indicate an inverse relationship whereas positive values indicate a direct relationship between the variables. Any values between -0.90 and -1.00 on the negative side and values between 0.90 and 1.00 on the positive indicate good correlation. Only dry elongation and dry flexural strength exhibit good

correlation with T_g (K). Dry elongation having a negative correlation coefficient (-0.915) indicates elongation decreases with increasing T_g (K). This is expected since polymers that have high T_g's exhibit greatly reduced molecular motion when evaluated at room temperature and as such are very rigid. On the other hand, polymers with low T_g's, especially below the evaluation temperature, will have much more molecular mobility allowing for orientation of polymer chains during applied stress.

Table 19 shows all the correlation coefficients calculated for the polymer T_g and performance testing done using the data for this study. The following relationship describes how these numbers are used for data analysis[47]:

-1.00 = Perfect negative correlation – as one value increases the other decreases

-0.99 to -0.90 = Fairly strong negative correlation

-0.89 to -0.70 = Moderate negative correlation

-0.69 to -0.21 = No correlation

-0.20 to 0.20 = Random, with 0.000 being completely random

0.21 to 0.69 = No correlation

0.70 to 0.89 = Moderate positive correlation

0.90 to 0.99 = Fairly strong positive correlation

1.00 = Perfect positive correlation – as one value increases the other increases

Both dry and wet UTS, dry Young's Modulus and dry and wet Durometer hardness all show some correlation to T_g (K). However, these values are not nearly as strong as those of dry elongation and dry flexural strength. In fact, another method of determining correlations is through the use of R-squared values (square of correlation coefficients). Correlation coefficients less than -0.9 or 0.9 have R-squared values < 0.8,

which can be considered somewhat nebulous. This is part of the reason for the totality of this project, specifically to explore other polymer parameters that can explain and possibly predict formulated physical performance.

Table 15

Correlation Coefficients for Polymer T_g Study

Property	1	2	3	4	5	6	7	8	9	10	11	12	13	14
1 = Tg (K)	1.00													
2 = UTS	0.70	1.00												
3 = Elongation	-0.92	-0.78	1.00											
4 = Youngs Modulus	0.76	0.96	-0.86	1.00										
5 = Dry Durometer	0.83	0.95	-0.82	0.91	1.00									
6 = Wet Durometer	0.79	0.72	-0.73	0.70	0.78	1.00								
7 = Water Absorption	-0.54	-0.79	0.63	-0.75	-0.81	-0.47	1.00							
8 = Dry Adhesion	0.61	0.86	-0.72	0.88	0.84	0.72	-0.69	1.00						
9 = Wet Adhesion	-0.02	0.32	-0.16	0.41	0.25	0.13	-0.46	0.64	1.00					
10 = Total Stain Repellency	0.09	-0.23	0.12	-0.28	-0.16	0.40	0.50	-0.21	-0.49	1.00				
11 = Oil Stain Repellency	0.60	0.30	-0.55	0.37	0.35	0.79	-0.21	0.36	0.09	0.55	1.00			
12 = Water Stain Repellency	-0.28	-0.47	0.50	-0.58	-0.42	-0.03	0.74	-0.49	-0.65	0.84	0.01	1.00		
13 = Flexural Strength	0.91	0.87	-0.86	0.86	0.96	0.85	-0.73	0.77	0.17	0.02	0.53	-0.33	1.00	
14 = Shrinkage	-0.62	-0.61	0.77	-0.66	-0.63	-0.54	0.73	-0.59	-0.27	0.33	-0.41	0.66	-0.58	1.00

Correlation coefficients close to 0.00 are defined as a complete lack of correlation. Both wet adhesion and total stain repellency exhibit a near lack of correlation with T_g (K). Lack of correlation between T_g (K) and total stain repellency makes sense if only using the correlation table. Note that while neither oil-based nor water-based stain repellency shows good correlation with T_g, they do have opposite signs indicated that the general movement of the data is in opposite directions. This movement in opposite directions could explain the complete lack of correlation between total stain repellency and T_g.

Table 16

Correlation Coefficients with T_g (K).

Property	Correlation Coefficient
Dry Elongation	**-0.915**
Wet Elongation	-0.622
Dry Ultimate Tensile Strength	**0.701**
Wet Ultimate Tensile Strength	**0.725**
Dry Young's Modulus	**0.755**
Dry Durometer	**0.831**
Wet Durometer	**0.794**
Dry Adhesion	0.605
Wet Adhesion	**-0.020**
Dry Flexural Strength	**0.914**
Shrinkage	-0.617
Water-based Stain Repellency	-0.276
Oil-based Stain Repellency	0.596
Total Stain Repellency	**0.094**
Water Absorption	-0.536

The following 12 Figures are box plots of various performance properties plotted against the polymer T_g. These graphs reinforce the correlation coefficient data in Table 18 and are summarized for clarity in Table 19. With the exception of the polymer with a T_g of 290 K, all polymers having T_g's < 300 K exhibited tensile strengths < 700 psi tensile strength, while polymers with T_g's > 300 K were characterized by tensile strengths > 1000 psi (Figure 38). The lone exception, i.e., the polymer with a T_g of 290 K appears to be an outlier to these two disparately performing groups of polymers that is until the monomer composition is taken into account. This polymer is unique among the entire test set in that it has a near one-to-one balance of short and long chain pendant group monomers. The fact that this polymer has an unusually high tensile strength than would be expected from its T_g is another reason why Hansen Solubility Parameters were considered important.

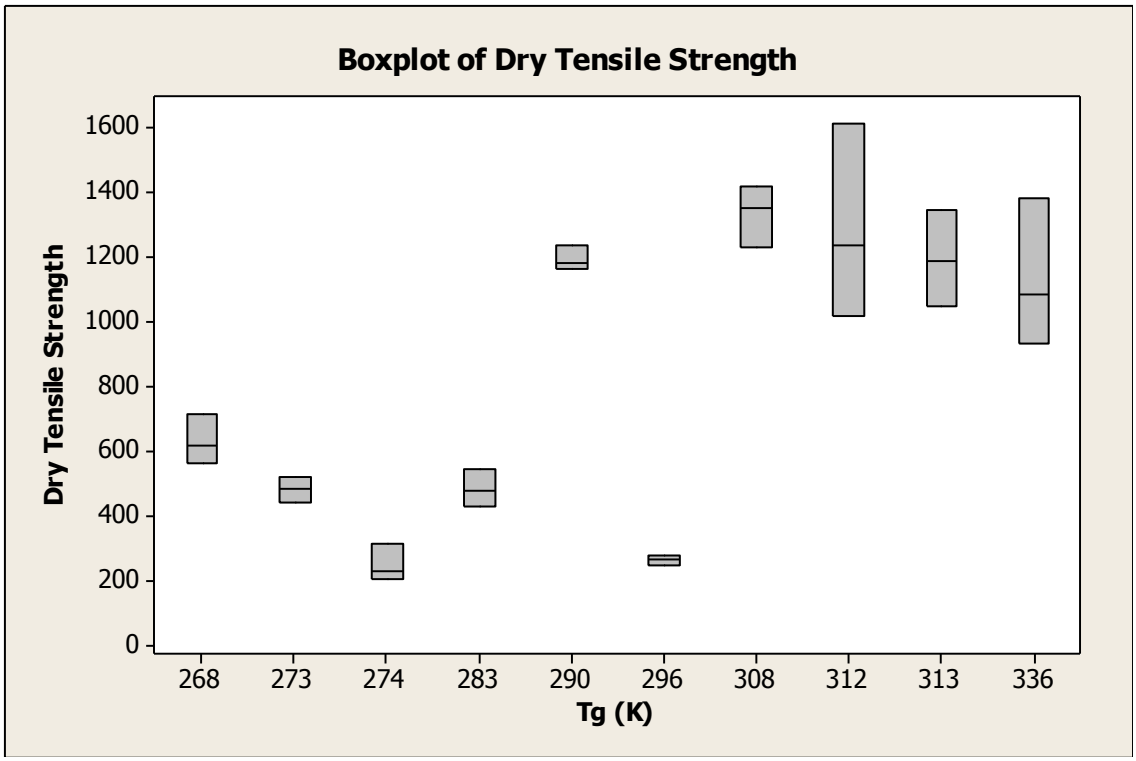

Figure 38. Boxplot of Dry Tensile Strength versus T_g(K)

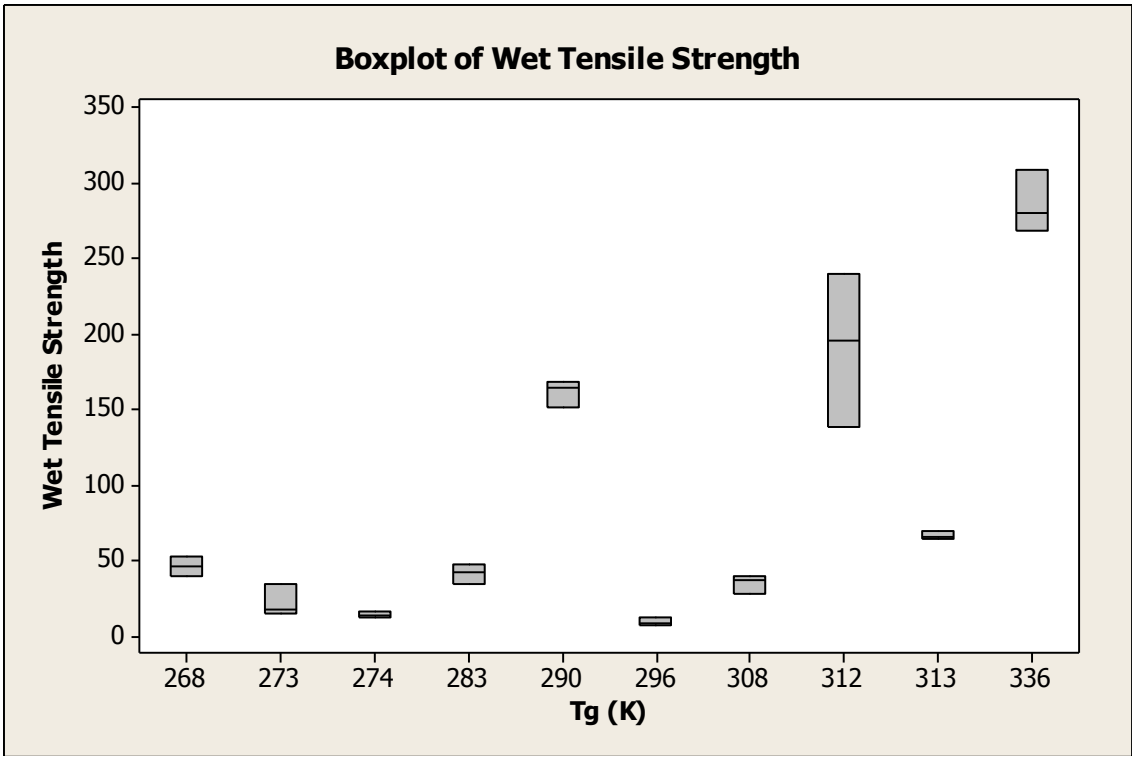

Figure 39. Boxplot of Wet Tensile Strength versus T_g(K)

The wet tensile strength of grout is far weaker, averaging a little more than only 9% of dry tensile strength. Most polymers (as tested in the grout), regardless of T_g, exhibit wet tensile strengths of less than 100 psi. This indicates that with the 24 hour water soaking step prior to tensile testing had a significant plasticizing effect. Three polymers exhibited tensile strengths > 150 psi, although they are far weaker as well. Again, the polymer with the more even balance of long and short chain pendant groups was one of the better performing polymers with respect to wet tensile strength.

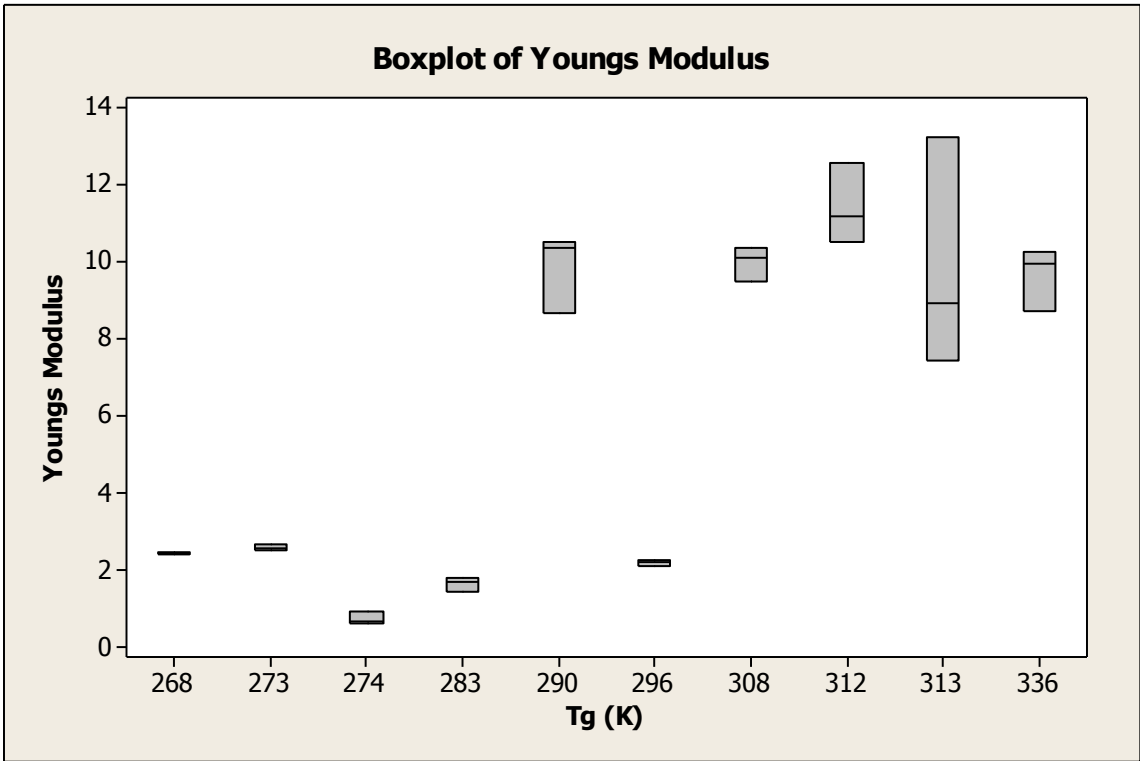

Figure 40. Boxplot of Young's modulus versus T_g (K)

The Young's modulus (dry), a measure of the grout stiffness upon tensile loading, behaved similar to dry tensile strength, with the grout containing polymer D (T_g = 290 K) showing better than predicted performance based upon T_g (Figure 40). The correlation coefficient shows some measure of correlation that as T_g increases, so does Young's Modulus. Curtzwiler et al.[52] noted a correlation between T_g and Young's modulus for a

broad range of polymers correlation coefficient > 0.9. The lower correlation coefficient noted here could be due to the increased sensitivity with greater number of similar polymers evaluated over a much narrower range.

Figures 41 and 42 show the dry and wet elongation properties as tested in tension loading. Overall, the wet elongation was > 375% greater than the dry elongation, with all wet elongation being at least 130% longer.

Dry elongation had a correlation coefficient of -0.915, indicating a good correlation between decreasing elongation with increasing polymer T_g. The correlation coefficient of -0.622 suggests a lack of correlation between wet elongation and T_g. The two polymers with the lowest T_g's have much lower than expected wet elongation values as a function of T_g as evidenced by the samples at the left on each graph of elongation versus T_g. Given that these two polymers are ethylene/vinyl acetate (EVA) co-polymers, the much reduced elongation could be a result of hydrolysis and deterioration of the polymer backbone forming free acetic acid and polyvinyl alcohol structures on the polymer backbone[53]. This makes the polymer more hydrophilic, resulting in reduced strength, and increased elongation.

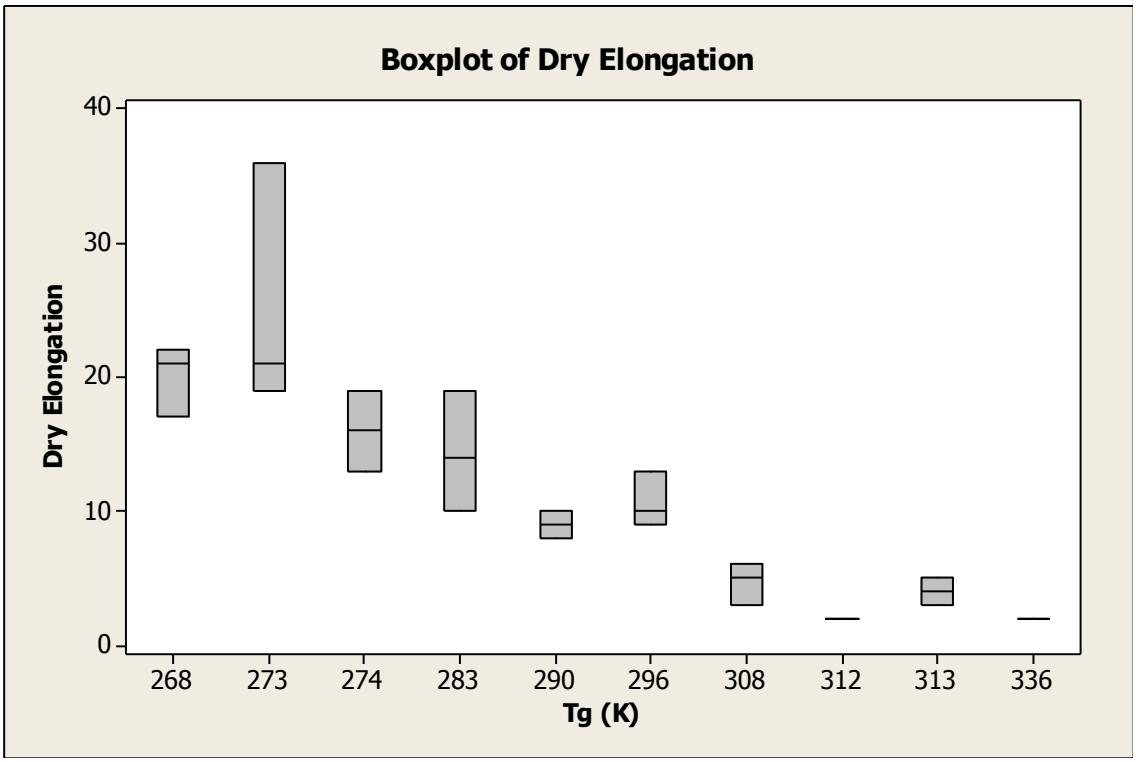

Figure 41. Boxplot of Dry Elongation versus T_g (K)

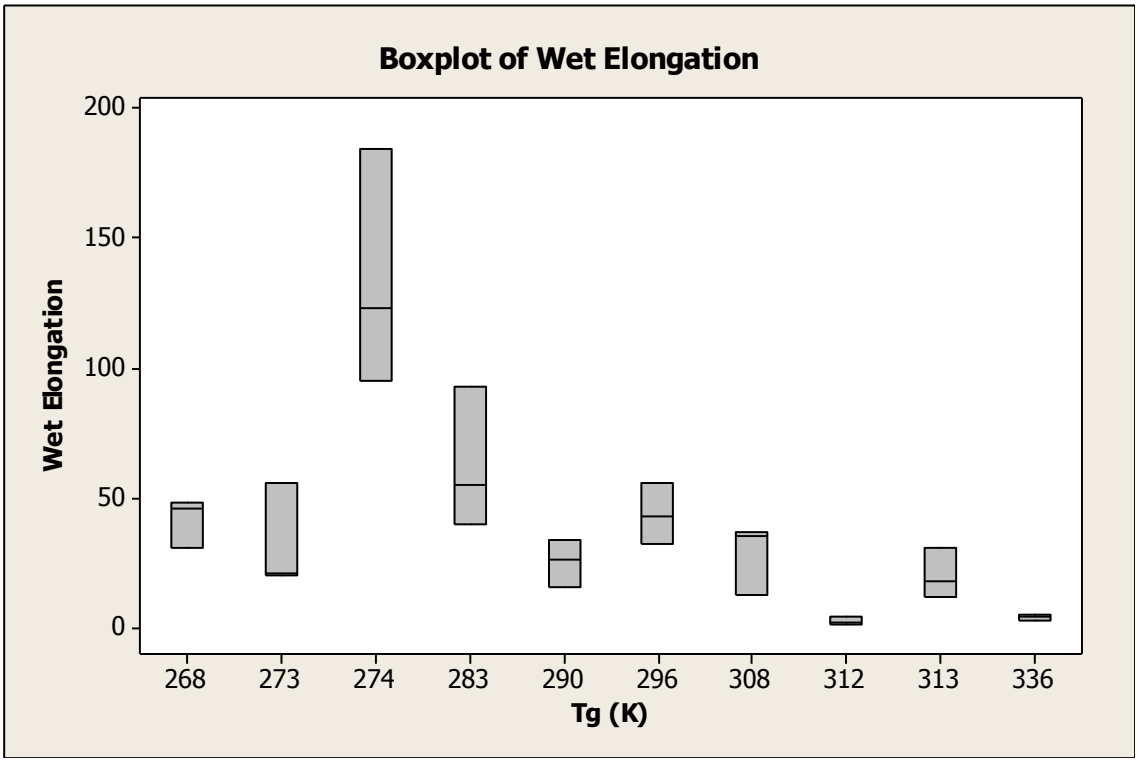

Figure 42. Boxplot of Wet Elongation versus T_g (K)

A strong, positive, correlation (0.914) was observed between flexural strength (dry tested) and polymer T_g. This is in agreement with the results reported by Kim et.al.,[54] where flexural strength was evaluated at different curing ages. Although Kim's work was with polymer modified cement mortars, the relationship is still clear that as T_g increases so does flexural strength.

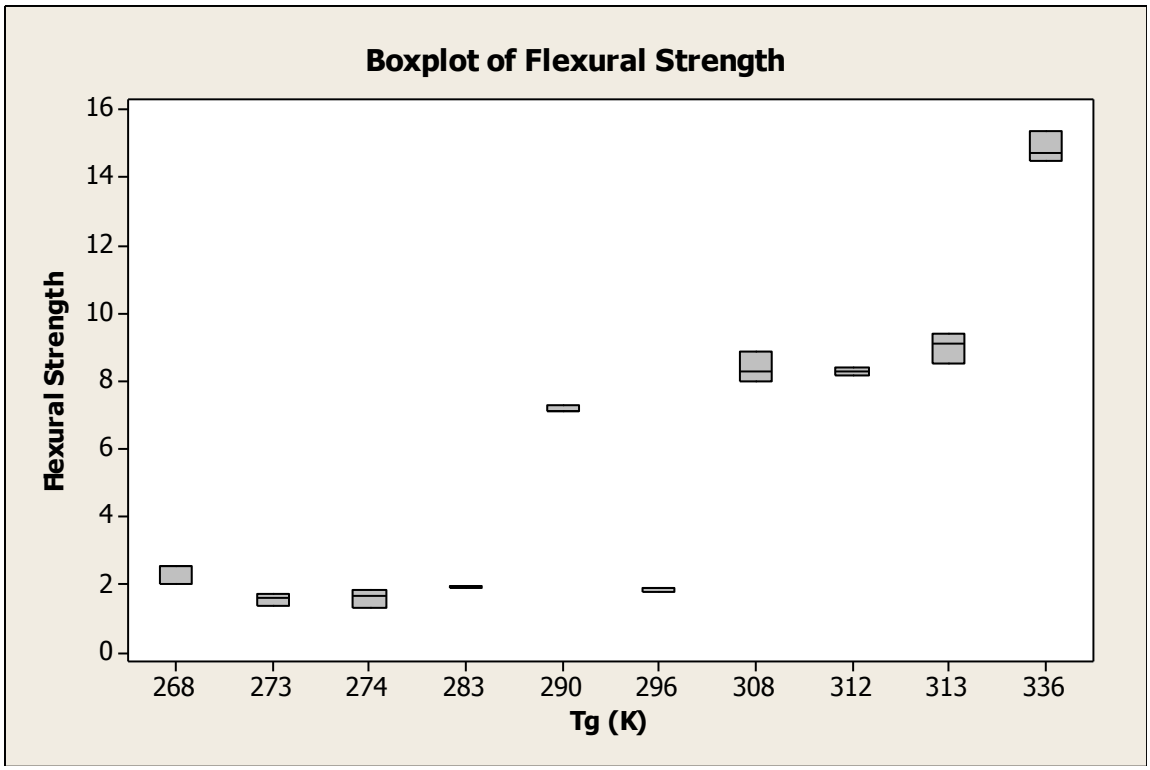

Figure 43. Boxplot of Flexural Strength (Dry) versus T_g (K)

Both dry and wet surface hardness (Shore D Durometer) show good correlation versus T_g, with values of 0.831 and 0.794 respectively. This indicates some correlation between hardness and T_g, which is expected. Figures 44 and 45 show that Polymer D is a potential outlier for correlation with between hardness and T_g both dry and wet.

For wet surface hardness, the roughly even concentration of long versus short chain groups could explain the relatively higher wet hardness. However, the pendant chain-group-length concentration does not explain the relative higher dry hardness.

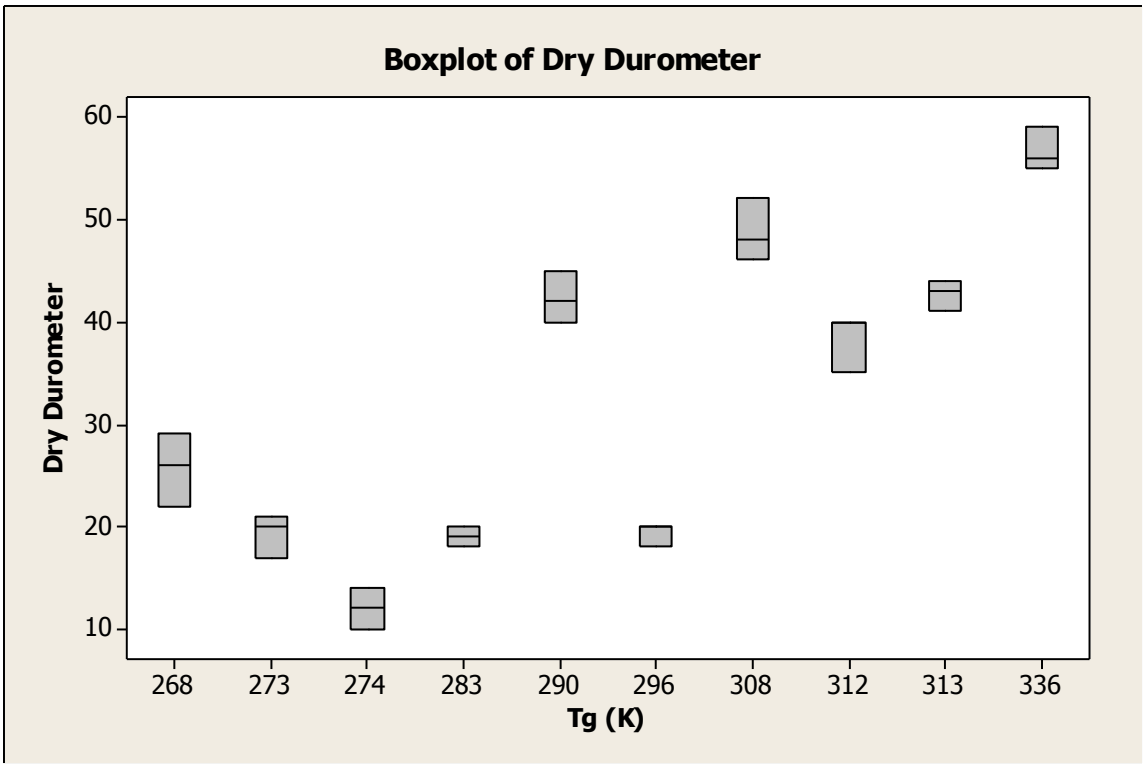

Figure 44. Dry Surface Hardness (Shore D Durometer) versus T_g (K)

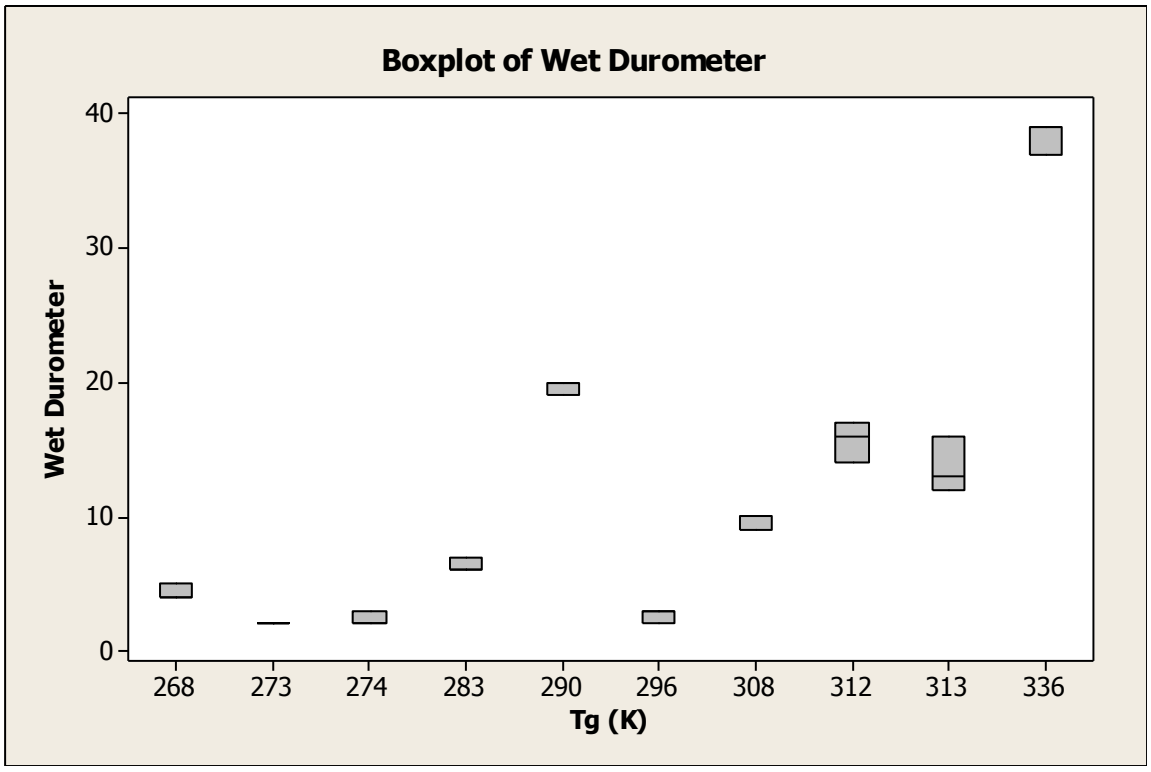

Figure 45. Wet Surface Hardness (Shore D Durometer) versus T_g (K)

Water absorption (correlation coefficient -0.536, Figure 46) did not exhibit good correlation with polymer T_g. While two of the worst performing (highest water absorption) polymers had very low T_g's, the polymer with the lowest T_g was one of the better performing polymers.

The best performing samples were A and D. Sample A comprises mostly of aromatic monomer (styrene), and sample D had the near one-to-one balance of long and short chain monomer pendant groups as reported earlier. This highlights the need to explore other polymer variables besides T_g for performance correlation, especially with respect to water-absorption.

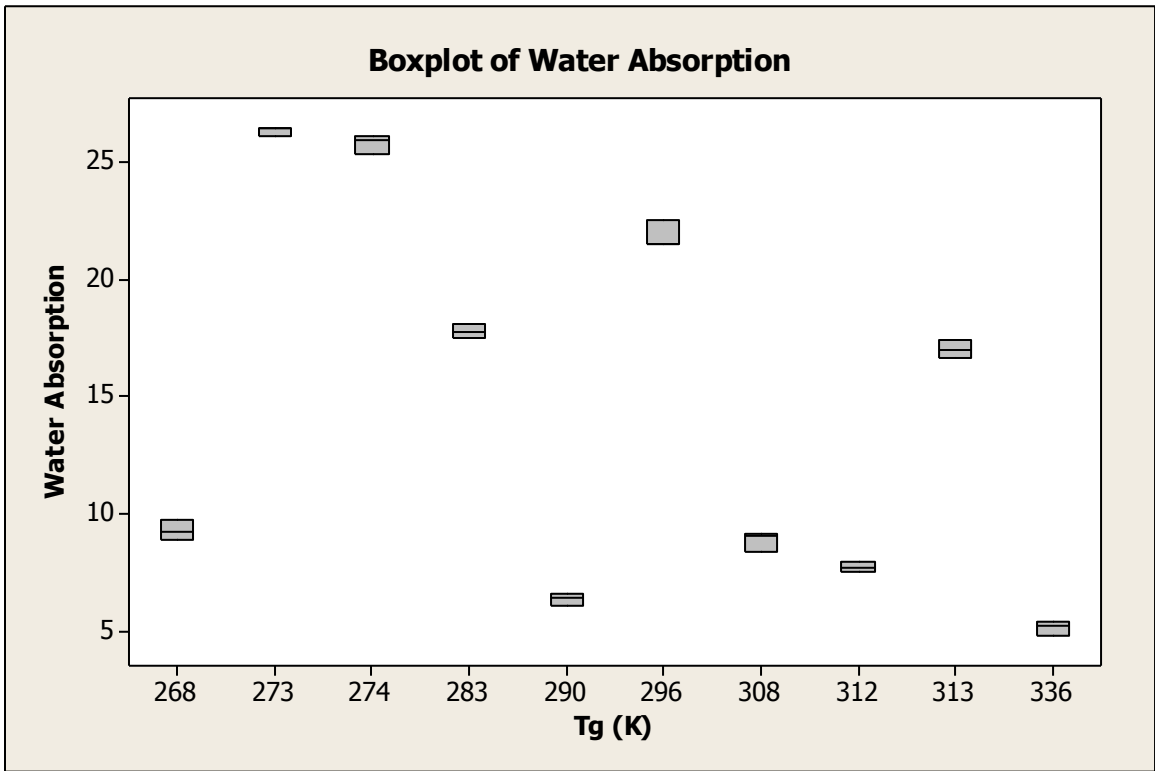

Figure 46. Water-absorption versus T_g (K)

Curtzwiler et al.[52] noted a direct correlation between modulus and polymer T_g. Lower modulus materials have more mobility, thus the adhesion is more dynamic, which often leads to weaker adhesion. This research shows a correlation between Young's modulus and dry adhesion (correlation coefficient 0.875). Toledo et al.[55] reported a correlation between T_g and adhesion (dry) and this research also found that adhesion improves as the testing (service) temperature decreased below the polymer T_g.

There does not appear to be a correlation between adhesion and T_g (correlation coefficient 0.605). However, if sample D was excluded from the evaluation, the correlation coefficient increased to 0.892, suggesting a good correlation between dry adhesion and T_g. The removal of sample D did not affect the correlation of wet adhesion to T_g. Sample D, with a balance of long and short chain monomer pendant groups has the best adhesion regardless of wet or dry testing (Figures 47 and 48). Wet adhesion

performance is on average only about 17% of the dry adhesion performance indicating a lot of plasticization by water for each sample, which reduced the adhesion significantly in most cases. Sample D maintained the highest amount of wet adhesive strength compared to dry (31%).

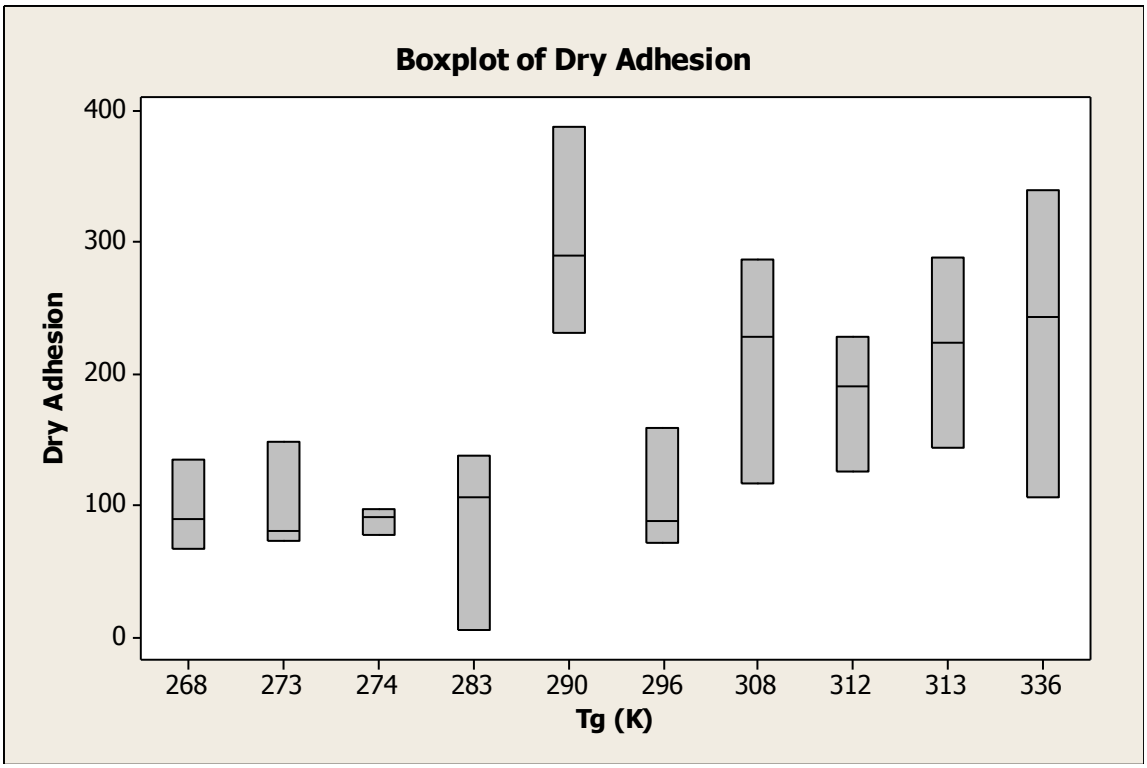

Figure 47. Dry adhesion versus T_g (K).

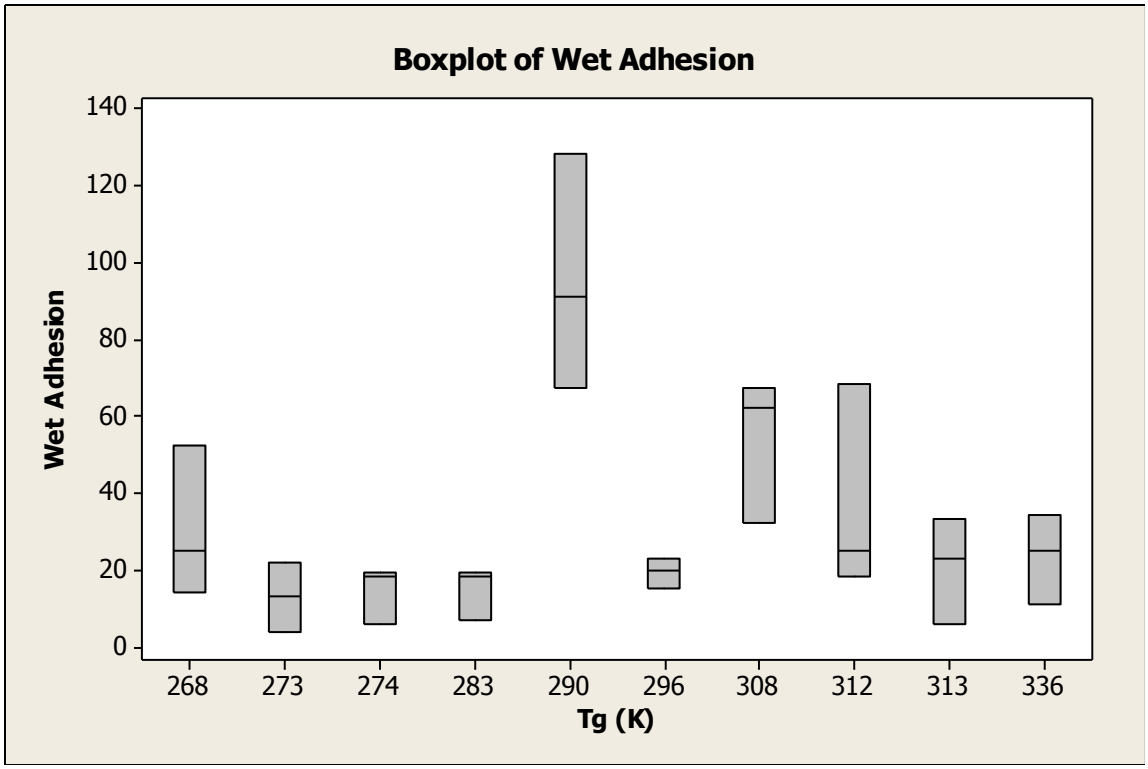

Figure 48. Wet Adhesion versus T_g (K).

An earlier study had shown a direct correlation between shrinkage and cracking, i.e., more shrinkage was associated with more cracking[7]. These samples did not show any appreciable cracking since these formulations were optimized against cracking.

Figure 49 shows the lack of correlation between shrinkage and T_g (correlation coefficient -0.617). Most samples exhibited about 8% shrinkage, except samples I and L (T_g's at 274 and 273 K respectively). The average shrinkage was about 5% if these two samples were removed.

Correlation coefficients for stain repellency were 0.596 and 0.296 for oil-based stains and water based stains respectively. The overall correlation coefficient for stain repellency (oil and water based stain repellency combined) was 0.094.

The positive, albeit weak, correlation coefficient suggests some polymer hardness may be beneficial in helping repel oil based stains. The fact that the polymers with the best oil-based stain repellency also have the highest content of either long chain or aromatic pendant monomer groups gives more credence to evaluating stain repellency as a function of solubility parameters.

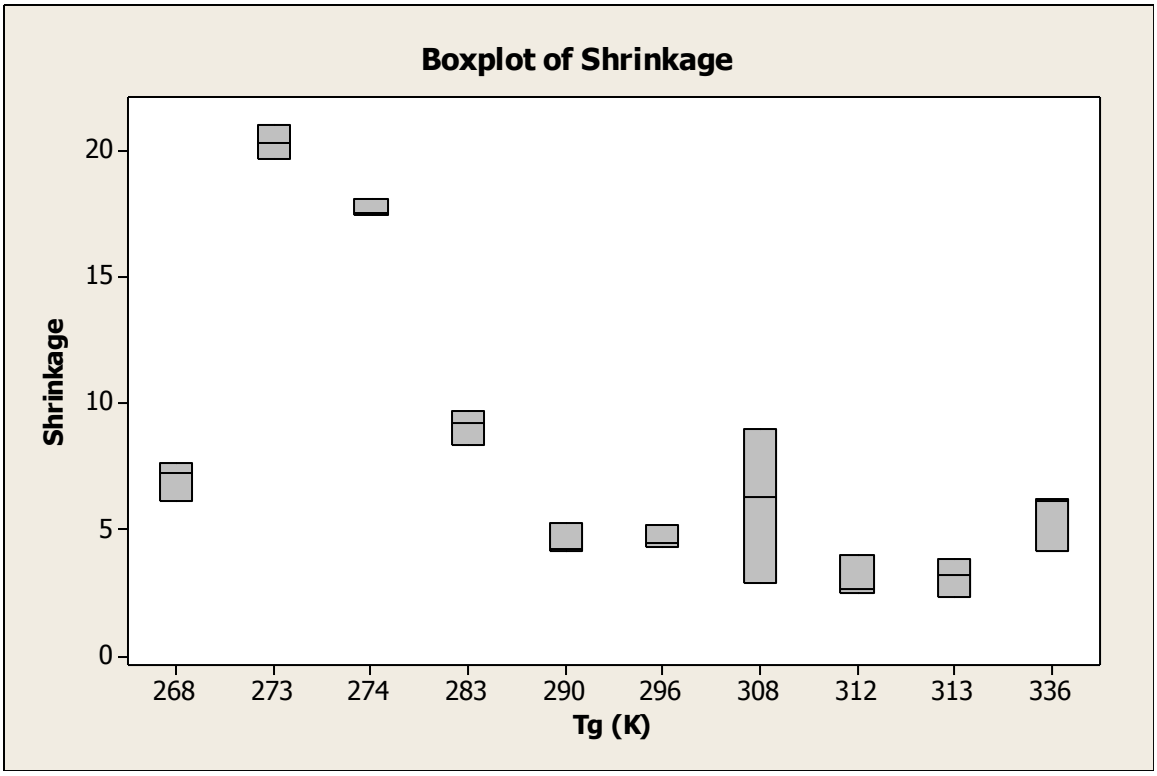

Figure 49. Boxplot of Shrinkage versus T_g (K)

Water-based stain repellency did not correlate with T_g, but the negative correlation coefficient suggests that softer polymers may be better for water-stain repellency. Most soft polymers have higher concentrations of short chain monomer pendant groups further highlighting the need to evaluate stain repellency as a function of solubility parameters.

It is interesting to note that the broad type of stain repellency (oil versus water) appear to be affected by opposite types of monomer composition. This is highlighted by

the fact that the overall correlation coefficient for stain repellency was 0.094 suggesting a near lack of correlation.

One of the best performing samples for total stain repellency is Sample D, whose near 1:1 balance of short and long chain monomer pendant groups, appears to resist both water and oil based stains more effectively.

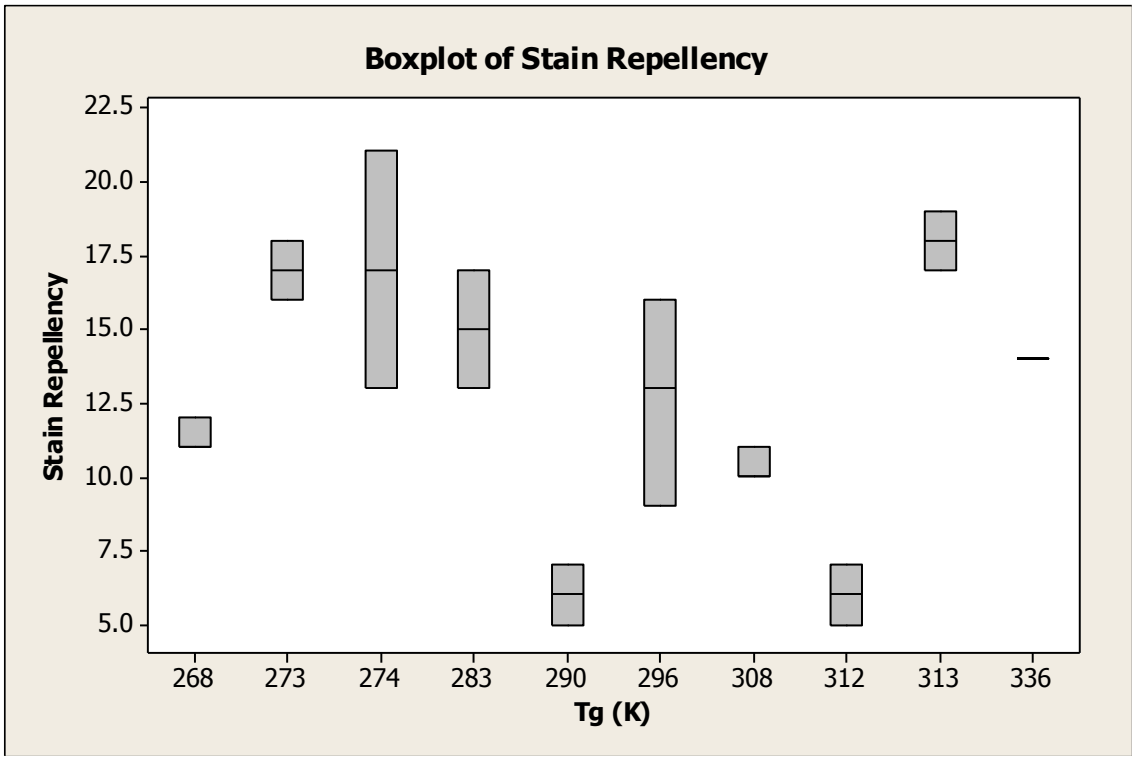

Figure 50. Stain Repellency versus T_g (K)

Correlations between each of the tested properties were also evaluated (Table 19). Correlation coefficients in blue are fairly strong, those in yellow are moderate, no color indicates no correlation and red indicates randomness. Four fairly strong correlation coefficients were noted (Table 20).

Table 17

Fairly Strong Correlations Between Performance Data

Property-to-Property Correlation	**Correlation Coefficient**
UTS – Young's Modulus	0.960
UTS – Surface Hardness (Dry – Durometer)	0.948
Young's Modulus – Surface Hardness (Dry – Durometer)	0.911
Flexural Strength – Surface Hardness (Dry – Durometer)	0.960

CHAPTER IV – HANSEN SOLUBILITY AND GROUP CONTRIBUTION THEORY

Hansen Solubility Parameters (HSP)

Adhesion theory shows that for any material to adhere to another, the Work of Adhesion (WA) equation must be satisfied. Equation 4 is the Dupre equation assuming the phases are separated by dry air, as is the case when adhering materials together such as stain materials (food items, etc.) to the surface of construction materials (i.e. grout).

$$WA = \Upsilon_A + \Upsilon_S - \Upsilon_{AS} \qquad \text{Equation 4}$$

Where:

Υ_A = surface free energy of adherend (stain item)

Υ_S = surface free energy of substrate (grout)\

Υ_{AS} = surface free energy of adherend-substrate interaction

A positive value for this equation indicates a stable system, i.e. good bonding of the stain item to the substrate (which is undesirable in this application). A negative value indicates instability, which leads to lack of adhesion (which is desirable in this case).

The WA is derived from solubility parameters. Even though no actual dissolution occurs there is a chemical interaction between the substrate and the adherend, which can be interpreted as a chemical affinity for or against solubility theory.

To further delve into solubility of materials onto substrates, a basic understanding of the concept of solubility must be derived. The basic concept of solubility that like dissolves like works well for small molecules. However, the size of polymers and the composition of household chemicals renders this principle useless. This is due in part to the fact that most polymers have fairly strong dispersion forces holding them together but have fairly weak polar and hydrogen bonding forces. Even polyvinyl chloride, which has

plenty of strongly polar bonds, is non-polar when compared to other polar compounds such as methyl chloride. Household items are even more complicated in that they are formulations that include inorganic and organic materials. As such, many scientists have attempted to develop mathematical expressions for polymer solubility based upon experimental evidence.

Starting with the basic solubility equation, the Gibb's Free Energy Equation:

$$\Delta G = \Delta H - T\Delta S \qquad \text{Equation 5}$$

Where:

ΔH = enthalpy

T = temperature

ΔS = entropy

For dissolution to occur ΔG must be negative. With very small molecules the entropy term is usually positive due to the chaotic nature of a mixture of small molecular components. However, the entropy term becomes much smaller, but still positive, with polymeric materials. This is due to the fact that there are fewer possible molecular arrangements to separate individual polymer chain from each other due to chain length (molecular weight) and entanglements. For dissolution to occur, the enthalpy must be smaller than the entropy term ($T\Delta S$), possibly negative, or at least very small positive.

Hildebrand developed an equation for the enthalpy of mixing of polymers and solvents:

$$\Delta H = \Phi_S \Phi_P (\delta_S - \delta_P)^2 \qquad \text{Equation 6}$$

Where:

Φ_S = volume fraction of solvent

Φ_P = volume fraction of polymer

δ_S = Cohesive Energy Density (CED) of solvent

δ_P = CED of polymer

These CED values are commonly referred to as solubility parameters. In most cases the solubility parameters are experimentally determined by the enthalpy (or heat) of vaporization. This technique does not work with polymers as their molecular weights prevent their vaporization. Using direct solubility experimentation, Hildebrand spent much of his career determining solubility parameters for solvents and solvent-polymer interactions.

Solubility is a function of solvent and solute interactions, specifically their intermolecular and intra-molecular forces. Hildebrand's solubility parameter is a single value that encompasses the dispersive, polar and hydrogen bonding molecular forces. His values work well for mainly aliphatic systems, but they are not as useful in systems with more polar or hydrogen bonding character. Certain estimates have been carried out to separate the component values. The first involved only the dipole moment (or polarity) and the overall dispersive forces. These two forces can be directly calculated or measured. The third parameter, hydrogen bonding, cannot be easily determined.

Charles Hansen, in his doctor dissertation in 1967[56], was one of the first to put forward a combined solubility parameter based upon the three component values.

$$\delta^2_T = \delta^2_D + \delta^2_P + \delta^2_H \qquad \text{Equation 7}$$

Where:

δ^2_T = Total Hansen Solubility Parameter

δ^2_D = Dispersion component of HSP

δ^2_P = Polar component of HSP

δ^2_H = Hydrogen bonding component of HSP

Hansen determines the solubility parameters of polymeric materials by attempting to dissolve them in a series (usually 30 or more) [57, 58] of solvents with known and varying solubility parameters and component parameter values. The solvents in which the polymeric material is soluble in (and the degree of solubility) helped determine the solubility parameters of the polymer. Typically, this was done by plotting the solvent solubility parameters into spherical coordinates using the three component values (dispersive, polar and hydrogen bonding) as the axes and marking the solvents that polymer is soluble in. The polymer solubility parameters were estimated (fairly closely) to be the center of the circle of compatible polymers.

Group Contribution Theory (GCT)

Charles Hansen may have developed the most prominent solubility theory method employed, but he was by no means the only person working on this problem Teas[59], Burrell[60], Skaarup (with Hansen)[61], Koenhen and Smolders[62], van Krevelen and Hoftyzer[63], Beerbower (with Hansen)64 and Barton[65, 66]. The Group Contribution Theory (GCT) proposed by Hoftyzer and Van Krevelen is the focus of this study[63].

To gain a better understanding of GCT, it is important to understand how the component values are determined for solvents. The polar component is directly related to the dipole-moment while the hydrogen bonding component is correlated with the hydrogen bonding number. Hildebrand defined well how to determine total solubility as well as the dispersive component.

Hoftyzer-Van Krevelen derived several formulas to estimate the component solubility parameters of any organic material based upon molar attraction constants for the dispersive and polar components. It has been shown that the hydrogen bonding energy is relatively constant per structural unit, thus the equation was modified to reflect this fact.

$$\delta_d = \Sigma F_{di} / V \qquad \text{Equation 8}$$

Where:

δ_d = Dispersive component of HSP

F_{di} = GC Factors for the dispersion component of the molar attraction constant

V = Molar volume

$$\delta_p = \sqrt{(\Sigma F^2_{pi})} / V \qquad \text{Equation 9}$$

δ_p = Polar component of HSP

F_{pi} = GC factors for the polar component of the molar attraction constant

V = Molar volume

$$\delta_h = \sqrt{(\Sigma E_{hi} / V)} \qquad \text{Equation 10}$$

δ_h = Hydrogen bonding component of HSP

E_{hi} = Hydrogen bonding energy per structural unit

V = Molar volume

Using these equations and molar attraction constants and hydrogen bonding energy for each chemical structural component, the component HSP values for any molecule can be determined.

Example Calculation of HSP values by GCT:

The methods for calculating the monomer HSP values by GCT are found in Properties of Polymers: Their Correlation with Chemical Structure; Their Numerical Estimation and Prediction from Additive Group Contribution by D.W. Van Krevelen, specifically chapter 7: Cohesive Properties and Solubility.

More specifically the method chosen was that of Hoftyzer-Van Krevelen. The individual solubility component values can be calculated using the following formulas

The relative values for each of structural units within a monomer molecule can be found in Table 7.8, page 213 of Van Krevelen's book. However, we are only utilizing a small part of that table since our polymer choice limited the types of structural units table 21, below, was constructed using that data table as a reference.

Table 18

GCT Constants for Molar Attraction and Hydrogen Bonding Energy

Structural Unit	**F_{di}**	**F_{pi}**	**E_{hi}**
-CH_3	420	0	0
-CH_2	270	0	0
-CH	80	0	0
-C	-70	0	0
-AROMATIC	1430	110	0
-COO-	390	490	7000
-COOH	530	420	10000
-OH	210	500	20000
-CN	430	1100	2500

Molar mass and molar volume data used for these and other calculations are listed in Table 22 and are derived from either Mark[67] or Brandrupt[68].

Table 19

Monomer Data

Monomer	**Molar Mass (g/mol)**	**Molar Density (g/cm^3)**	**Molar Volume (cm^3/mol)**
Vinyl Acetate	86	0.934	92.08
Methyl Methacrylate	100	0.94	106.38
Butyl Acrylate	128	0.895	143.02
Butyl Methacrylate	142	0.894	158.84
2-Ethyl Hexyl Acrylate	184	0.885	207.91
Styrene	104	0.909	114.41
Ethylene	24	1.18	20.34
Versatic Acid	202	0.871	231.92
Acrylonitrile	53	0.81	67.1
Methacrylic Acid	85	1.015	83.74
Acrylic Acid	72	1.051	68.51

Using equations 7, 8 and 9, as well as data from both tables, below is an example calculation for 2-Ethyl Hexyl Acrylate Monomer. Please note that the double bond functionality will be considered as a component of the backbone of a polymer, as such, it will be considered as a single bond between to CH_2 groups.

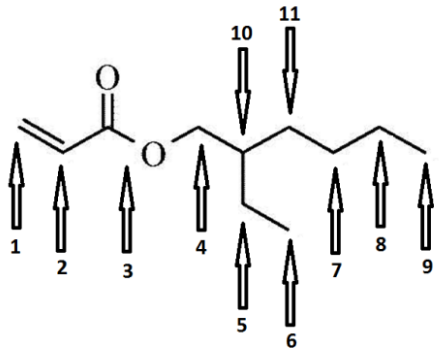

Figure 51. 2-EHA with numbered groups.

Table 23 shows how each of the structural units are classified for purposes of the calculations.

Table 20

Structural Units in 2-EHA

Structural Unit Number	**Structural Unit**
1	$-CH_2$
2	$-CH_2$
3	-COO-
4	$-CH_2$
5	$-CH_2$
6	$-CH_3$
7	$-CH_2$
8	$-CH_2$
9	$-CH_3$
10	-CH
11	$-CH_2$

This shows there are two $–CH_3$ groups, seven $–CH_2$ groups, one –CH group and one –COO- group to utilize with equations 7, 8 and 9 to determine the HSP component value Cohesive Energy Densities for this monomer. Below is the example of the worked out calculation for 2-EHA.

Using equations 7, 8 and 9, below are the individual calculations for the HSP component values for the monomer 2-Ethyl Hexyl Acrylate:

$$\delta_d = \Sigma F_{di} / V$$

$$\delta_d = \Sigma (420 \times 2) + (270 \times 7) + (80 \times 1) + (390 \times 1) / 207.91$$

$\delta_d = \Sigma\ (840 + 1890 + 80 + 390) / 207.91$

$\delta_d = 3200 / 207.91$

$_d = 15.39$

$\delta_p = \sqrt{(\Sigma\ (0 \times 2)^2 + (0 \times 7)^2 + (0 \times 1)^2 + (490 \times 1)^2 / 207.91}$

$\delta_p = \sqrt{(\Sigma\ (490)^2) / 207.91}$

$\delta_p = \sqrt{(240100) / 207.91}$

$\delta_p = 490 / 207.91$

$\delta_p = 2.36$

$\delta_h = \sqrt{(\Sigma\ E_{hi} / V\ )}$

$\delta_h = \sqrt{(\Sigma\ (0 \times 2) + (0 \times 7) + (0 \times 1) + (7000 \times 1) / 207.91}$

$\delta_h = \sqrt{(7000 / 207.91)}$

$\delta_h = \sqrt{\ 33.67}$

$\delta_h = 5.80$

We now have all three component values; now simply use equation 7 to obtain the total HSP for 2-Ethyl Hexyl Acrylate as follows:

$\delta_T = \sqrt{\ (\delta^2_p + \delta^2_d + \delta^2_h)}$

$\delta_T = \sqrt{\ ((15.39)^2 + (2.36)^2 + (5.80)^2)}$

$\delta_T = \sqrt{\ (236.85 + 5.57 + 33.64)}$

$\delta_T = \sqrt{\ 276.06}$

$\delta_T = 16.62$

Thus 16.62 is the total HSP parameter for 2-Ethyl Hexyl Acrylate. Table 24 shows the compilation of the component and total HSP values for each monomer as calculated by this process.

Repeating this process for each monomer table xx shows the HSP values as calculated by GCT.

Table 21

Monomer HSP Data

Monomer	δ_d	δ_p	δ_h	δ_T
Vinyl Acetate	12.53	5.29	8.69	16.14
Methyl Methacrylate	14.89	4.62	8.12	17.58
Butyl Acrylate	13.70	3.41	6.98	15.75
Butyl Methacrylate	14.99	3.07	6.63	16.68
2-Ethyl Hexyl Acrylate	15.39	2.35	5.80	16.62
Styrene	15.40	0.95	0.00	15.43
Ethylene	8.57	0.00	0.00	8.57
Versatic Acid	18.46	2.55	6.03	19.59
Acrylonitrile	14.70	20.73	6.86	26.32
Methacrylic Acid	15.33	4.95	10.86	19.43
Acrylic Acid	12.85	6.13	12.08	18.67

Using the data from table 24 and from the monomer compositions, the following was done to calculate the total and component HSP values for each polymer. Polymer B with a monomer composition

$\delta_{D\text{-Polymer B}}$ = (Monomer S = 0.835 % x 15.40) + (Monomer 2-EHA = 0.158 % x 15.39) + (Monomer MAA = 0.07 % x 15.33)

$\delta_{D\text{-Polymer B}}$ = (Monomer S = 12.859) + (Monomer 2-EHA = 2.432) + (Monomer MAA 1.073) = 16.36

$\delta_{P\text{-Polymer B}}$ = (Monomer S = 0.835 % x 0.95) + (Monomer 2-EHA = 0.158 % x 2.35) + (Monomer MAA = 0.07 % x 4.95)

$\delta_{P\text{-Polymer B}}$ = (Monomer S = 0.793) + (Monomer 2-EHA = 0.371) + (Monomer MAA = 0.347) = 1.51

$\delta_{H\text{-Polymer B}}$ = (Monomer S = 0.835 % x 0.00) + (Monomer 2-EHA = 0.158 % x 5.80) + (Monomer MAA = 0.07 % x 10.86)

$\delta_{H\text{-Polymer B}}$ = (Monomer S = 0.00) + (Monomer 2-EHA = 0.916) + (Monomer MAA = 0.762) = 1.68

$\delta_{T\text{-Polymer B}} = \sqrt{[\ (\delta_{D\text{-Polymer B}} = 16.36)^2 + (\delta_{P\text{-Polymer B}} = 1.51)^2 + (\delta_{H\text{-Polymer B}} = 1.68)^2\ ]}$

$\delta_{T\text{-Polymer B}} = \sqrt{[\ (267.65) + (2.28) + (2.82)\ ]}$

$\delta_{T\text{-Polymer B}} = \sqrt{[\ 272.75\ ]}$

$\delta_{T\text{-Polymer B}}$ = 16.52

Using the same method as above table 25 was constructed to give the calculated component and total HSP values according Hoftzyer-Van Krevelen method.

Table 22

Polymer HSP data as calculated by Hoftyzer-VanKrevelen

Polymer	**δ_d**	**δ_p**	**δ_h**	**δ_T**
A	16.33	1.45	1.98	16.51
B	16.36	1.51	1.68	16.52
C	14.95	4.20	7.71	17.34
D	14.60	3.95	7.75	16.99
E	14.52	4.19	7.73	16.97
F	13.33	4.76	8.22	16.37
H	14.87	2.61	4.29	15.70
I	11.41	2.99	4.92	12.76
J	12.53	5.29	8.69	16.14
L	11.89	3.59	6.04	13.79

Compare these with the values as determined experimentally by Hansen in table 26.

Table 23

HSP Values for Polymers from Hansen

Polymer	**δ_D**	**δ_P**	**δ_H**	**δ_T**
A	17.9	2.2	4.2	18.7
B	18.0	1.6	4.0	18.5
C	15.6	6.2	5.1	17.6
D	16.3	6.4	5.3	18.3
E	15.7	6.4	5.3	17.8
F	15.9	6.8	5.6	18.2

Table 23 (continued).

H	15.5	4.6	4.8	17.0
I	15.9	4.9	5.0	17.2
J	16.0	7.2	5.9	19.5
L	15.7	5.3	5.3	17.5

Since this study is focused on the relevance of HSP to water absorption and stain repellency, only localized interaction phenomena are of interest, and the molecular weight of the polymers and its effect upon HSP was ignored.

CHAPTER V – PERFORMANCE VERSUS HANSEN SOLUBILITY PARAMETER

Numerous studies have correlated polymeric material performance to its T_g, but exceptions do exist. For such cases performance needs to be correlated with the monomer composition. HSP has been used for multiple purposes, including solvent selection, chemical resistance, and polymer compatibility in multiple fields including coatings science.

Since we now know that polymer T_g can be a useful tool to predict physical performance but not stain repellency, how good of a tool can HSP be in predicting stain repellency or ease-of-clean properties. Furthermore, if HSP can generally be used to predict stain repellency performance how can it be employed in practical terms?

This project is a continuation of two previously published studies[1, 2] regarding RTU grout. The first published in 2013 focused on the extreme T_gs of polymer used in this application. The results suggested that high strength and toughness were more positively affected by high polymer T_g, while flexibility was improved by low polymer T_g. The second study published in 2014 investigated the effects of fibers, fillers and a broader range of polymer T_g. Results from this study suggested that factors other than polymer T_g effected performance properties. The general trends of the data suggested performance followed T_g, but there were outliers. Upon further investigation it was found that polymers with a more even blend of short versus long chain pendant groups were shown to have better than predicted performance. Long chain groups in this case are defined as three carbons or longer, including aromatic groups.

This current research utilized an optimized formulation where the only difference in the grout formulations was the amount of propylene glycol phenyl ether (PPh) used to

coalesce the grouts. The amount of coalescent was determined for each polymer to be able to form a film at 50 °F by a minimum film formation temperature (MFFT) bar. Volume, weight solids, filler content, fiber content, water content and PVC were all kept constant.

Chain growth polymers polymerized via unsaturated/vinyl bonds using emulsion polymerization were used in this study. All polymers are commercial materials supplied by both Dow Chemical Company and Wacker Chemical Corporation. There are pure acrylics, styrenated acrylics, vinyl acrylics, ethylene-vinyl acetate (EVA), hydrolytically stable EVA and pure vinyl acetate (PVA) used in this study.

All grouts were evaluated using the same protocol with the data first being plotted and analyzed according to T_g. The data was then analyzed for trends and correlation versus Hansen Solubility Parameters (HSP). HSP values for the polymers in this study were taken from *Hansen Solubility Parameters A User's Handbook* (2007).[3] The component values of dispersion (δ_D), polarity (δ_P) and hydrogen bonding (δ_H) were used as well as total HSP (δ_T).

Hildebrand first utilized rudimentary solubility parameters which worked mainly with non-polar materials[4]. Prior to Hildebrand the rule of thumb that like dissolves like was one of the best solubility indicators available. Hildebrand determined that the Cohesive Energy Density (CED) could be used to predict some solubility behavior:

$$\delta = \sqrt{(\Delta H_v - RT) / V_m} \qquad \text{Equation 11}$$

Where:

δ – solubility

ΔH_v - heat of vaporization

R - universal gas constant

T - temperature (K)

V_m - molar volume.

Hildebrand values and his equation for CED did not adequately describe solubility behavior for polar compounds. CED units are $MPa^{1/2}$ (SI), or $cal^{1/2}cm^{-3/2}$ (American Standard), but for brevity sake they will be omitted for the remainder of this paper. Other scientist contributed to solubility theory, but it was not until Charles Hansen's Doctoral Dissertation *The Three Dimensional Solubility Parameter*[5] that a greater understanding of solubility was reached. His worked showed the contributions of dispersion components or Van derWaals forces, polarity, and hydrogen bonding to total solubility. Hansen showed that:

$$\delta^2_T = \delta^2_D + \delta^2_P + \delta^2_H \qquad \text{Equation 12}$$

The derivation of this formula and its components is beyond the scope of this research, as such, we will work with the HSP component and total solubility parameters. It is important to note that solubility parameters cannot be directly determined for polymers using standard techniques employed for low molecular weight solvents. This is because polymers do not vaporize. As such, polymer HSP values must be determined experimentally by dissolving (or attempting to) the polymers in a series of solvents with known HSP values. Additionally, many scientists, including Van Krevelen, have used chemical group contribution theory (GCT)[6] to determine polymer HSP values. However, to reduce complications, GCT values will not be used in this study.

Performance versus HSP

Solubility parameters for polymers cannot be directly determined since the heat of vaporization cannot be measured for polymers. As such, other methods of determining solubility parameters must be used. A method was developed for determining polymer solubility parameters by dissolving a polymer in a range of solvents, typically 30, with a wide range of solubility themselves. The solubility of the polymer in each solvent is then determined by various means (typically turbidity, viscosity and separation or lack thereof). Once the polymer-solvent solubility is determined, a 3D plot is constructed using the three HSP values (dispersion, polarity and hydrogen bonding). Once this is done, the center point of the solubility sphere is determined, and this is the spot that denotes the total solubility parameter and the component HSP values.[26]

Each of the polymers in this study was analyzed for quantitative monomer content by mole percent in the backbone. Using this information, combined with the monomer HSP values listed in Hansen Solubility Parameters A User's Handbook, the total and HSP component solubility parameters were calculated for each polymer. One monomer's HSP values had to be estimated by plotting similar monomers with different alkyl pendant group lengths and extrapolating to estimate the monomer HSP values. Since all of the monomer HSP values are based upon non direct experimentation, as in correlating polymer HSP with solvent HSP that can lead to a range of HSP that is somewhat inaccurate, this calculated estimate was deemed acceptable.

Table 28 shows the HSP component and total solubility parameters for each monomer used in the backbones of the polymers used in this study. The total solubility was calculated using Equation 12.

Table 24

HSP Values for Monomers on Polymer Backbones used in this Study

Monomer	**δ_D Dispersion**	**δ_P Polar**	**δ_H Hydrogen Bonding**	**δ_T Total HSP**
Acrylic acid (AA)	17.7	6.4	14.9	15.9
Acrylonitrile (AN)	16.0	12.8	6.8	21.6
Butyl acrylate (BA)	15.6	6.2	4.9	17.5
Butyl methacrylate (BMA)	15.6	6.4	6.6	18.1
2-Ethylhexyl acrylate (2-EHA)	14.8	4.7	3.4	15.9
Ethylene (E)	15.0	2.0	3.8	15.6
Meth-acrylic Acid (MAA)	15.8	2.8	10.2	19.0
Methyl methacrylate (MMA)	15.8	6.5	5.4	17.9
Styrene (S)	18.6	1.0	4.1	19.1
Veova-10 (VV)	15.6	2.1	5.3	16.6
Vinyl acetate (VA)	16.0	7.2	5.9	18.5

Table 29 shows the HSP and total solubility parameters for each of the polymers used in this study. The calculations for these polymer solubility parameters were done using the values for monomer concentrations from Table 7 and the monomer solubility parameters from Table 11. One example calculation for polymer B is shown:

$\delta_{D\text{-Polymer B}}$ = (Monomer S = 0.835 % x 18.6) + (Monomer 2-EHA = 0.158 % x 14.8) + (Monomer MAA = 0.07 % x 15.8) = 18.0

$\delta_{P\text{-Polymer B}}$ = (Monomer S = 0.835 % x 1.0) + (Monomer 2-EHA = 0.158 % x 4.7) + (Monomer MAA = 0.07 % x 2.8) = 1.6

$\delta_{H\text{-Polymer B}}$ = (Monomer S = 0.835 % x 4.1) + (Monomer 2-EHA = 0.158 % x 3.4) + (Monomer MAA = 0.07 % x 10.2) = 4.0

$\delta_{T\text{-Polymer B}} = \sqrt{[\ (\delta_{D\text{-Polymer B}} = 18.0)^2 + (\delta_{P\text{-Polymer B}} = 1.6)^2 + (\delta_{H\text{-Polymer B}} = 4.0)^2\ ]}\ = 18.5$ –

Using equation 2

Table 25

HSP Values for Polymers

Polymer	**δ_D Dispersion**	**δ_P Polar**	**δ_H Hydrogen Bonding**	**δ_T Total HSP**
A	17.9	2.2	4.2	18.7
B	18.0	1.6	4.0	18.5
C	15.6	6.2	5.1	17.6
D	16.3	6.4	5.3	18.3
E	15.7	6.4	5.3	17.8

Table 25 (continued).

F	15.9	6.8	5.6	18.2
H	15.5	4.6	4.8	17.0
I	15.9	4.9	5.0	17.2
J	16.0	7.2	5.9	19.5
L	15.7	5.3	5.3	17.5

Using the values in Table 12 and the test results, Pearson Correlation Coefficient (PCC) values were calculated and shown in Table 13. Table 14 shows the summation of the strength of the PCC values.

Table 26

PCC Values for Performance Properties and HSP

Property	**δ_D Dispersion**	**δ_P Polar**	**δ_H Hydrogen Bonding**	**δ_T Total HSP**
UTS	0.50	-0.18	-0.19	0.60
Elongation	-0.68	0.27	0.30	-0.79
Young's modulus	0.62	-0.25	-0.26	0.70
Dry Durometer	0.61	-0.27	-0.27	0.70
Wet Durometer	0.44	-0.29	-0.40	0.37
Water absorption	-0.62	0.37	0.37	-0.59
Dry adhesion	0.39	0.02	-0.04	0.60
Wet adhesion	0.23	0.00	-0.06	0.30
Total stain repellency	-0.21	-0.06	-0.18	-0.42
Oil stain repellency	0.48	-0.46	-0.62	0.21
Water stain repellency	-0.56	0.22	0.19	-0.64
Flexural strength	0.72	-0.44	-0.45	0.70

Table 26 (continued).

Shrinkage	-0.41	0.07	0.16	-0.54
Wet UTS	0.90	-0.72	-0.74	0.67
Wet elongation	-0.57	0.29	0.28	-0.59

Table 27

Summation of Strength of PCC Values for HSP Parameters

PCC Strength	**δ_D Dispersion**	**δ_P Polar**	**δ_H Hydrogen Bonding**	**δ_T Total HSP**
Perfect	0	0	0	0
Strong	2	1	1	4
Moderate	10	2	3	8
Weak	3	9	9	3
Zero	0	3	2	0

Based solely on the strength of PCC values it appears that total HSP exhibits the best overall correlation to performance based upon solubility only, with dispersion HSP component values very close. Both total and dispersion HSP have 12 (of 15) values that are either strong or moderate, but total HSP has more strong PCC values. Polar and hydrogen bonding HSP values both have over 12 weak or lower correlations with polar having the most with 13 weak or lower correlations, including 3 zero correlations with hydrogen bonding having 2 zero correlations.

Looking at only the mechanical properties (UTS, FS, Durometer, YM and elongation - all wet and dry), the best correlations exist with total HSP, with the exception of wet UTS. With wet UTS the dispersion HSP value has a strong correlation,

whereas the total HSP only has a moderate correlation. Additionally, wet Durometer only shows a moderate correlation with the dispersion HSP and a weak correlation with total HSP. However, total HSP still shows correlation to all of the mechanical properties and in most cases the best correlation of all the solubility parameters.

Comparing total HSP to T_g for PCC strength, T_g has only six mechanical performance parameters that have PCC strengths of moderate or strong, whereas total HSP has seven performance parameters that are either moderate or strong. Elongation, YM, and dry Durometer show strong correlations for both total HSP and T_g, but T_g also shows strong correlations with dry UTS and wet Durometer, whereas total HSP only shows moderate correlation with dry UTS and a weak correlation with wet Durometer. For mechanical properties it appears that T_g is a better performance predictor than total HSP, although inexplicably FS shows a moderate correlation with HSP but only a weak correlation with T_g. This could be due to the fact that in some way, HSP takes into account the pendant groups effect, whereas T_g only takes into account the gross effect of pendant groups.

Total HSP PCC values are the highest for both wet and dry adhesion. Dry adhesion appears to have the same PCC strength and nearly the same PCC value for both total HSP and T_g. However, wet adhesion shows zero correlation to T_g but a moderate correlation to total HSP. This makes sense given that adhesion between two materials is increased with increased interfacial interaction, which is increased by similar solubility parameters. Thus, total HSP appears to be a better indicator for adhesion, especially if the solubility parameters for the substrate are known. If the solubility parameters of both the substrate and material used can be matched (or close to), adhesion will be increased.

With regard to the properties that are exposed to liquid materials and are not mechanical properties at first glance it appears that T_g is a better performance predictor. This is due to the fact that there are two strong PCC values (water absorption and OSR) and one moderate (WSR). However, T_g shows zero correlation with TSR. Total HSP and component HSP values for dispersion and hydrogen bonding each have four PCC values that exhibit correlations. However, the component values are nearly always weaker than total HSP and T_g for that matter (with the exception of T_g's zero correlation to TSR).

Stain repellency appears to be governed strongly by T_g, based upon PCC values. With a 0.91 for OSR and a -0.62 for WSR these are the best performance predictors for OSR or WSR. However, T_g alone is terrible for TSR. Total HSP shows at least a moderate correlation to TSR with a value of -0.42. This shows that lower total HSP values have better overall stain repellency, whereas T_g can predict performance either good or bad for only water-based or oil-based stains and they are in contradiction to each other. As polymer T_g increases, OSR gets better, but WSR gets worse. Conversely, as polymer T_g decreases OSR gets worse, but WSR gets better. This leaves a quandary as to how to pick appropriate polymers for stain repellency. It appears that total HSP, while showing only a moderate correlation is a better predictor of total stain repellency. In other words as total HSP decreases so too does TSR.

As to the component values and stain repellency, hydrogen bonding has only one moderate correlation, with OSR, but it is the strongest correlation of all the HSP values. This indicates that the best parameter to focus on for improving OSR is to decrease the hydrogen bonding parameter, which will also have the effect of decreasing the total HSP,

which should also improve TSR. WSR appears to be affected most by the polar HSP component with decreasing WSR with increasing polarity. This makes sense due to the fact that water itself is highly polar. Thus, decreasing the polar content of the polymer will increase WSR and also increase TSR.

Table 32 shows a comparison of the PCC values for each property versus T_g and HSP side-by-side. Note that the blue highlighted properties show PCC values that are more than 0.1 greater than that for the PCC value for the other characteristic. For example, dry elongation has -0.92 PCC value versus T_g, but is weaker by more than 0.1 (precisely a difference of 0.13) than the PCC value versus HSP of -0.79. This suggests the polymer T_g is a better predictor of performance.

There are five properties that are clearly better predicted by polymer Tg: dry elongation, wet and dry surface hardness by Shore D Durometer, dry flexural strength and oil stain repellency. While water-based stain repellency and total stain repellency (water and oil combined) are better predicted by HSP.

The oil stain repellency curiosity of being better predicted by polymer T_g can be explained if the data is further scrutinized. The first issue with the stain repellency rating in general is that it is non continuous data. The data is a subjective scale of zero to four for each stain and while experience has shown that this method is suitable to compare one sample to another it is difficult to strictly apply statistical analysis. The second difficulty comes from the fact that while most of the water based stains exhibited a range of performance from zero to four, while most of the oil based stains were either very low or very high with not much middling performance. This has the potential to statistically

skew, thus biasing the data. So this oil-based correlation to polymer T_g and not HSP should be further explored.

The other values, while some may be higher than the other, are too close to make a definitive differentiation between whether polymer T_g or HSP is a better predictive tool based upon PCC values. However, given how close that the HSP values are to each this may have influenced the PCC values.

Table 28

Correlation Coefficient Comparison Table: Polymer T_g vs HSP

Property \ Correlation Coefficient	**Versus T_g (K)**	**Versus HSP**
Dry Elongation	**-0.92**	-0.79
Wet Elongation	-0.62	-0.59
Dry UTS	0.70	0.60
Wet UTS	0.73	0.67
Dry Youngs Modulus	0.76	0.70
Dry Durometer	**0.83**	0.70
Wet Durometer	**0.79**	0.37
Dry Adhesion	0.61	0.60
Wet Adhesion	-0.20	0.30
Dry Flexural Strength	**0.91**	0.70
Shrinkage	-0.62	-0.54
Water-based Stain Repellency	-0.28	**-0.64**
Oil-based Stain Repellency	**0.60**	0.21
Total Stain Repellency	0.09	**-0.42**
Water Absorption	-0.54	-0.59

Polymer D was further scrutinized for variability in HSP values by utilizing differing monomer molar concentrations. Each of the four highest concentration monomers: MMA, BA, 2EHA, and BMA were used in test calculations by increasing the highest molar concentration monomer by 10% and reducing the next highest molar concentration monomer by 10%. This was repeated with the next two monomers by

changing their molar concentrations. These example calculations were done in an attempt to determine the overall variability of potential HSP values for a given polymer as the monomer concentrations are slightly changed. Table 33, below shows the high end, low end as well as the calculated values used in this research. The average percentage difference between the lowest and highest calculated HSP value is 3.4% with the total HSP value having only a 1.7% difference. With such small differences in calculated HSP values which were based upon an assumed variance in the actual monomer molar concentrations, this small difference suggests that the PCC values would not change by much, if all, if the data for each polymer were re-evaluated for correlations to HSP values. This also shows that even with a 10% error in monomer molar concentration identification that the data in this research is fairly robust.

Table 29

High, Low and Research Example Calculated HSP Values for Polymer D

Example	**δ_D**	**δ_P**	**δ_H**	**δ_T**
Low End	14.40	3.85	7.54	16.70
Research	14.60	3.95	7.75	16.99
High End	14.58	3.99	7.20	16.74

Lastly, in an attempt to determine if HSP values can be used to determine if any specific stain will either be repelled or easy to clean (or remove) the HSP values some of the staining agents were estimated by GCT. Since most of the stains are complex mixture: brake fluid, motor oil, red wine, ketchup, mustard, soy sauce, coffee and cola, we used only the stains that we could be reasonably sure of the structure. Skydrol is a tributyl phosphate ester, soya oil is a combination of triglycerides with relatively known concentrations (linoleic acid ~ 55%, oleic acid ~ 23%, palmitic acid ~ 11%, linolenic acid

~ 7% and stearic acid ~ 4%), and vinegar (5% acetic acid in water). Table 34 shows the calculated HSP values for those three staining agents.

Table 30

Calculated HSP Values for Select Staining Agents

Staining Agent	**δ_D**	**δ_P**	**δ_H**	**δ_T**
Skydrol	16.18	6.90	6.89	18.89
Vinegar	15.53	15.74	41.43	46.96
Soya Oil	15.94	1.54	4.69	16.68

Using these values and the stain repellency data for those three stains for each polymer correlation coefficients were calculated. Vinegar and soya oil both had PCC values of 0.22 and 0.15 respectively, while Skydrol had a PCC value of – 0.81. At first glance this suggests that correlation between staining of vinegar and soya oil are not well predicted by HSP and Skydrol is fairly well predicted. However, this is complicated by the fact that of the three staining agents only Skydrol has a spread of data. Vinegar only showed very minor staining with a rating of one out four on one of the ten samples, and soya oil only exhibited the same minor stain of one out of four on only two of the ten samples.

To further investigate the stain repellency of both vinegar and soya oil, Hansen's relative energy difference (RED) value were calculated. RED values are defined as[57]:

$$(R_a)^2 = 4(\delta_{D2} - \delta_{D1})^2 + (\delta_{P2} - \delta_{P1})^2 + (\delta_{H2} - \delta_{H1})^2 \qquad \text{Equation 13}$$

This is the difference between two different molecules in a three dimensional Hansen space. If you divide this value by the interaction radius (R_0), you obtain the RED value for two mixed systems. The larger the red value the less likely the two materials

will dissolve together. Under normal circumstances we would know the R_0 value and be able to directly determine RED values. In this case, since we are dealing with multiple uncertainties (GCT calculations, monomer concentration estimations and estimation of staining agents specific compositions), we will only use the R_a values themselves.

Table 35 shows the R_a values between each polymer used in this study and each of the three focused stain agents. The R_a values are italicized and in red to show which polymers exhibited staining.

Table 31

HSP Distance Values between Polymers and select Staining Agents

Polymer	**R_a – Skydrol**	**R_a – Soya Oil**	**R_a – Vinegar**
A	***6.4***	4.0	39.9
B	***7.0***	4.2	40.3
C	***2.2***	4.7	37.6
D	***1.7***	5.0	37.3
E	***1.9***	4.9	37.3
F	***1.4***	5.3	***36.9***
H	***3.4***	***3.2***	38.3
I	***2.8***	***3.4***	38.0
J	***1.1***	5.8	36.6
L	***2.5***	3.8	37.6

The only samples to show staining with soya oil are polymers H and I, which coincide with the lowest R_a values and since the next highest R_a value for soya oil is 3.8 it would stand to reason that according to Hansen's original concept where a RED value of 1.0 is the borderline between solubility and not that the R_0 for soya oil is between 3.4 and 3.8.

Vinegar only showed slight staining on one sample. All of the R_a values for vinegar are very high. So one could conclude that the very high R_a values indicate a lack

of staining (or interaction) with vinegar, thus HSP values can predict fairly accurately stain repellency or ease-of-clean properties with vinegar: with one outlier being polymer F. However, since the R_a values are so large and we have a potential outlier we cannot estimate the R_o value of vinegar.

Skydrol showed stain with each sample with varying staining performance from 0.5 to four. However, the correlation between stain repellency data and R_a values was high at – 0.81, thus showing that while we do not know the precise R_o value for Skydrol, we can predict that as the R_a value gets larger, the stain repellency gets better, thus showing that HSP values can be used to predict stain repellency or ease-of-clean properties against Skydrol.

Using R_a values, based upon HSP values for polymers and staining agents, we have shown that it is possible to predict stain repellency; thus proving the original hypothesis that HSP values can predict stain repellency if all of the variables of the system are known.

CHAPTER VI – THESIS SUMMATION AND CONCLUSIONS

The original premise of this research was two-fold, first as a work project and second as a Master's Thesis. The work component was designed to learn about the RTU grout market both from an economic importance perspective and as a technical formulating perspective so that Wacker could utilize this information to aid with internal product development for use in this market sector. The Master's Thesis component was designed to gain a better scientific understanding of how RTU grouts were formulated. Along the way the scientific portion developed into determining how polymer Tg and Hansen Solubility Parameters (HSP) could be used to aid in predicting polymer performance within RTU grouts in an attempt to use this information to push the boundaries of performance of RTU grouts.

In short, the physical properties; dry elongation, surface hardness (wet and dry) and flexural strength all can all be correlated fairly well with polymer T_g. While water-based, oil-based and total stain repellency correlate much better with HSP. With the remaining properties having correlations somewhere in between the two, but mostly stronger with polymer T_g.

It was learned during this research that filler particle size and oil absorption (OA) value can have profound effects upon physical performance, as well as particle size distribution. Smaller particle sizes, at equal density, allows for a higher packing density, which will improve strength properties, especially as CPVC is approached (but not exceeded). This packing, then physical strength performance can be improved upon by varying the particle sizes so that larger particles can be successively distributed within a matrix of increasingly smaller particle size filler particles. Lower OA values allow for

more filler to be incorporated on a by weight (or volume) basis since the lower OA values require less binder material to aid in dispersing them and preventing flocculation of filler particles. Thus the optimal filler package would contain a distribution of larger to smaller particle sizes with the largest particle size compromising the largest volume and the smallest particle size comprising the smallest volume to ensure the best packing. Utilizing fillers with low OA values will also allow for more filler to be used thus increasing the PVC, while keeping below the CPVC. Using low OA value fillers leads to higher CPVC and vice versa for high OA value fillers.

Filler hardness was found to not be of significant importance at least will respect to the properties and formulations utilized in this study. In general, fiber content was of little significance as well. While the use of fibers did marginally improve tensile strength properties, these properties can also be improved through judicious use of filler and choice of polymer.

The strongest correlations between polymer T_g and performance were with flexural strength and tensile elongation. Both properties had correlation values higher than 0.9, indicating strong correlations. Elongation had a negative correlation indicating that as polymer T_g increased, elongation decreased simultaneously flexural strength increased as polymer T_g increased. Ultimate tensile strength (UTS), Young's modulus and surface hardness (by Shore D Durometer) all showed good correlations with polymer T_g, with all of these properties increasing with increasing polymer T_g. Water-absorption, adhesion, shrinkage and stain repellency (both oil and water-based) showed either weak or no correlation between the performance properties and polymer T_g.

Correlation between the primary strength properties and polymer T_g should not be surprising. The fact that flexural strength and elongation had the best correlations should also not be surprising since those two properties rely upon either stiffness for flexural strength or ductility for elongation and typically increased T_g gives stiffer material and decreased T_g gives more ductile behavior.

UTS, Young's modulus and surface hardness while showing good correlation with polymer T_g are more affected by polymer motion than flexural strength and elongation. These properties are also influenced more by side chains which may not necessarily equate to changes (up or down) in polymer T_g. Side chain effects can account for the slightly weaker correlation to polymer T_g in these physical strength properties.

Adhesion, as tested in both compressive and tensile shear as was utilized in various phases of this study is most certainly a physical property and as such affected by polymer T_g. However, the interfacial area between adhesive and adherend (substrate) is also affected by chemical contributions, in this case HSP. Since all of the polymers in this study had the same backbone and only varied in T_g and side chain composition, the side chain composition is also how the HSP varied. This variation also contributes to adhesion performance, which is why the relatively weak correlation between polymer T_g and adhesion. Coincidentally HSP correlation with adhesion was also relatively weak, highlighting the fact that both polymer T_g and HSP contribute to adhesion performance.

Water-absorption has a slightly better correlation with HSP, than with polymer T_g, but both are still fairly weak. This also highlights the combination of factors as they influence performance. Stain repellency has similar trends as with water-absorption.

Interesting as polymer T_g increases, oil stain repellency gets better, but water-based stain repellency gets worse and vice versa.

It was also shown quite convincingly for three select staining agents (Skydrol, vinegar and soya oil) that R_a and RED values can be used to accurately predict stain repellency. Thus as more information is learned about the chemistry of typical household or garage staining agents the better that polymeric systems can be designed to prevent those stains or at least make them easier to clean.

In van Krevelen's Porperties of Polymers[69] the author shows there is a relationship between side chain or methylene chain length and T_g. In fact with increasing chain length T_g passes through a minimum value at around 9 methylene units and then increases again. The theory is that with short chain lengths there exists a tendency for order with increasing disorder as chain length increases to approximately 9 units./ At about 9 methylene units the tendency increases for intermolecular interaction which then contribute to higher order and in some cases "side chain crystallization."

In a study by Yakout[70] the solubility of polycyclic aromatic compounds with activated carbon showed that with increased number of methyl groups the solubility with the activated carbon increased. By extension, this suggests that increased chain length of polymer side chains should increase organic solubility, thus becoming more hydrophobic. Combining these two concepts, Van Krevelen's of side chain length influence on properties and the specific case by Yakout on the specific solubility effect of methyl chain lengths could explain why the polymers with a more uniform blend of short and long chain side groups show better overall stain repellency to both oil based and water based stains. Whereas polymers with predominantly long chain side chains fared better

against water based stains and worse with oil based stains, while polymers with predominantly short chain side chains fared better against oil bases stains and worse with water bases stains.

This research only scratched the surface of the utility of HSP for predicting stain repellency or ease-of-clean properties. The project focused on only one type of polymer in one type of formulation with no variability. It only evaluated a handful of staining agents and fewer still ones with known chemical compositions. More work should be done to follow this up by expanding the polymers, formulations, and more importantly, evaluating the staining agents more thoroughly to determine their precise chemical compositions, thus their HSP values. Then a more comprehensive effort can be put forth to more broadly apply this research and truly determine the practical applicability of HSP for stain repellency prediction.

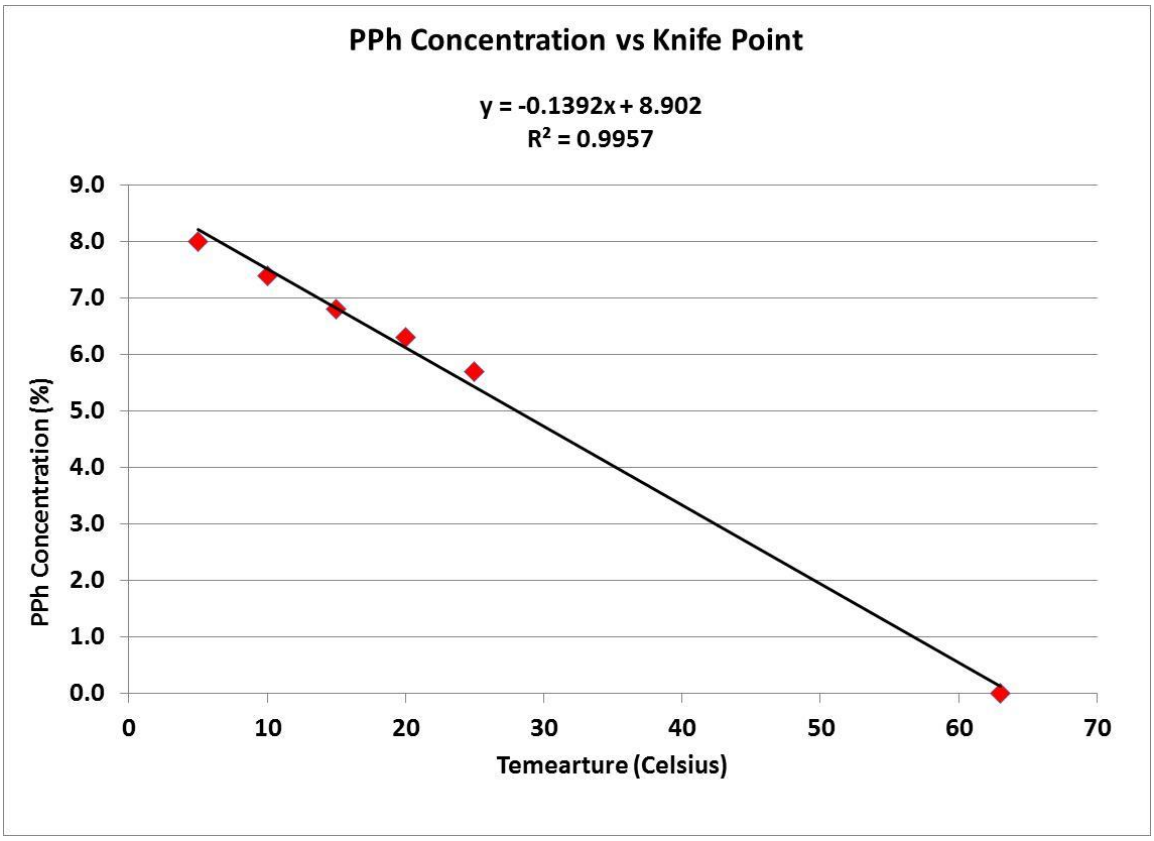

Figure A1. MFFT of Sample A with PPh by Knife Point

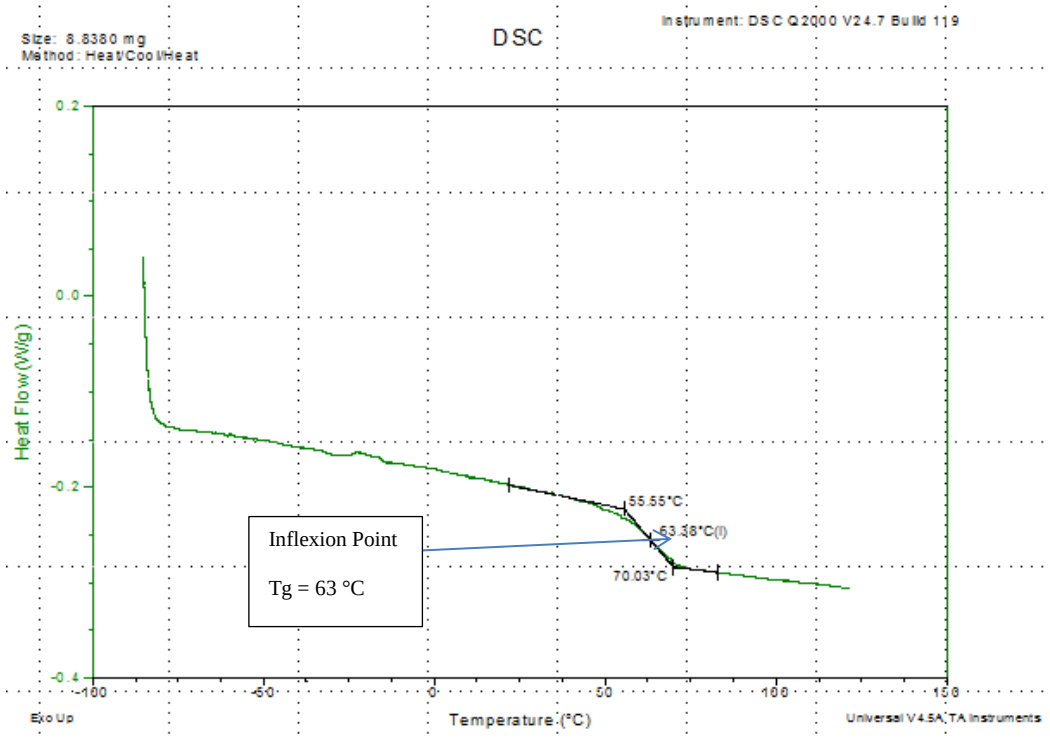

Figure A2. DSC Scan for Polymer A

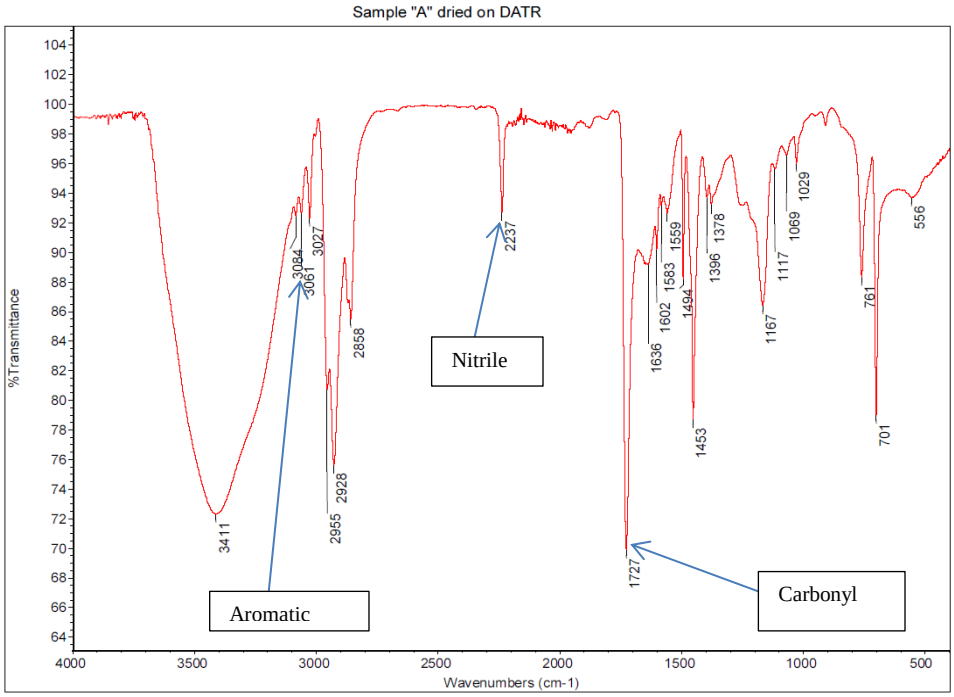

Figure A3. FT-ATR Spectra for Polymer A

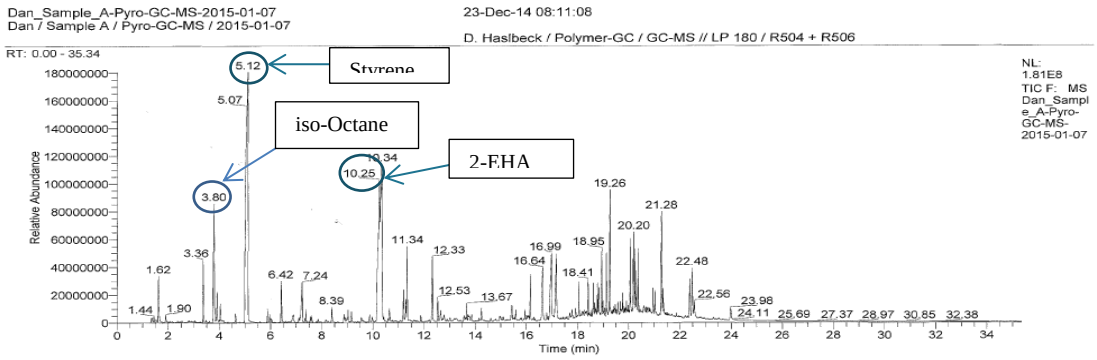

Figure A4. Pyrolysis-GC-MS Chromatograph for Polymer A

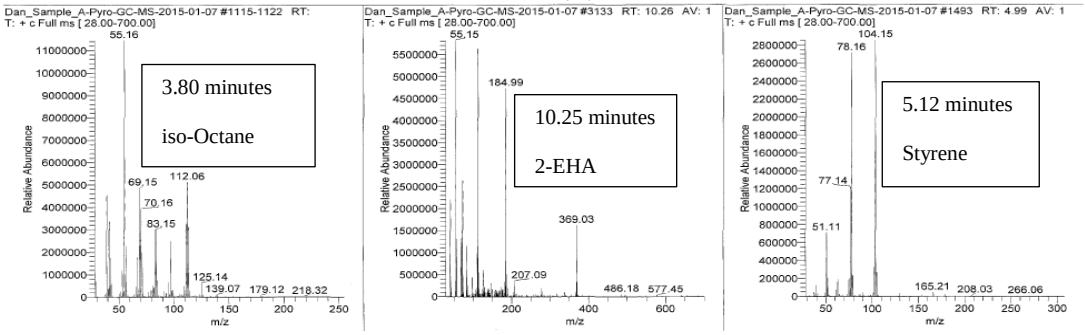

Figure A5. Total Ion Chromatograms for Components in Polymer A.

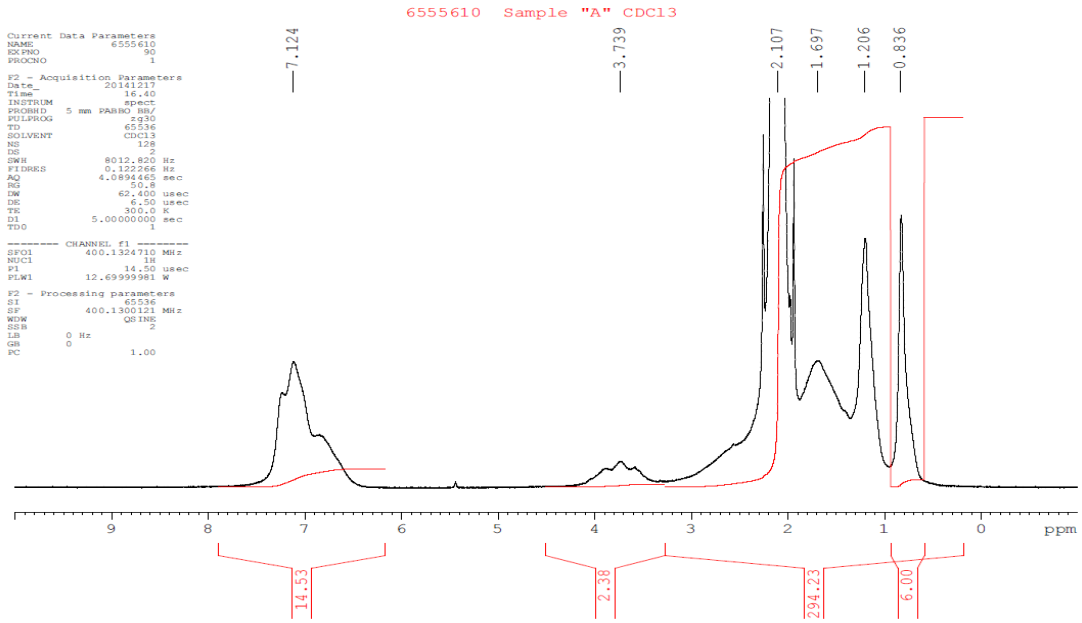

Figure A6. H^1-NMR Spectra for Polymer A

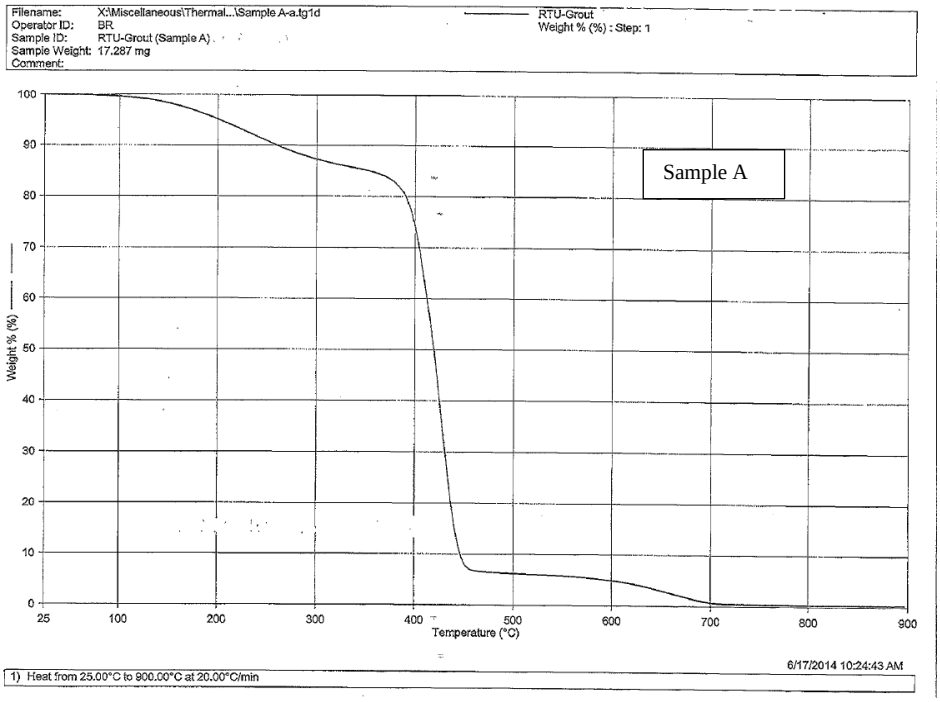

Figure A7. TGA Thermal Curve of Polymer A

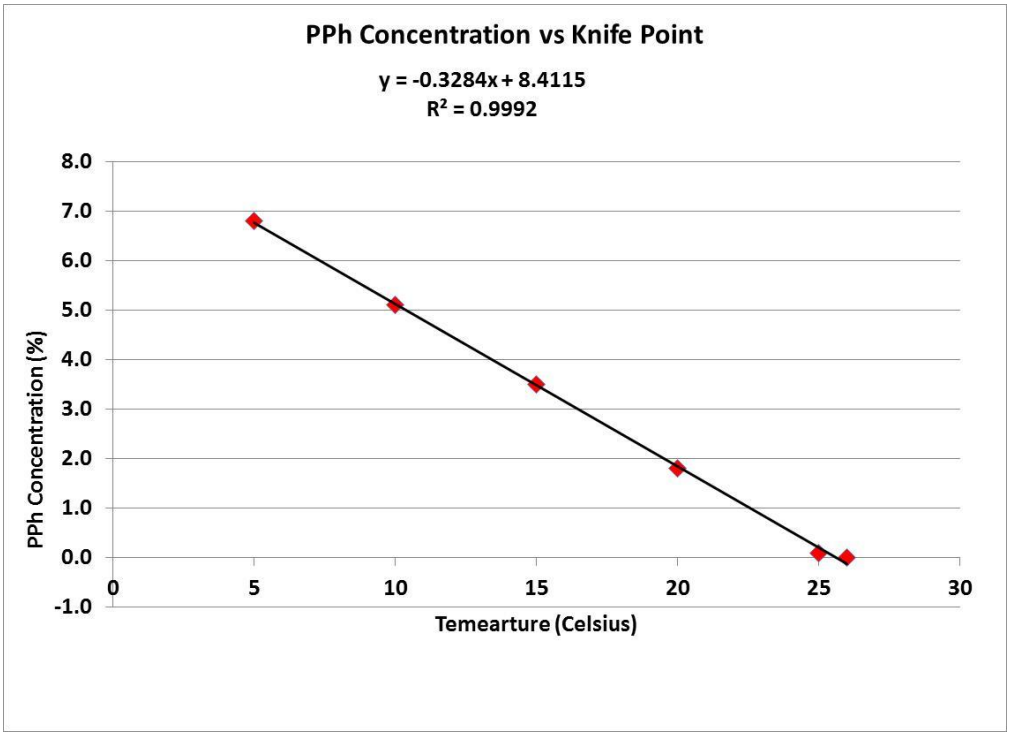

Figure A8. MFFT of Polymer B with PPh by Knifepoint

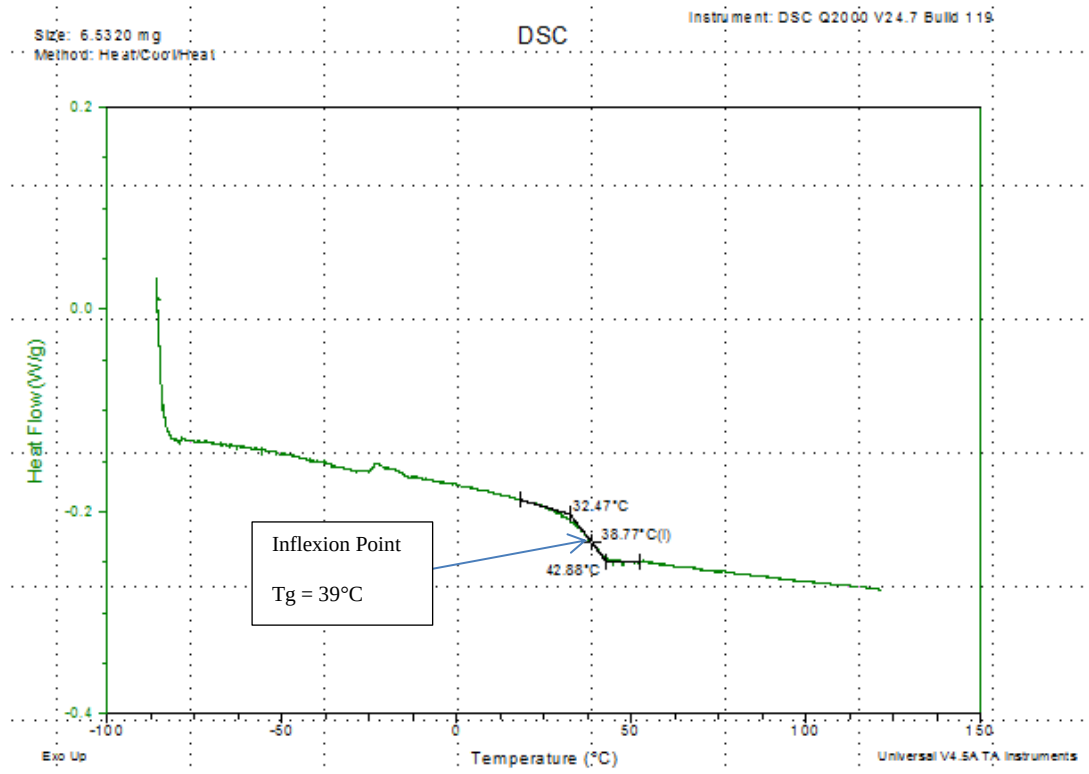

Figure A9. DSC Scan of Polymer B

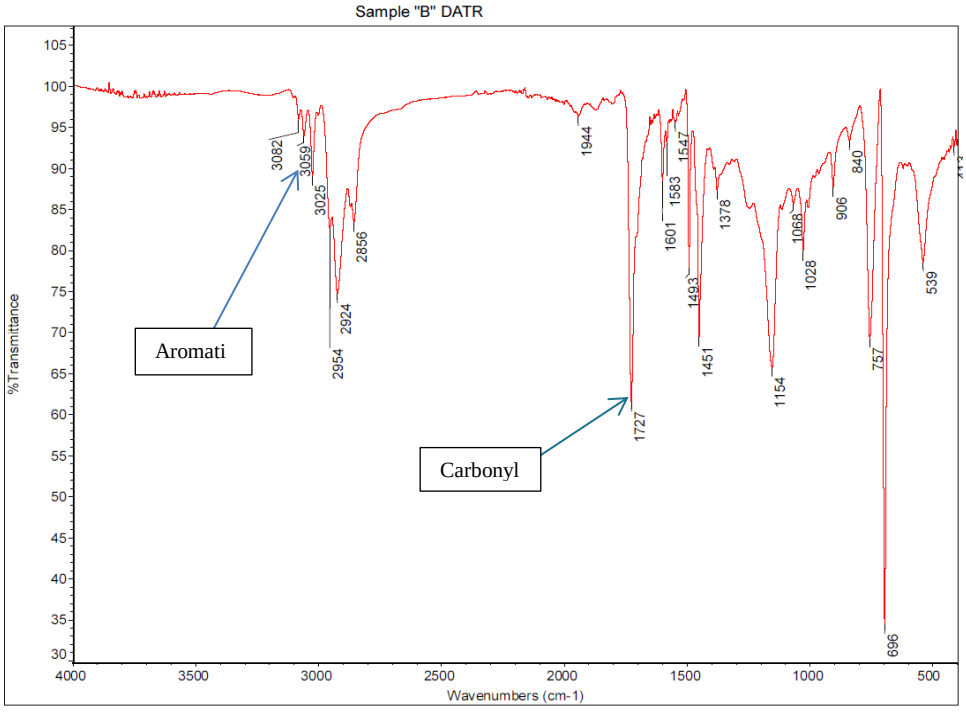

Figure A10. FT-ATR Spectra of Polymer B.

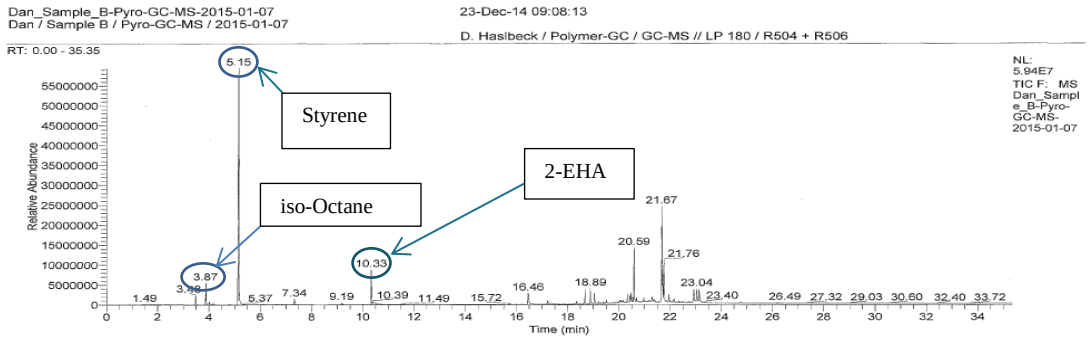

Figure A11. Pyrolysis-GC-MS Chromatograph for Polymer B.

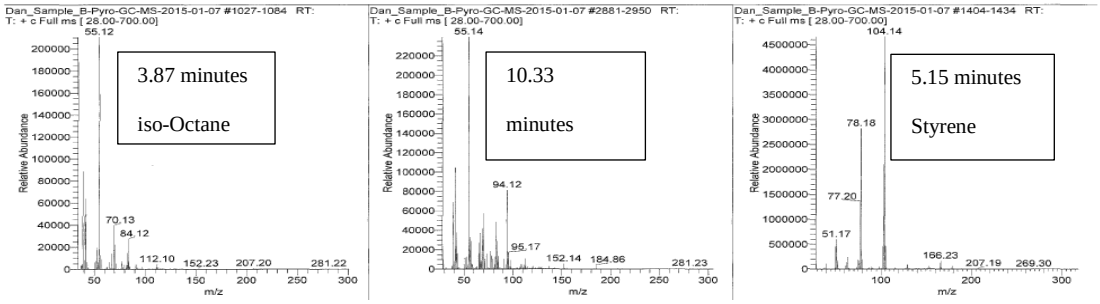

Figure A12. Total Ion Chromatograms for Components in Polymer B

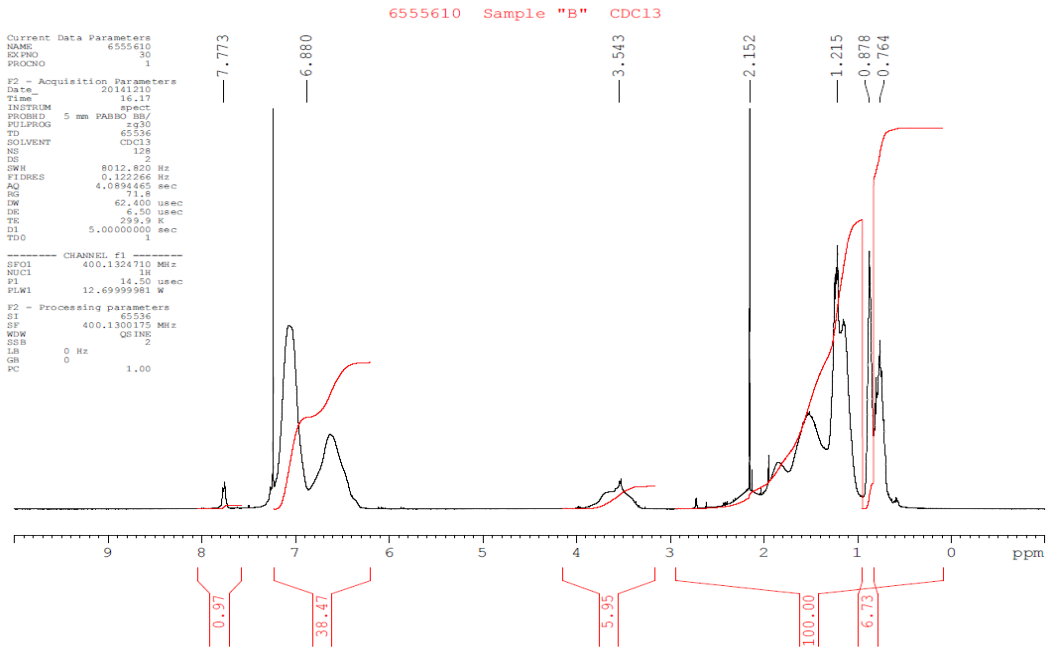

Figure A13. H^1-NMR Spectra for Polymer B

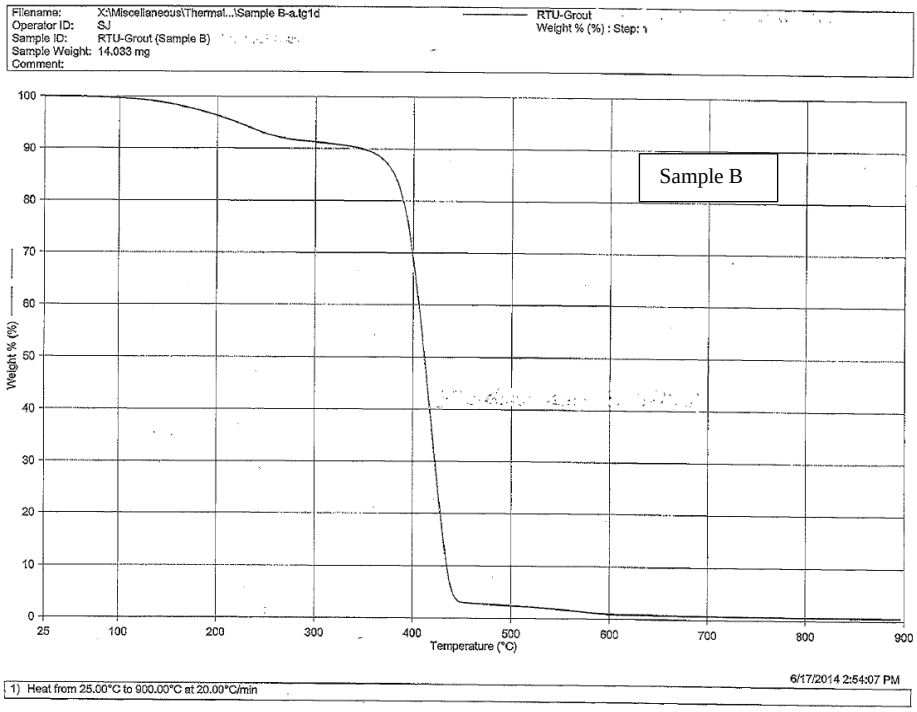

Figure A14. TGA Thermal Curve of Polymer B

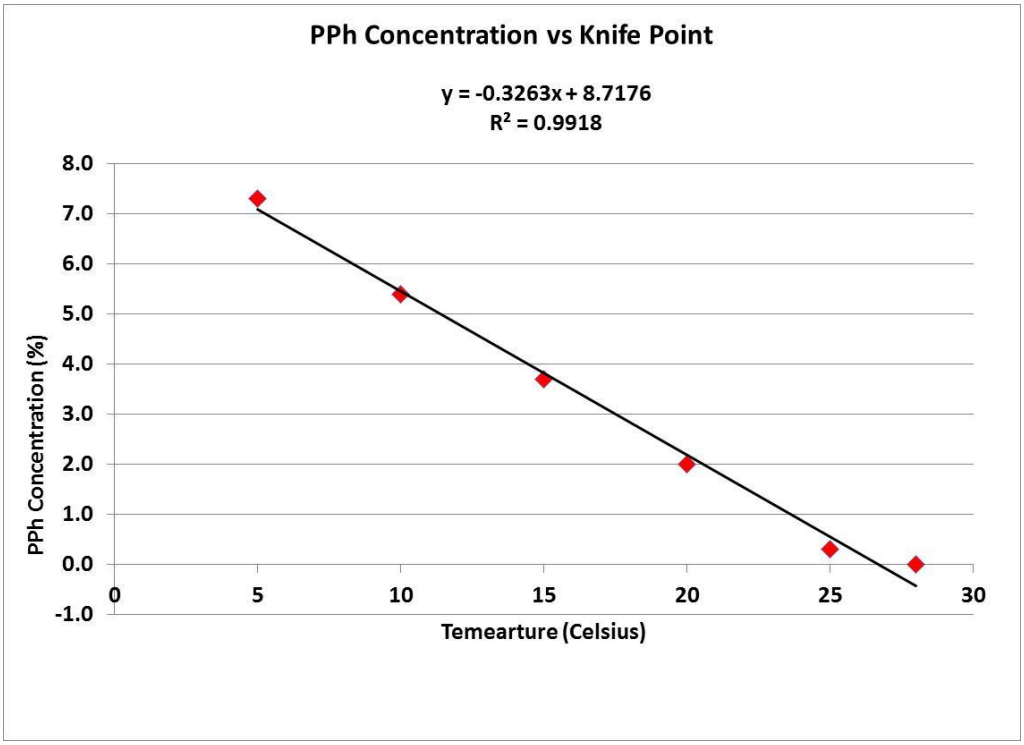

Figure A15. MFFT of Polymer C with PPh by Knifepoint

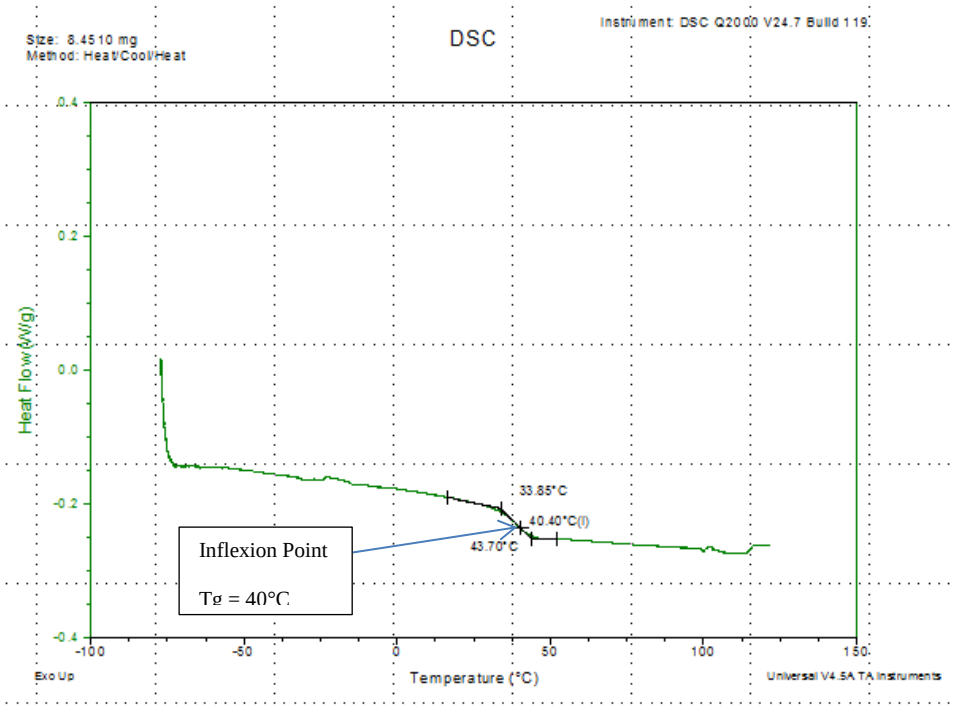

Figure A16. DSC Scan of Polymer C

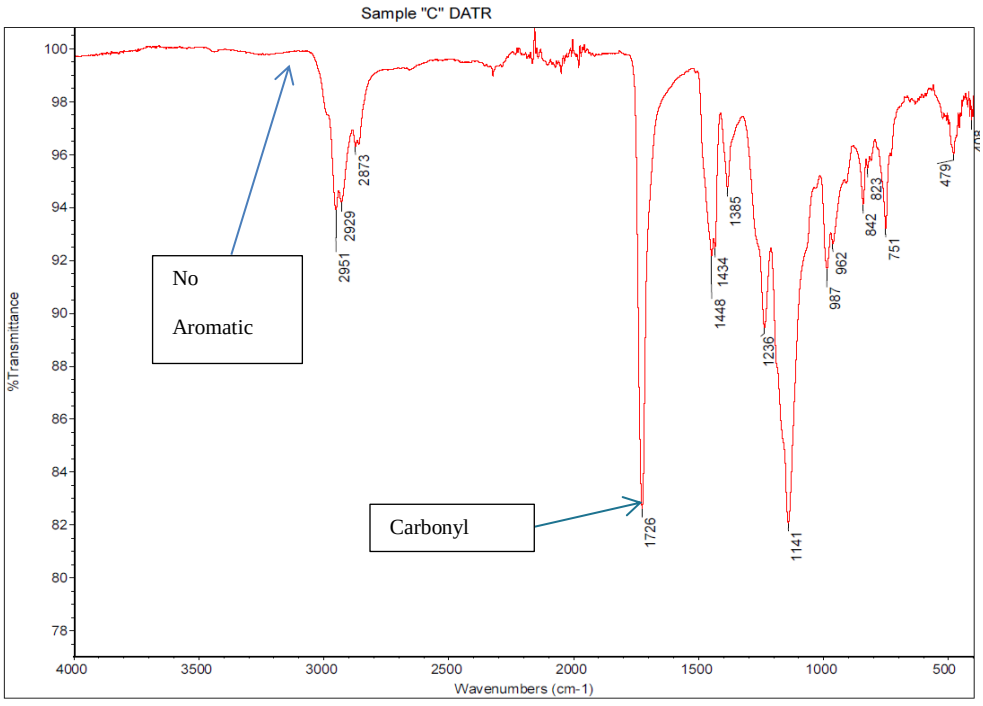

Figure A17. FT-ATR Spectra of Polymer C

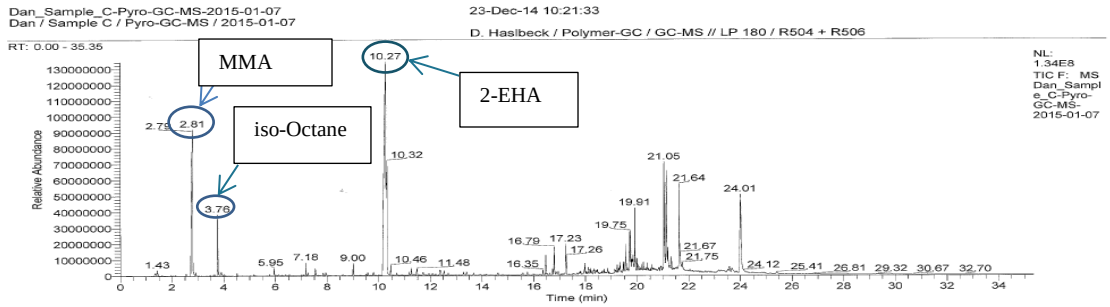

Figure A18. Pyrolysis-GC-MS Chromatograph of Polymer C

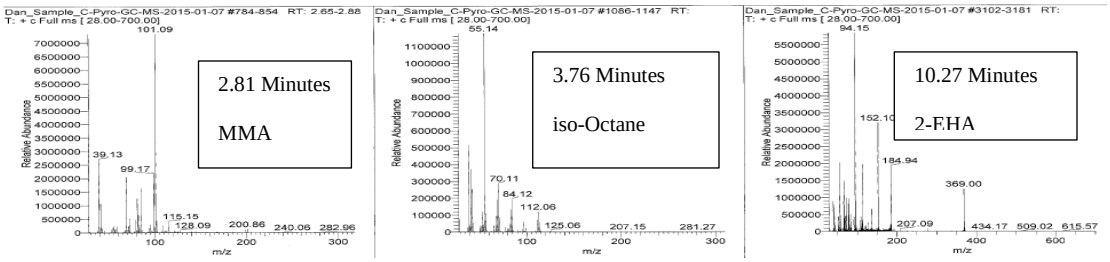

Figure A19. Total Ion Chromatogram of Components of Polymer C

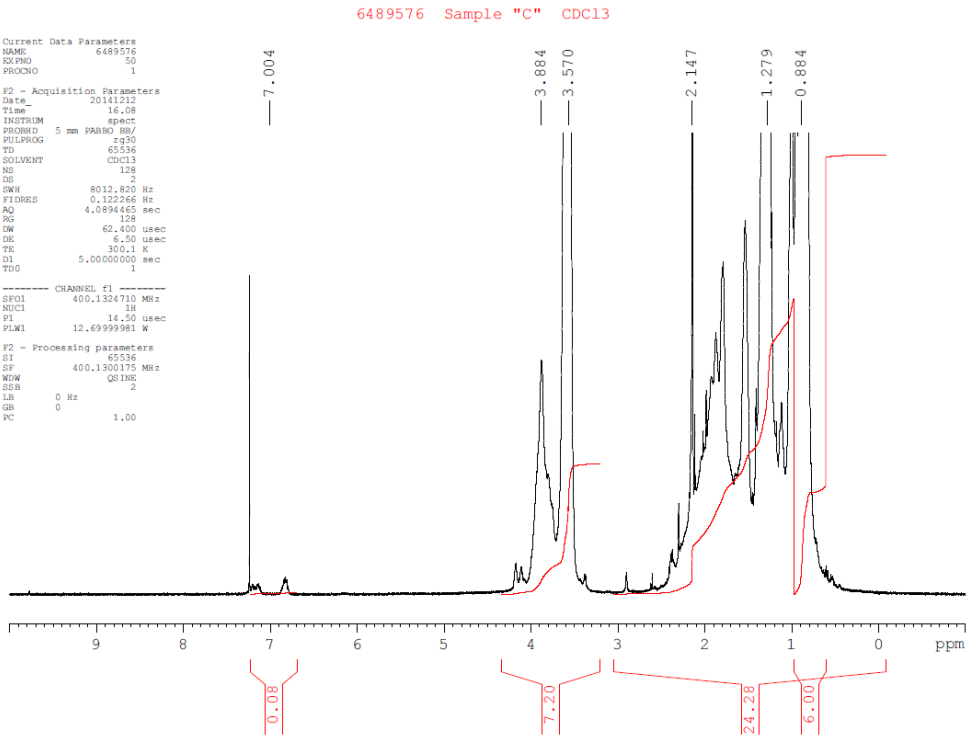

Figure A20. H^1-NMR Spectra of Polymer C

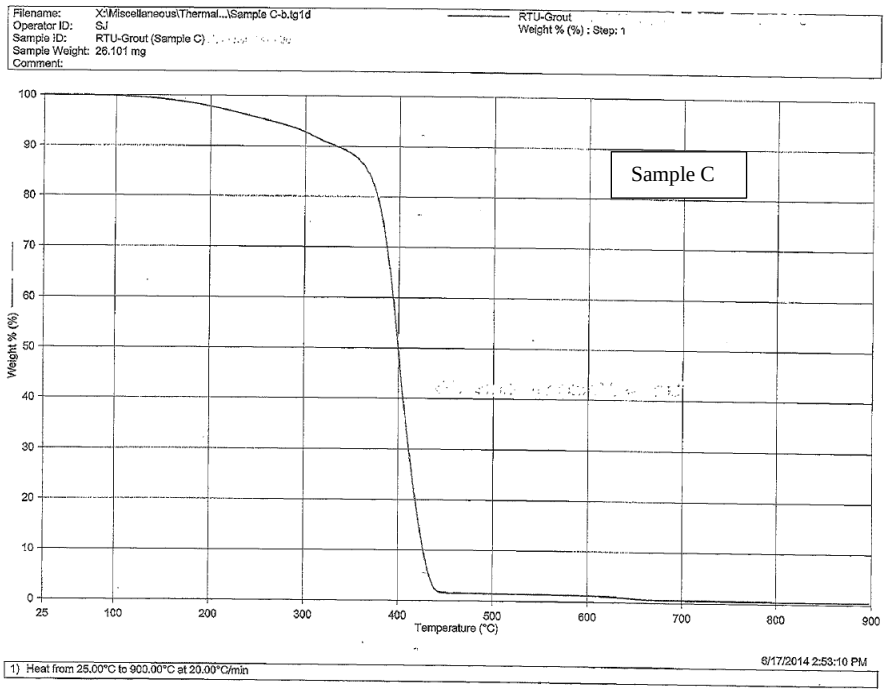

Figure A21. TGA Thermal Curve of Polymer C

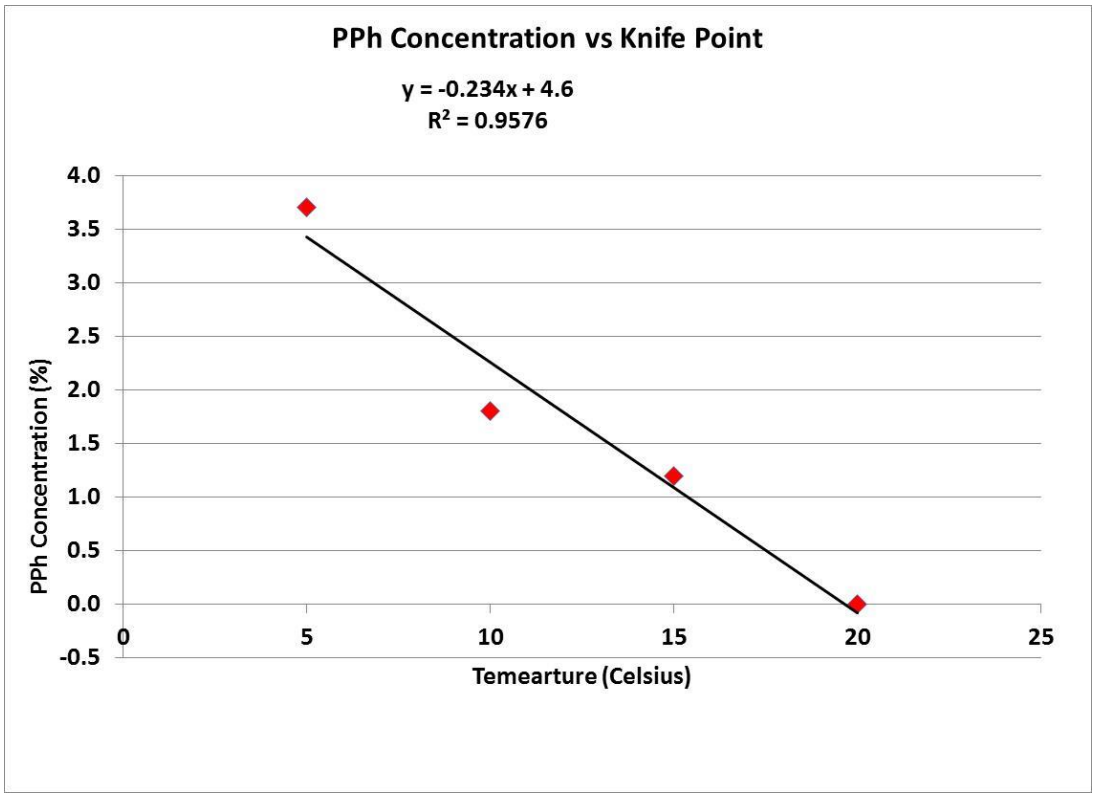

Figure A22. MFFT of Polymer D with PPh by Knifepoint

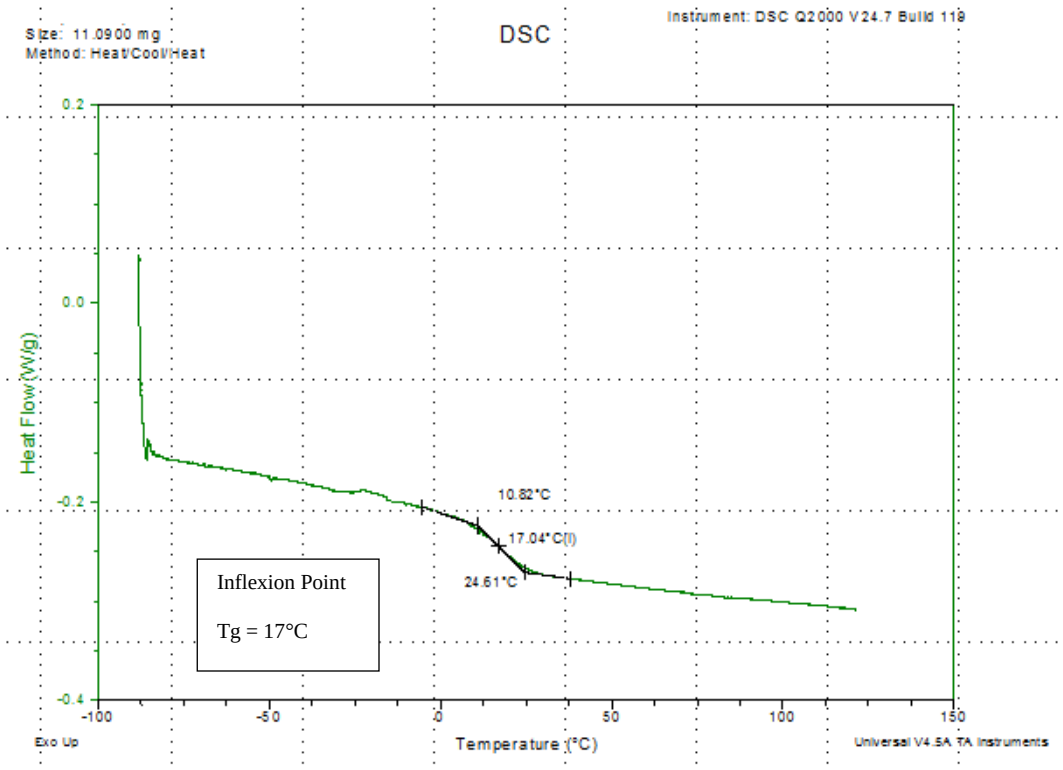

Figure A23. DSC Scan of Polymer D

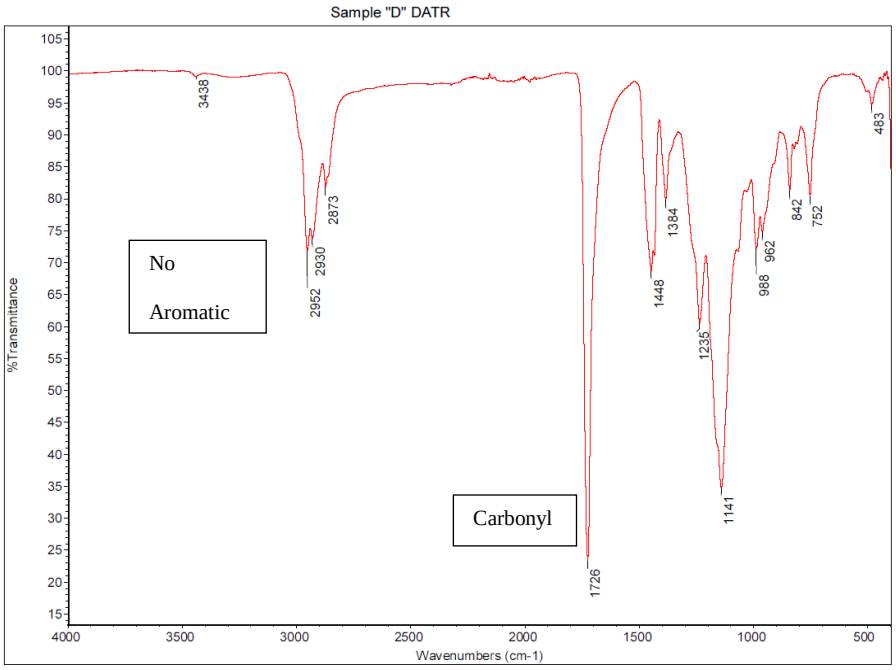

Figure A24. FT-ATR Spectra of Polymer D

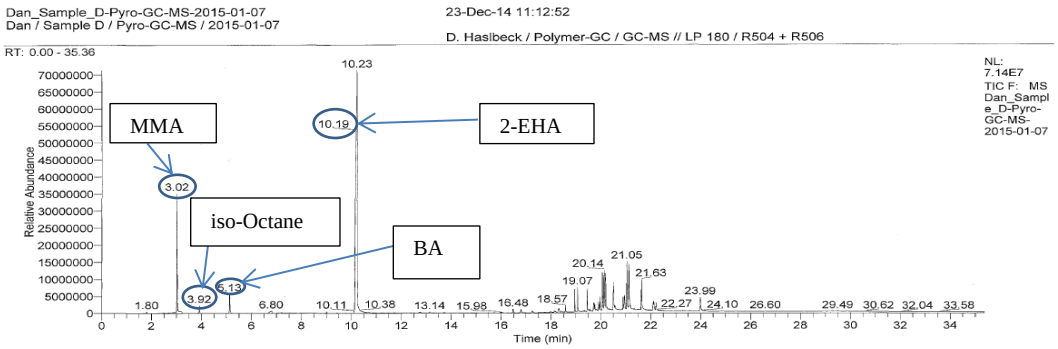

Figure A25. Pyrolysis-GC-MS Chromatograph of Polymer D

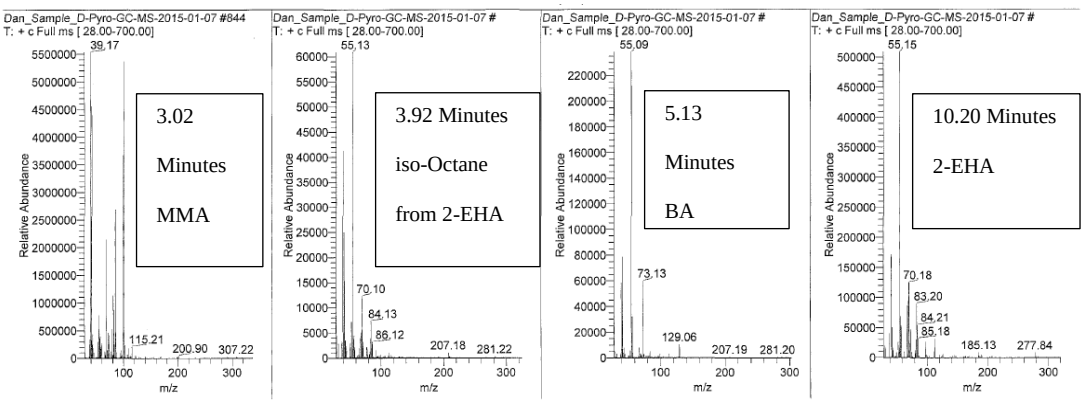

Figure A26. Total Ion Chromatogram for Components in Polymer D

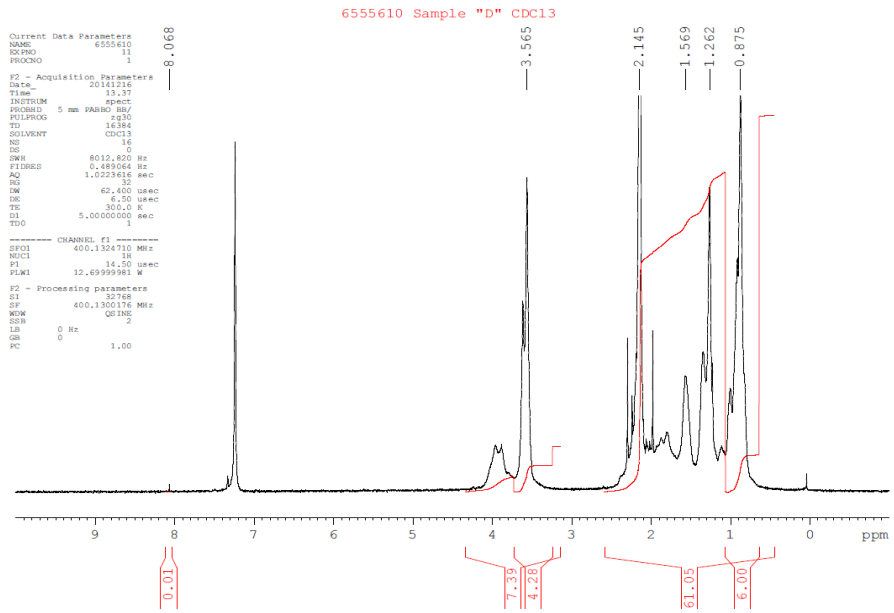

Figure A27. H^1-NMR Spectra for Polymer D

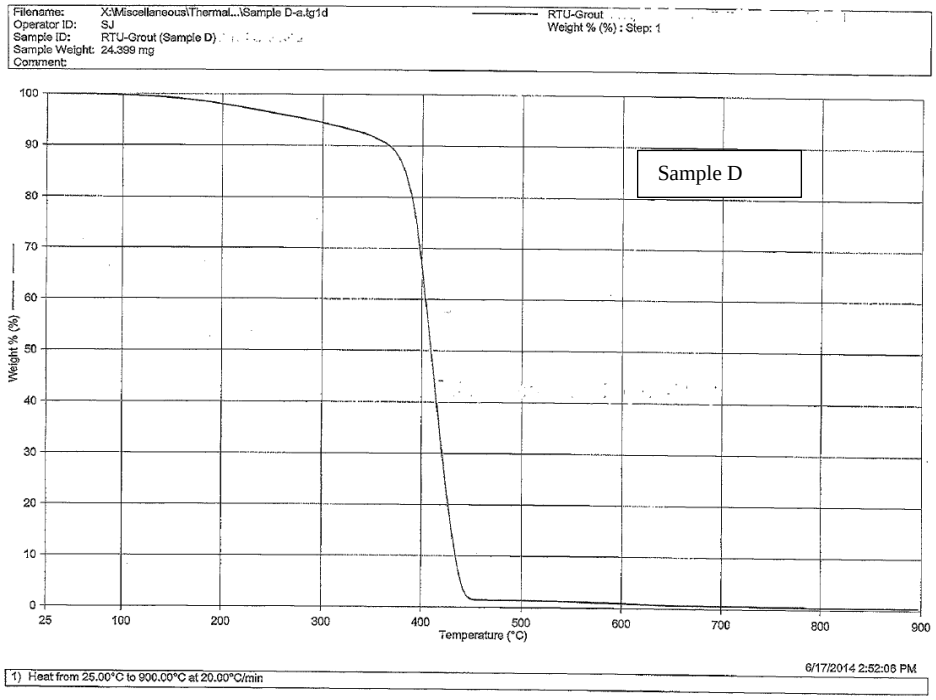

Figure A28. TGA Thermal Curve of Polymer D

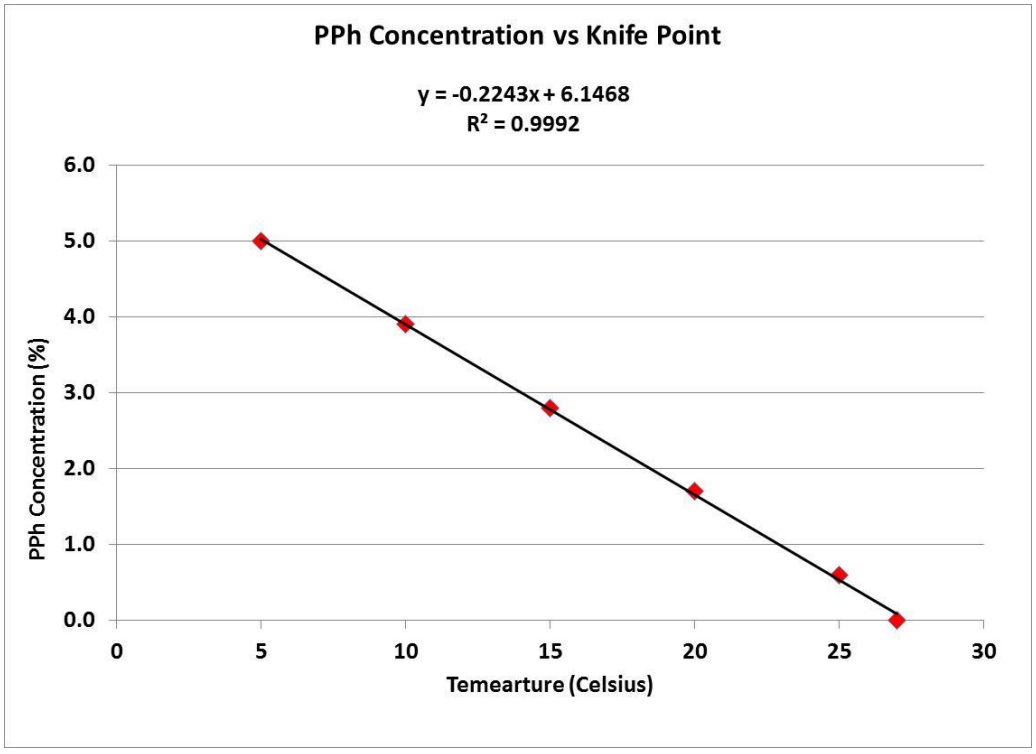

Figure A29. MFFT of Polymer F with PPh by Knifepoint

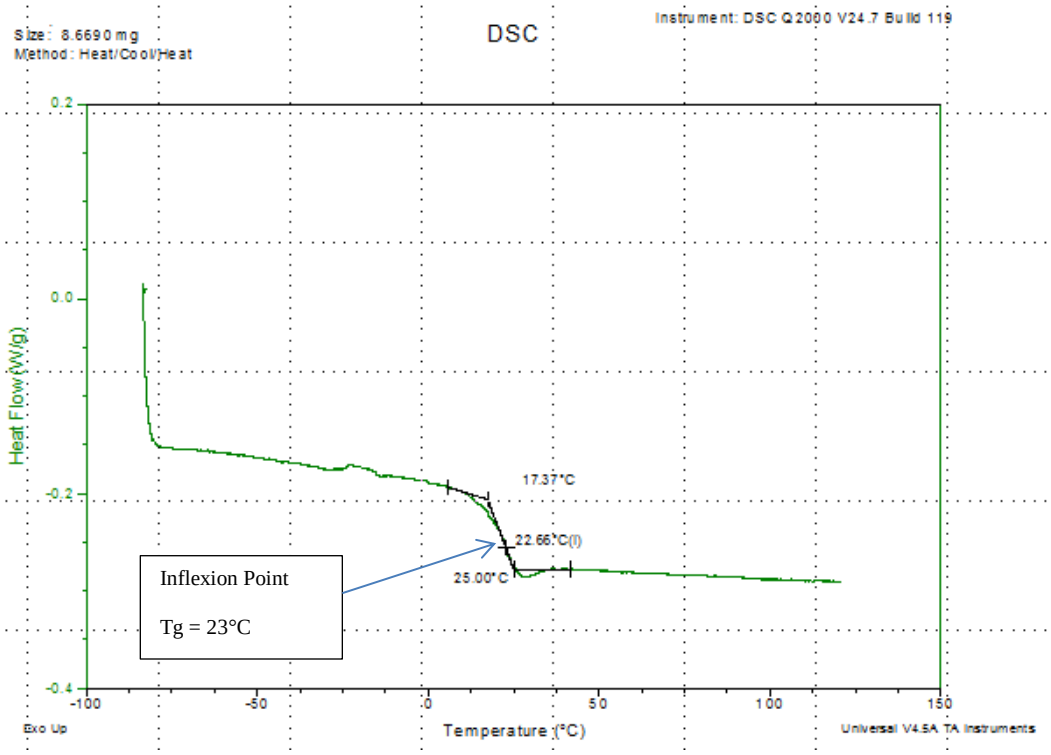

Figure A30. DSC Scan of Polymer F

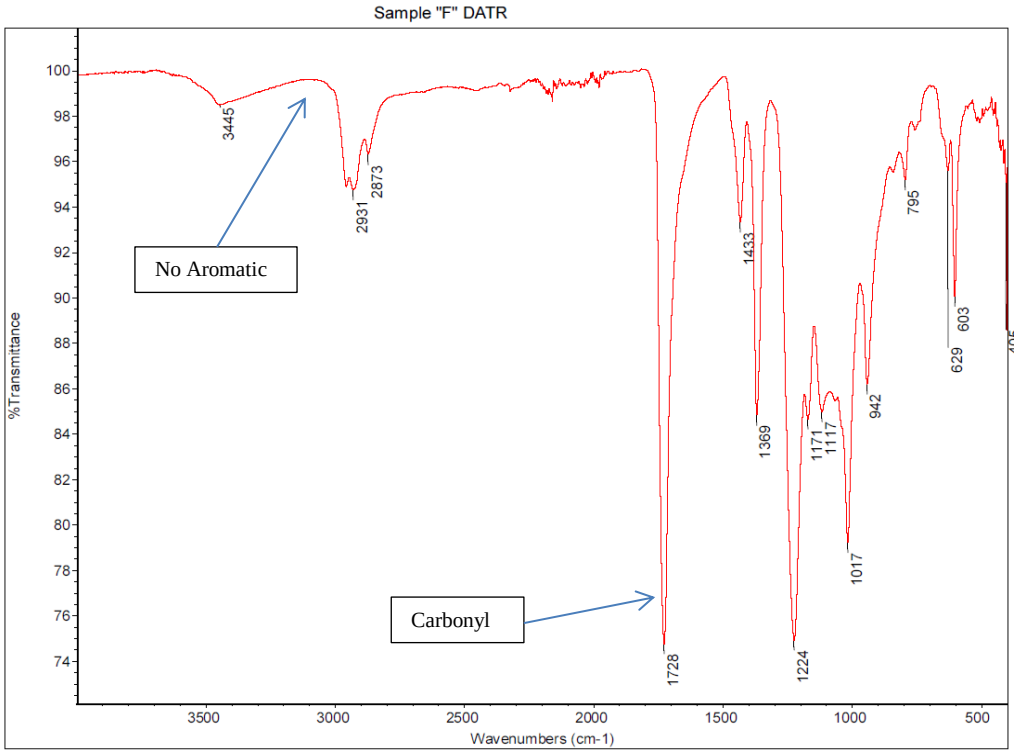

Figure A31. FT-ATR Spectra of Polymer F

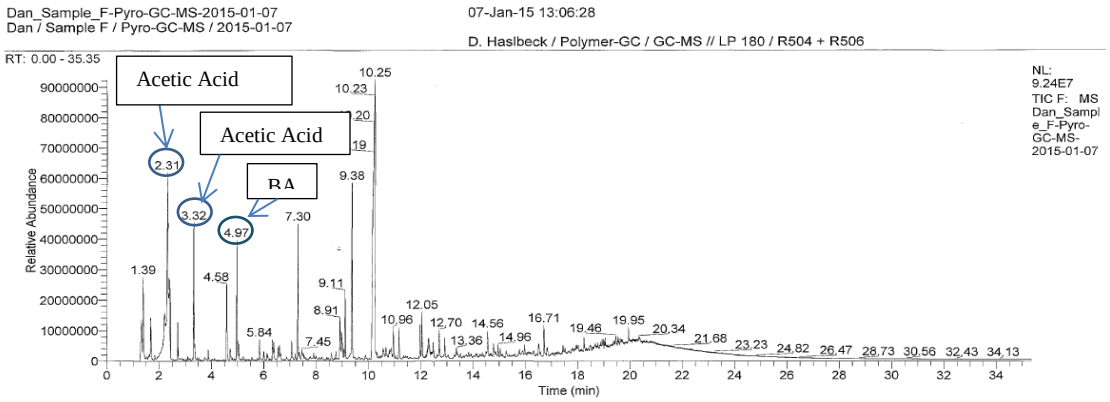

Figure A32. Pyrolysis-GC-MS Chromatograph of Polymer F

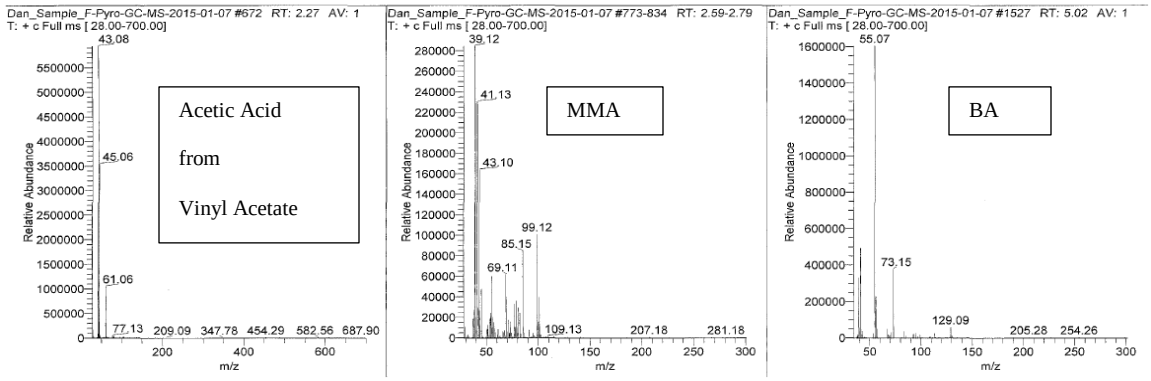

Figure A33. Total Ion Chromatogram for Components of Polymer F

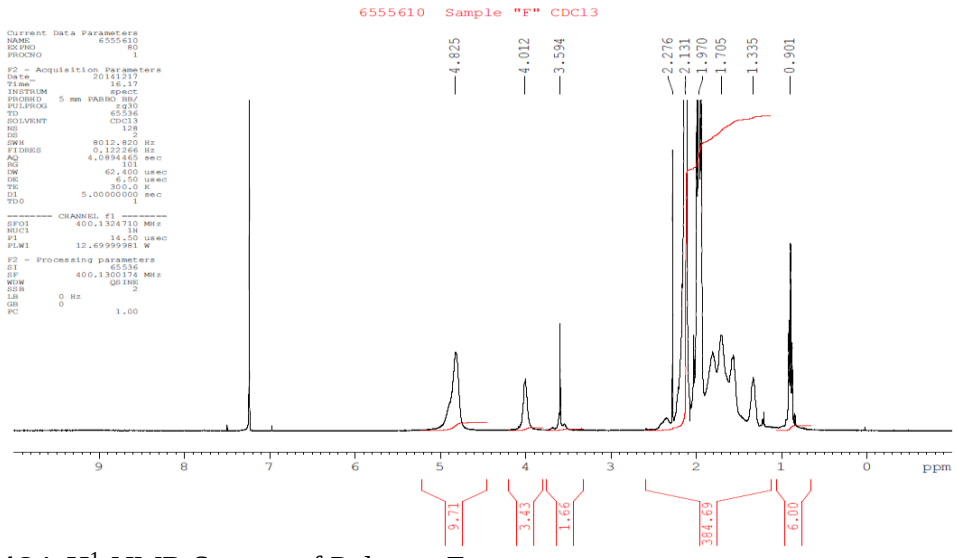

Figure A34. H^1-NMR Spectra of Polymer F

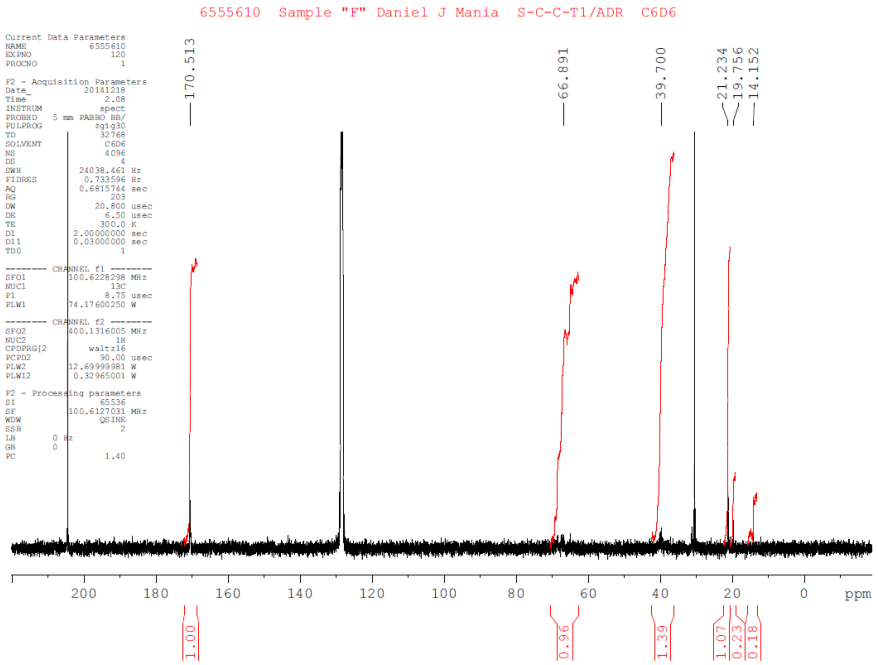

Figure A35. C^{13}-NMR Spectra of Polymer F

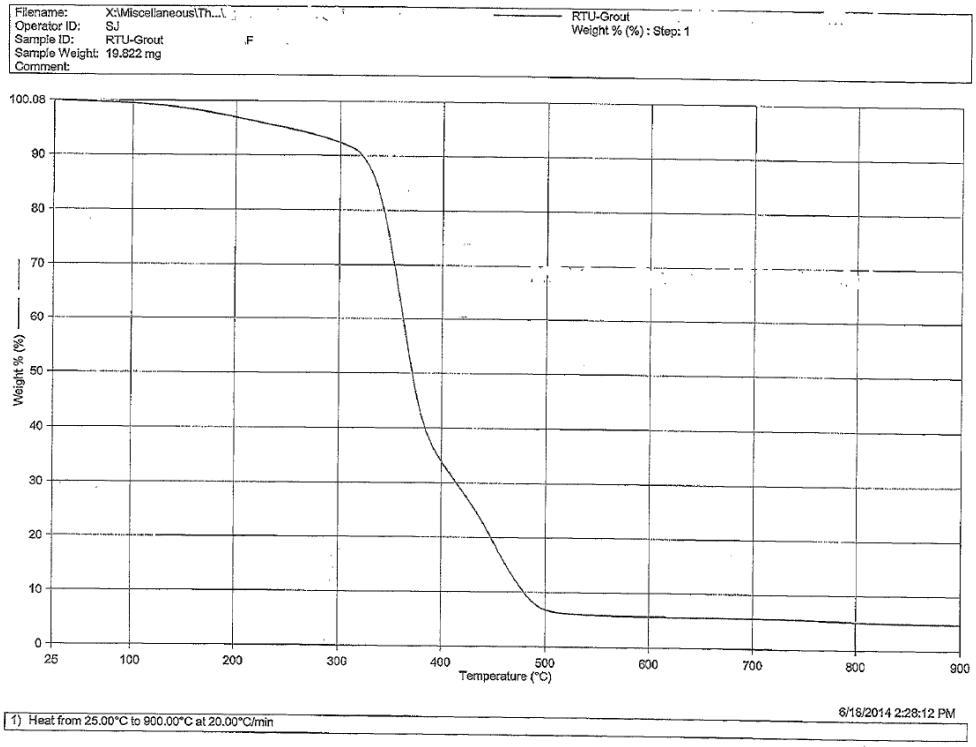

Figure A36. TGA Thermal Curve of Polymer F

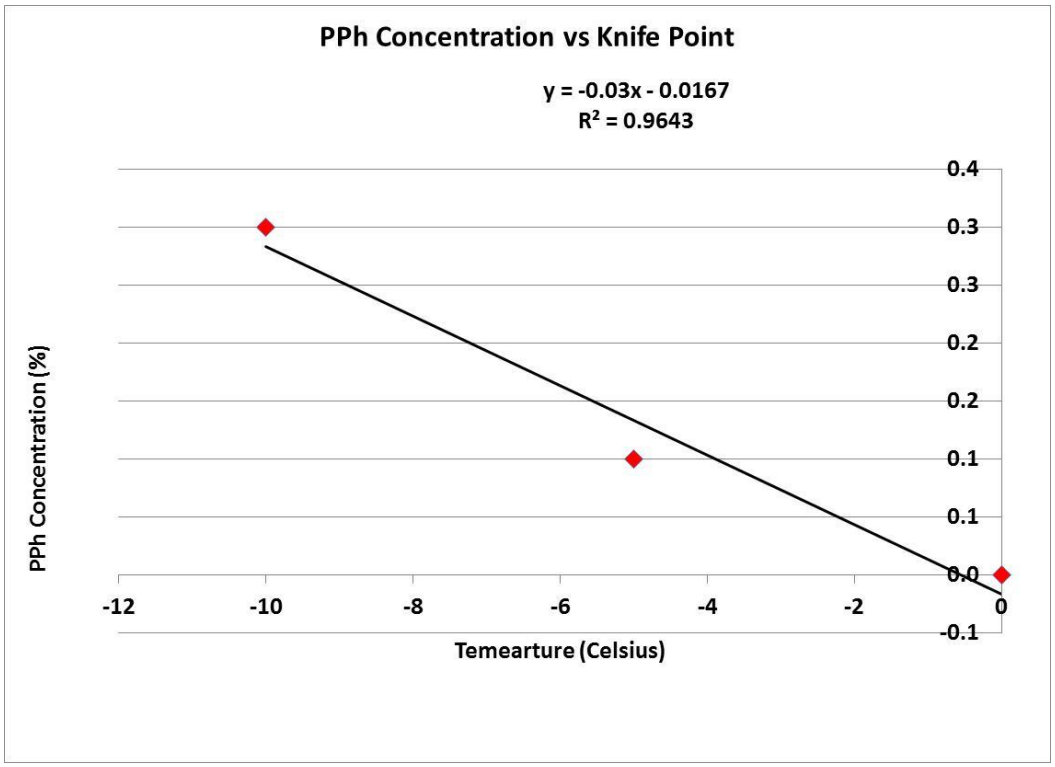

Figure A37. MMFT of Polymer H with PPh by Knifepoint

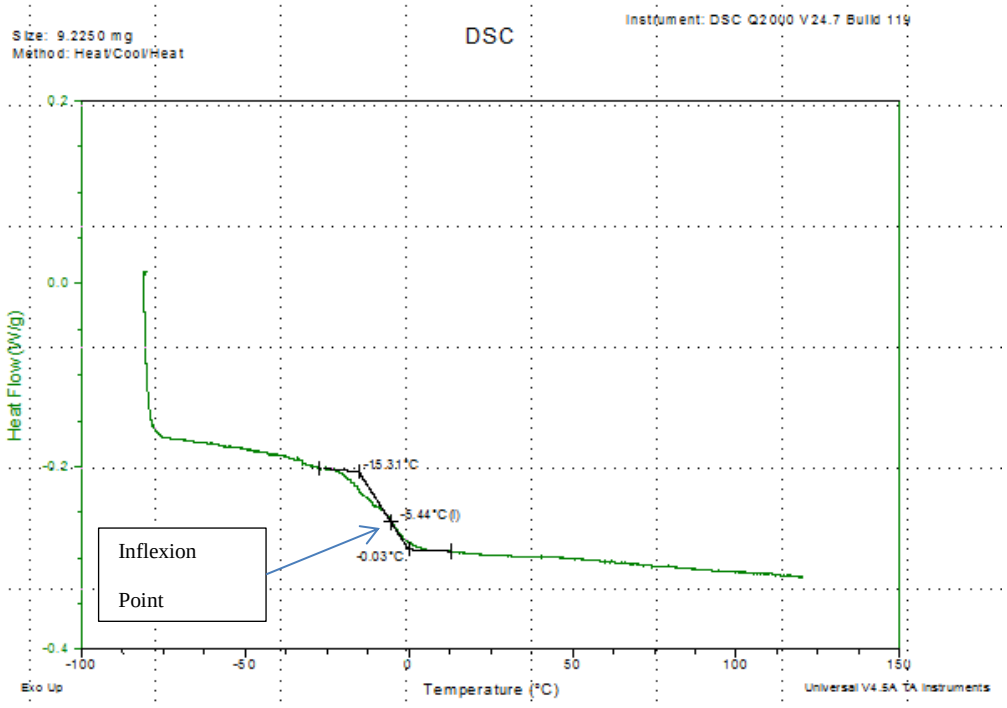

Figure A38. DSC Scan of Polymer H

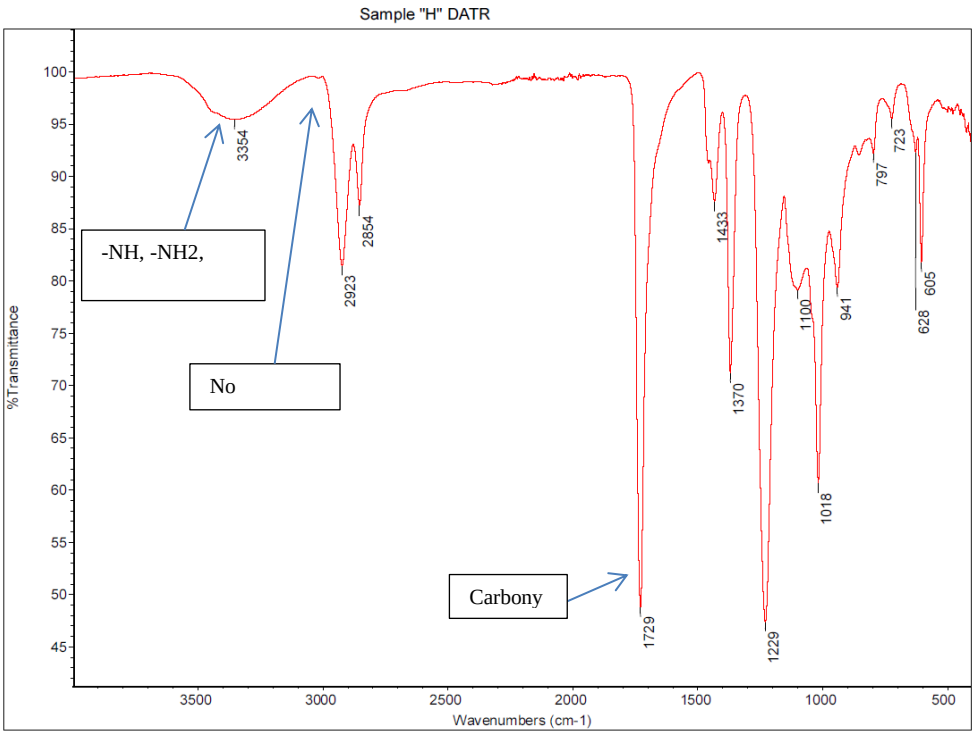

Figure A39. FT-ATR Spectra of Polymer H

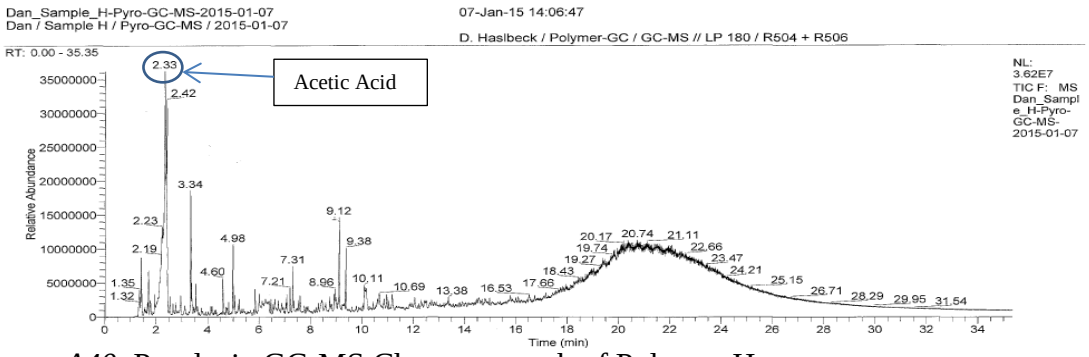

Figure A40. Pyrolysis-GC-MS Chromatograph of Polymer H

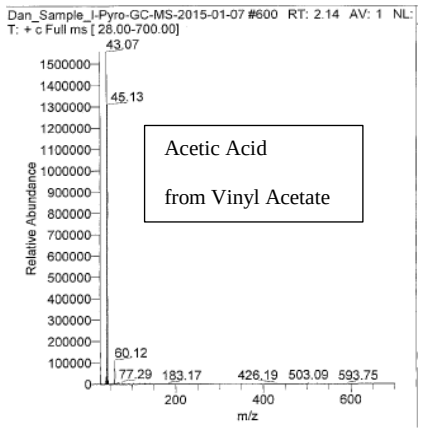

Figure A41. Total Ion Chromatogram of Components of Polymer H

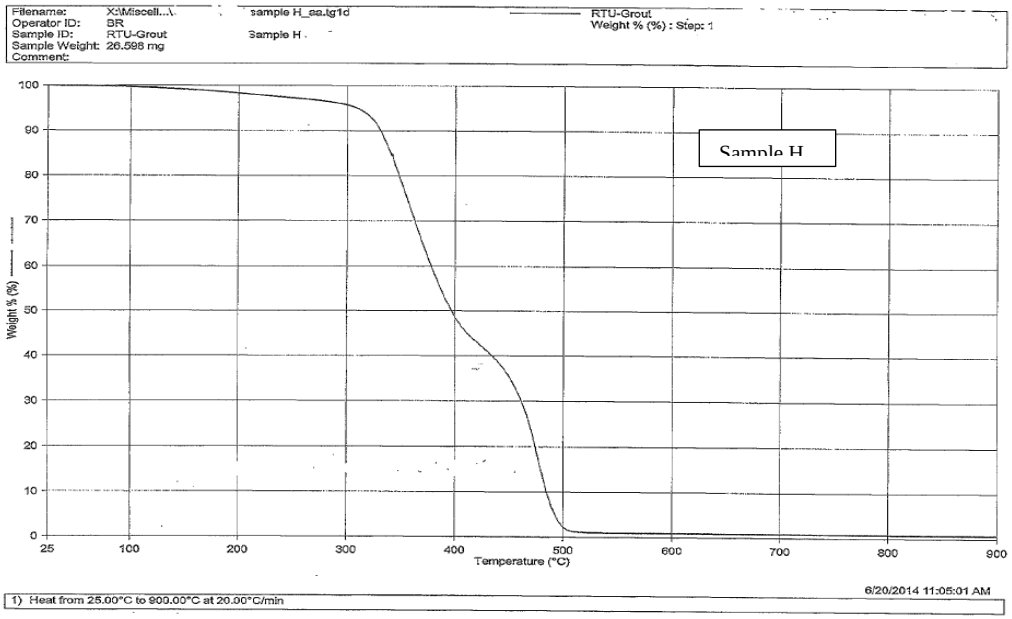

Figure A42. TGA Thermal Curve of Polymer H

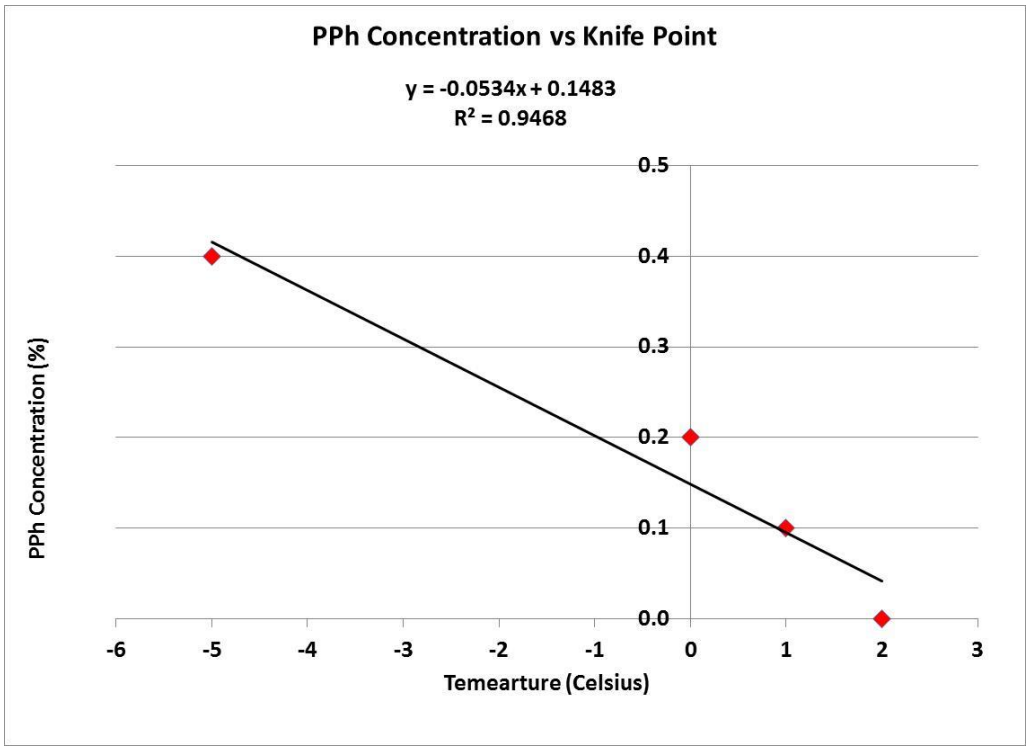

Figure A43. MFFT of Polymer I with PPh.

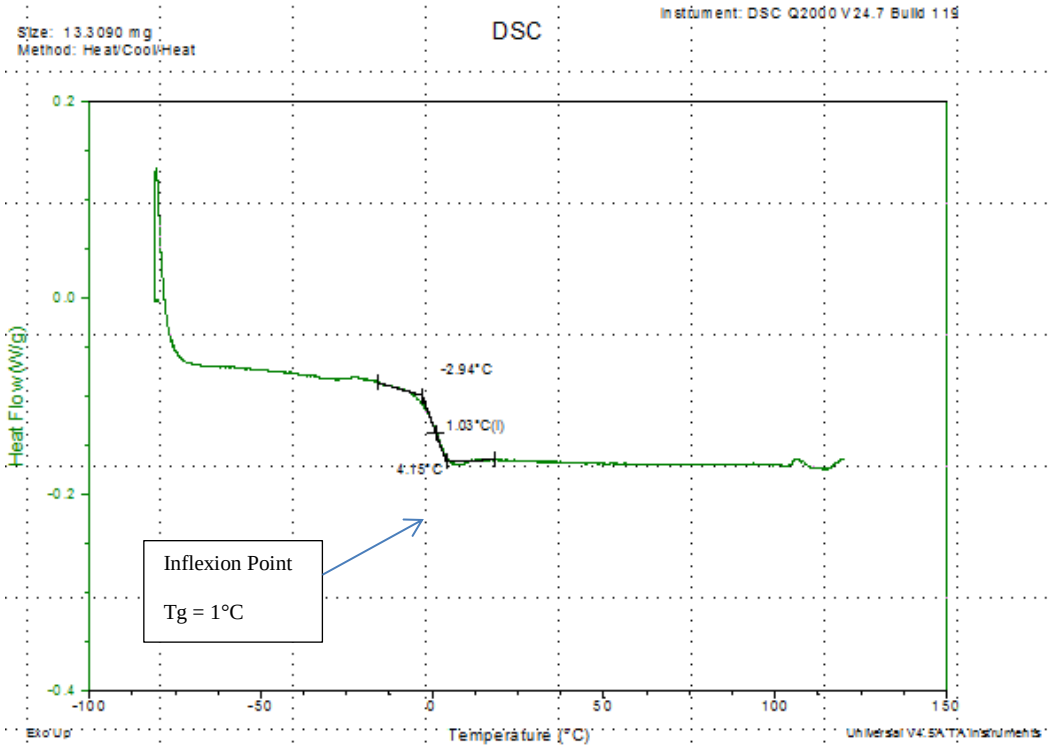

Figure A44. DSC Scan of Polymer I

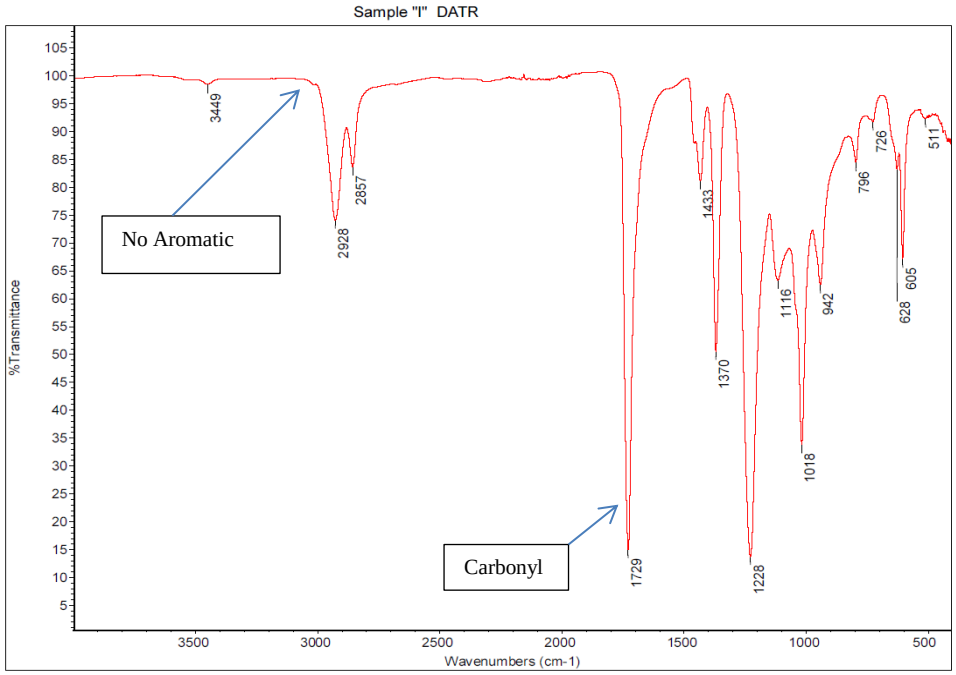

Figure A45. FT-ATR Spectra of Polymer I

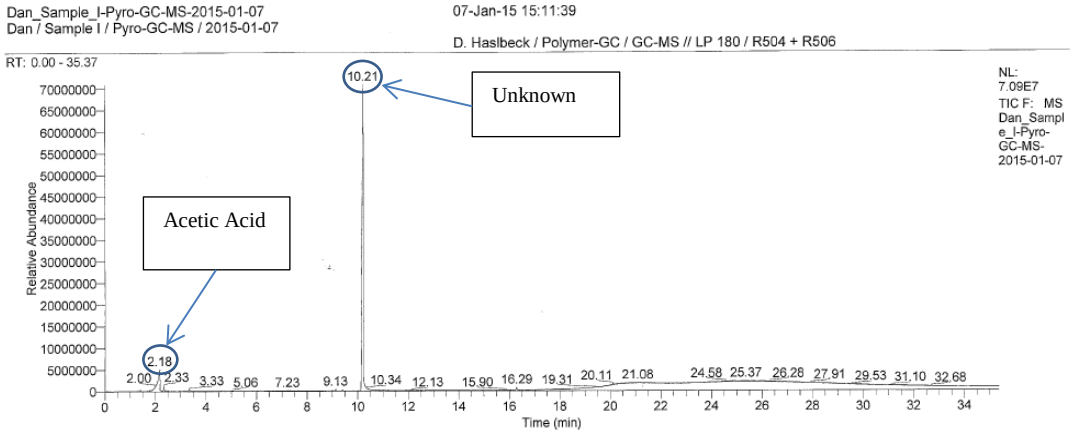

Figure A46. Pyrolysis-GC-MS Chromatograph of Polymer I

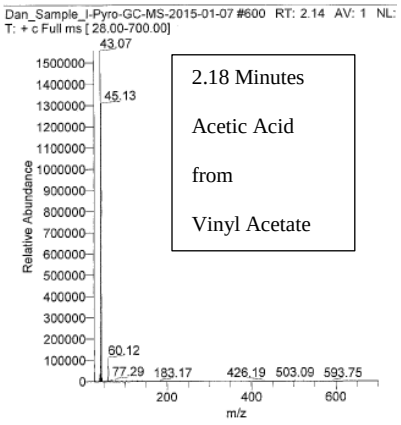

Figure A47. Total Ion Chromatogram of Components of Polymer I

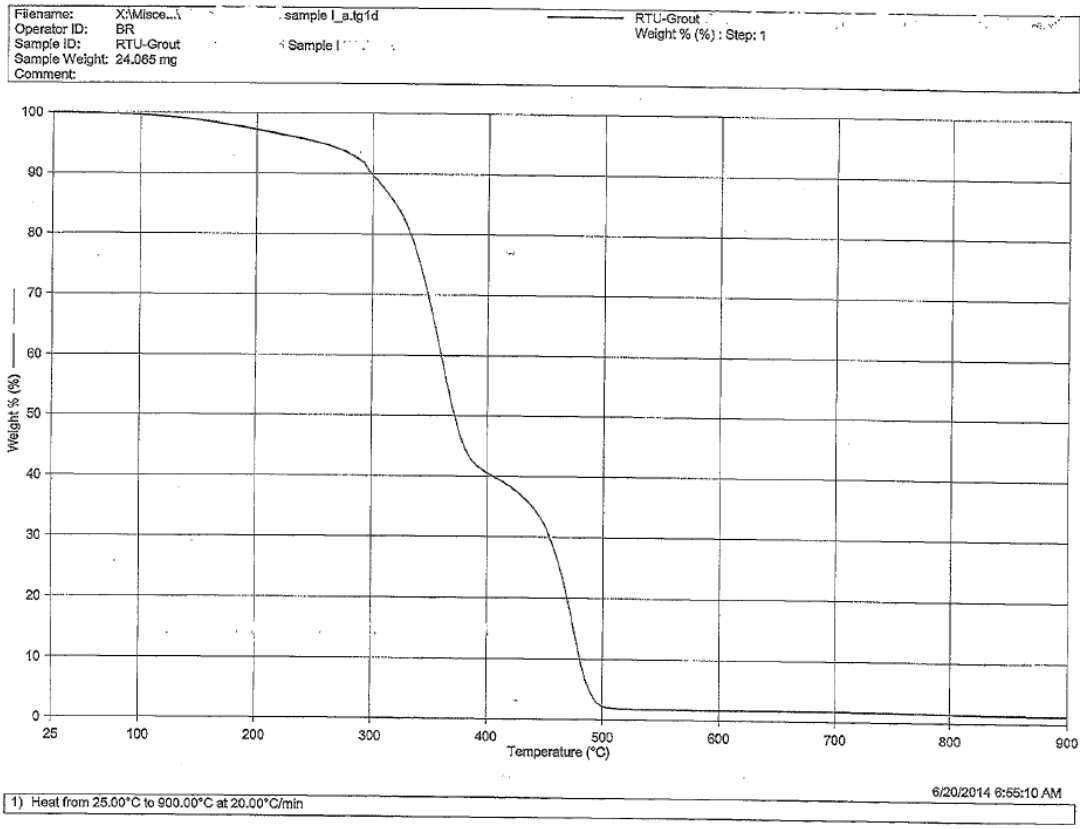

Figure A48. TGA Thermal Curve of Polymer I

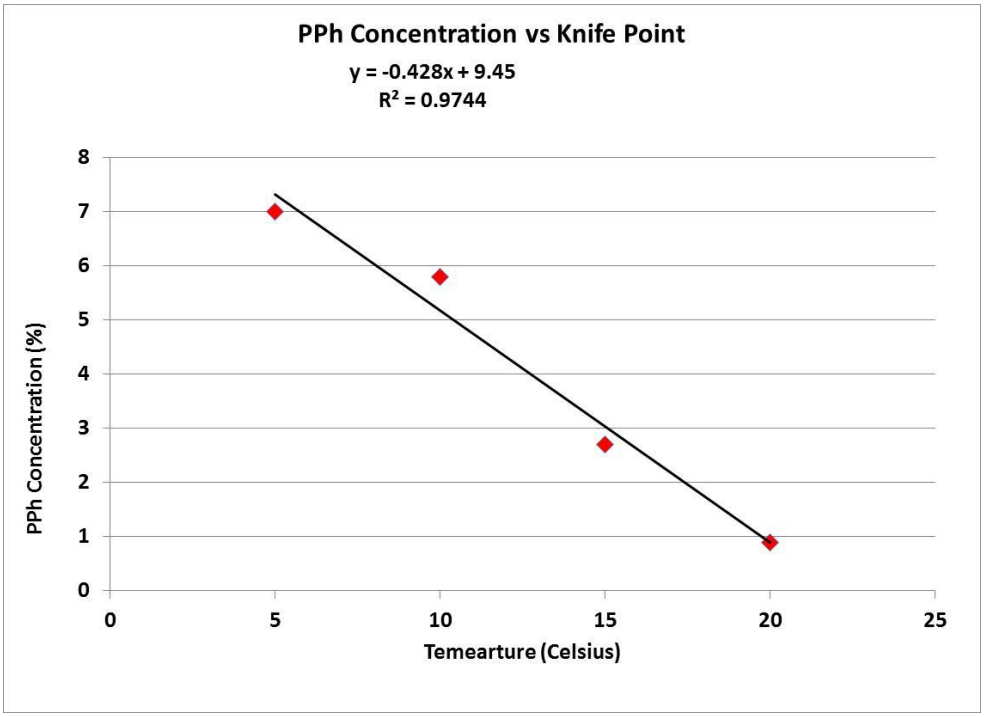

Figure A49. MFFT of Polymer J with PPh by Knifepoint

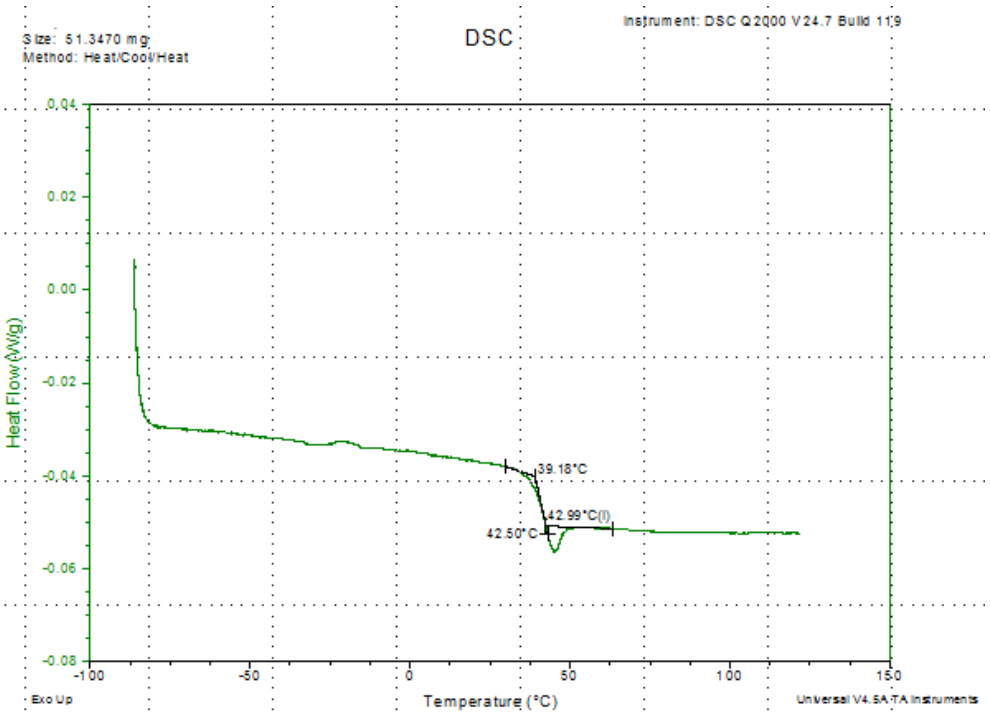

Figure A50. DSC Scan of Polymer J.

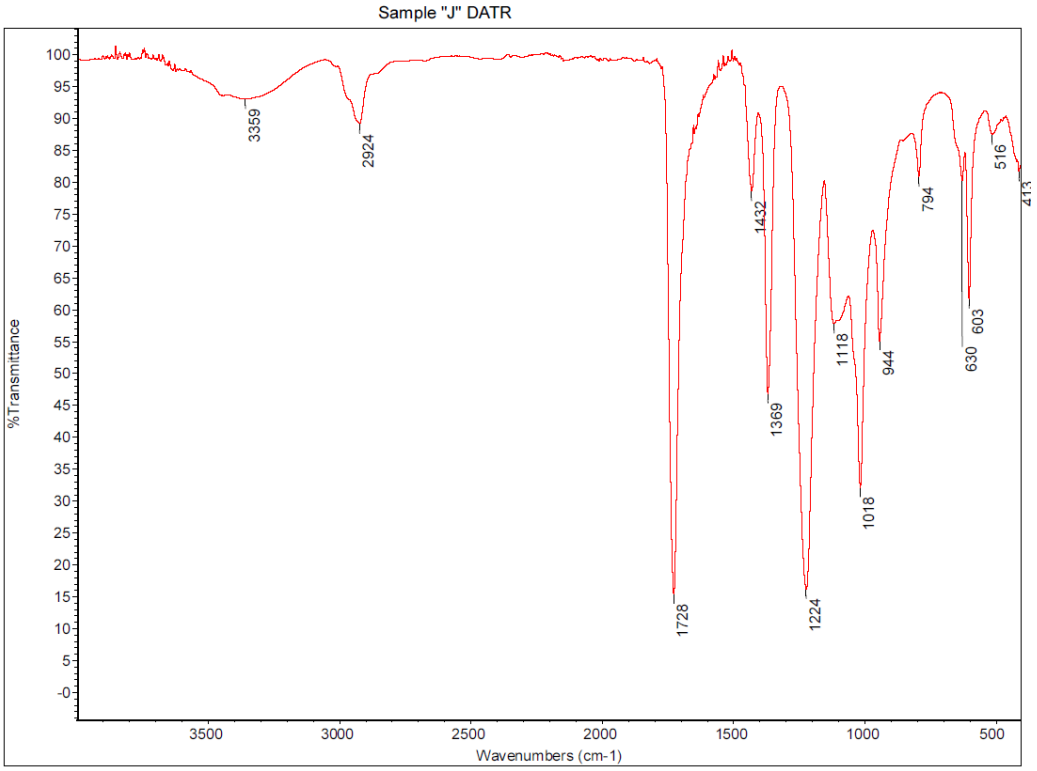

Figure A51. FT-ATR Spectra of Polymer J

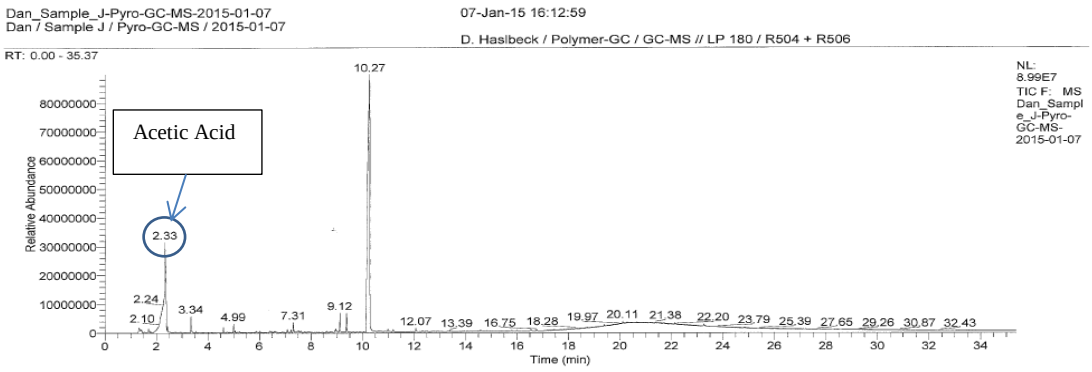

Figure A52. Pyrolysis-GC-MS Chromatograph of Polymer J

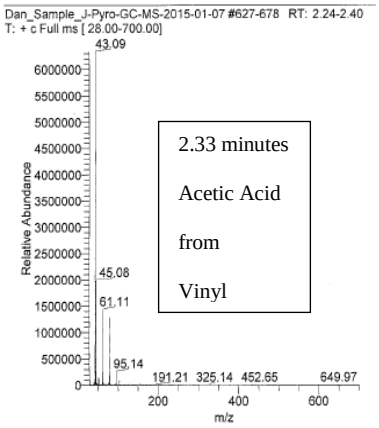

Figure A53. Total Ion Chromatogram of Components of Polymer J

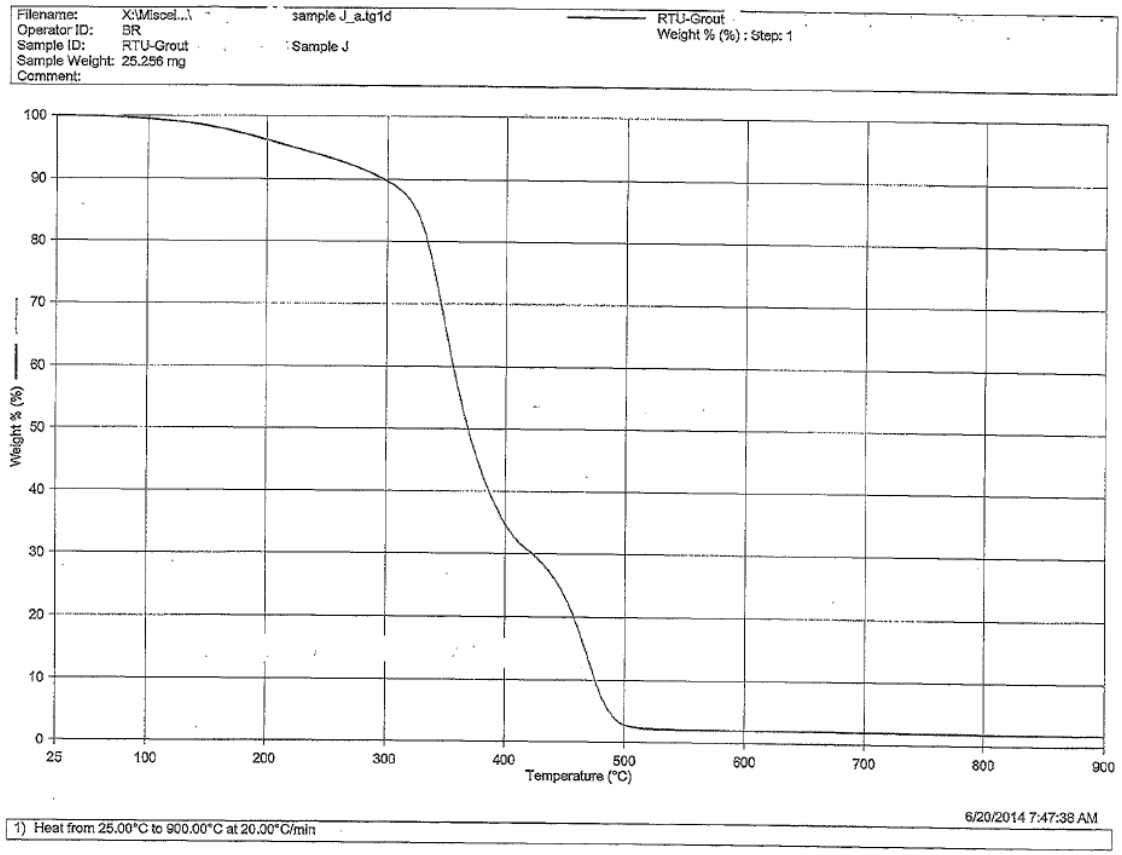

Figure A54. TGA Thermal Curve of Polymer J

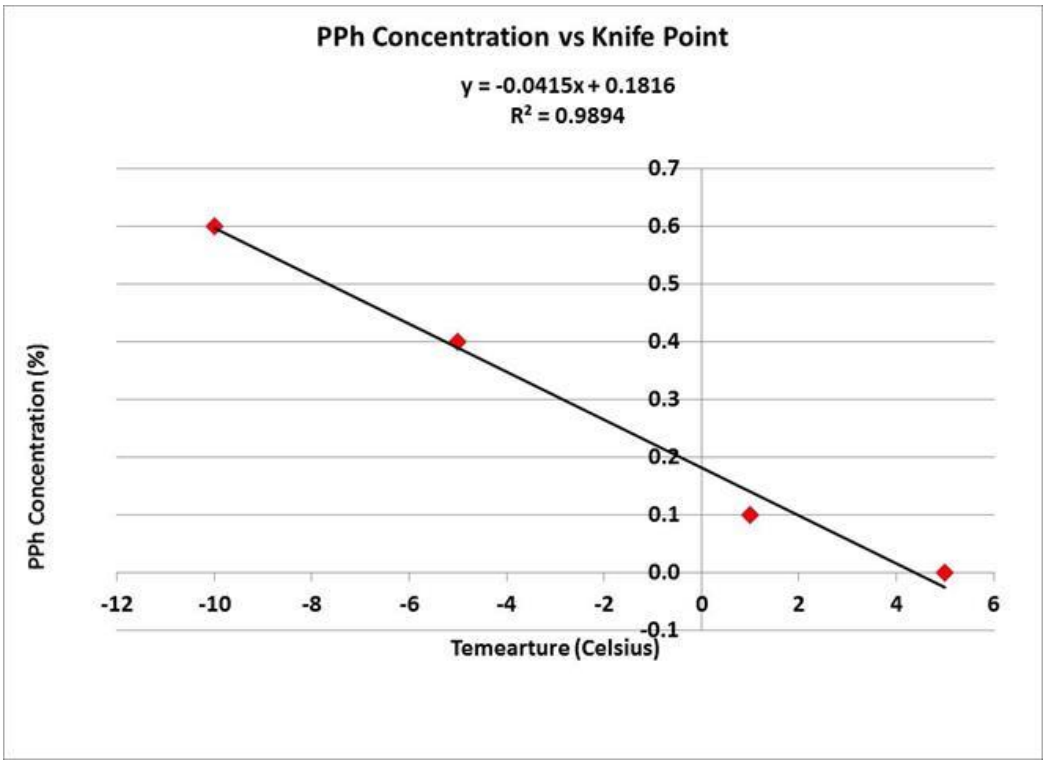

Figure A55. MFFT of Polymer L with PPh by Knifepoint

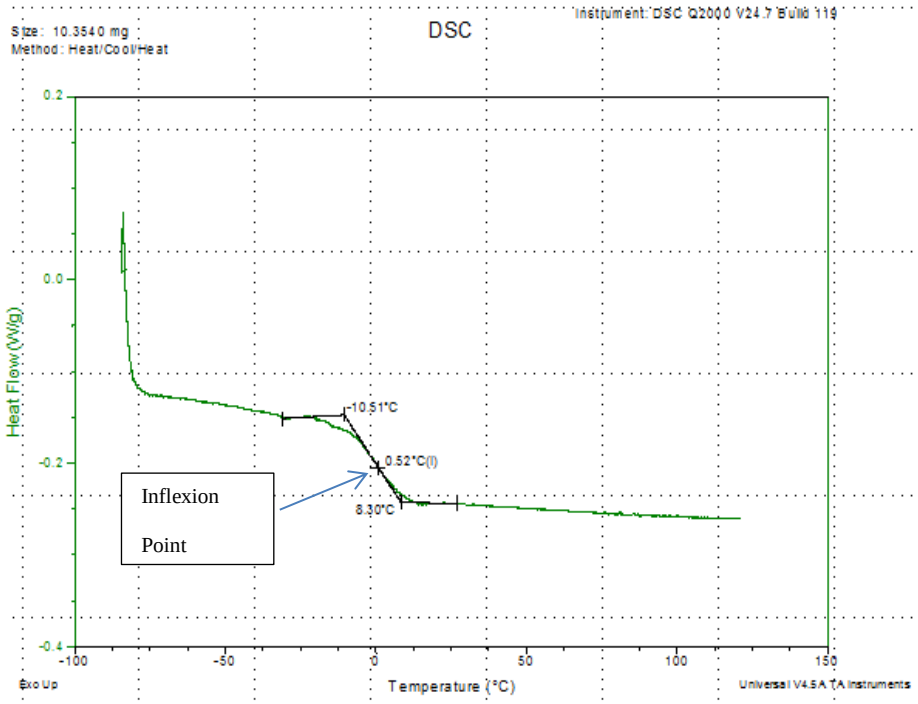

Figure 52. DSC Scan of Polymer L

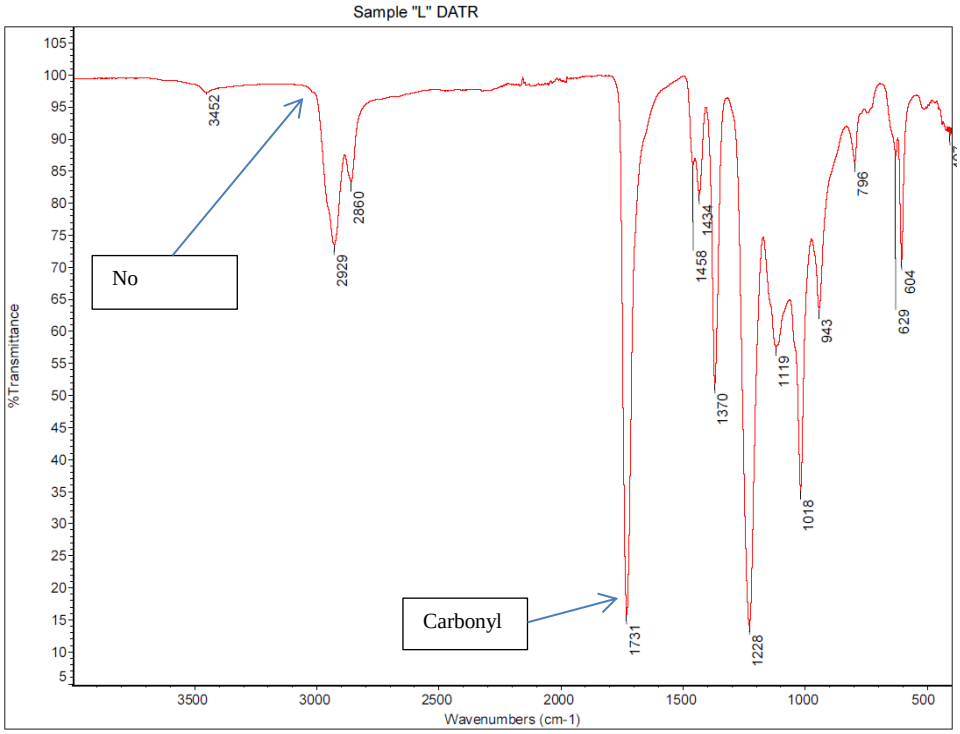

Figure A56. FT-ATR Spectra of Polymer L

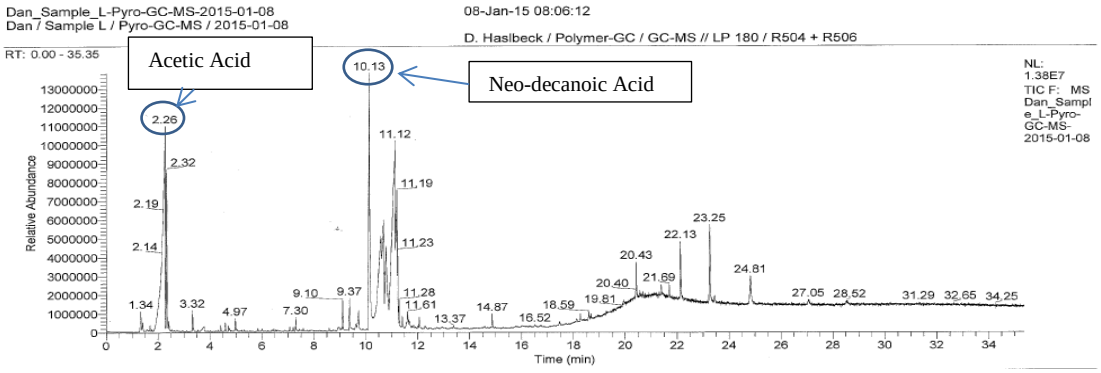

Figure A57. Pyrolysis-GC-MS Chromatograph of Polymer L

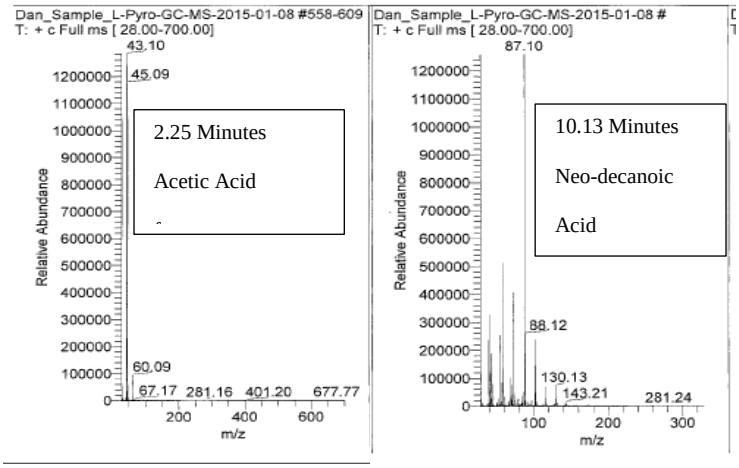

Figure 53. Total Ion Chromatogram of Polymer L.

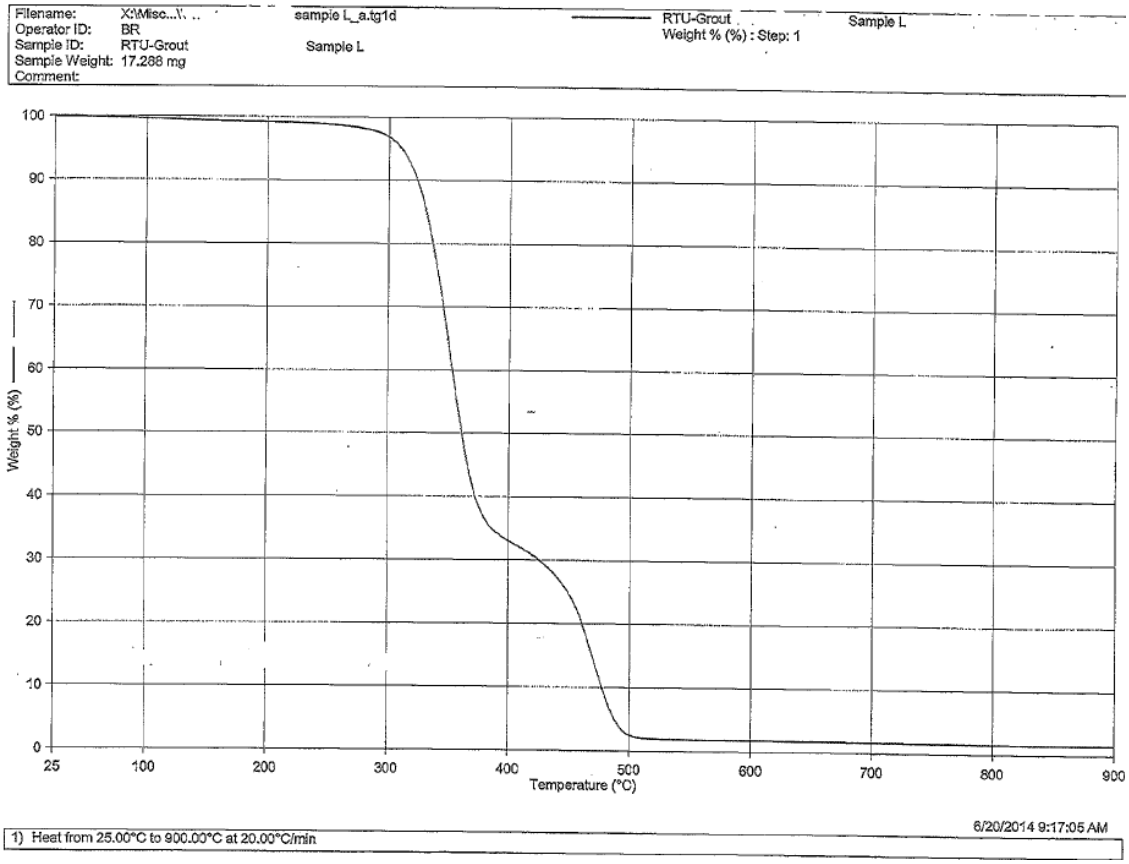

Figure A58. TGA Thermal Curve of Polymer L

APPENDIX B – Summarized and Averaged Raw Data

Table A1.

Comparative Grout Technology Data

Property / Technology	**RTU Average**	**Cement Only**	**Cement w/Dry Polymer**	**Cement w/Liquid Admixture**	**DIY Epoxy**	**Industrial Epoxy**
Water-Absorption (%)	13.0	7.7	9.7	7.8	0.7	0.3
UTS (MPa)	1.5	0.3	0.7	1.0	1.9	19.7
Elongation (%)	10.99	1.0	1.0	1.3	1.0	4.8
Total Stain Repellency	8.6	29.5	29.5	30.0	13.5	4.0
Volume Shrinkage*	13.3	9.9	20.9	12.6	5.5	12.5
Cracking	9.1	10.0	0.0	10.0	10.0	10.0
Lap Shear Adhesion (MPa)	0.42	1.4	1.7	1.2	1.1	1.3
Surface Hardness (Shore D Durometer)	29.8	80.0	73.0	68.0	70.0	72.0
Clean-up	9.0	10.0	10.0	10.0	9.0	1.0
Cost ($/gal.)	45	15	20	30	100	150

* Volume Shrinkage performed according to volume shrinkage determination via ASTM D 2697-03

Table A2.

Commercial RTU Grout Survey Data

Property / Sample	**A**	**B**	**C**	**D**	**E**	**F**	**G**	**H**	**I**	**J**
Water Absorption (%)	17.2	Fell Apart	11.4	10.5	Dissolved	87.9	98.2	10.3	12.8	15.7
UTS (MPa)	0.43	1.10	1.84	1.74	2.19	0.94	2.30	2.73	0.69	0.76
Elongation (%)	26.4	10.5	3.4	2.0	3.0	16.0	6.8	1.6	19.2	21
Total Stain Repellency	8.5	7.0	13.5	10.5	35.0	4.5	12.5	10.0	4.0	7.0
Volume Shrinkage*	7.8	2.4	11.2	10.9	18.0	4.1	39.7	18.8	9.9	10.4
Cracking	9.3	9.3	8.3	7.8	2.5	9.0	9.5	8.5	10.0	9.8
Lap-Shear Adhesion (MPa)	0.35	0.21	0.58	0.80	0.75	0.13	0.48	0.56	0.19	0.16
Surface Hardness (Shore D Durometer)	30	6	34	43	31	19	37	17	61	20
Clean-up	9.0	10.0	10.0	6.0	10.0	5.0	9.0	9.5	9.0	10.0
Application	7.6	8.0	9.5	9.0	6.0	8.3	8.6	8.0	7.9	8.0

* Volume Shrinkage performed according to volume shrinkage determination via ASTM D 2697-03

APPENDIX C – Property / Sample

Table A3.

Data from Paper Presented at 40th Waterborne Symposium, New Orleans, LA, 4 – 8 February 2013, samples 1 – 9.

	1	**2**	**3**	**4**	**5**	**6**	**7**	**8**	**9**
Grout PVC	80	80	80	80	80	80	80	80	80
Polymer T_g (K)	287	287	287	287	287	287	287	287	287
Filler OA Value	8	11	6	8	11	6	8	11	6
Filler Particle Size (µm)	6	6	21	6	6	21	6	6	21
Fiber Concentration (%)	3	6	0	3	6	0	3	6	0
Water Absorption (%)	8.6	10.5	29.1	8.4	9.4	25.6	8.8	10.0	25.6
UTS (MPa)	2.46	2.86	1.18	2.33	2.92	1.52	2.92	2.41	0.91
Young's Modulus (MPa)	0.3	0.6	0.6	0.4	0.6	0.6	0.5	1.5	0.3
Elongation	3.3	3.8	14.2	3.8	4.0	8.8	4.0	3.6	14.4
Total Stain Repellency	19.0	23.0	19.5	18.5	17.5	15.5	20.0	18.0	18.0
Volume Shrinkage (%)*	27.1	31.9	11.3	26.6	23.6	9.3	25.5	25.1	12.5
Cracking	4.5	5.8	5.3	5.0	6.0	8.8	4.3	4.8	6.5
Lap Shear Adhesion (MPa)	1.26	0.54	0.11	0.86	0.53	0.63	1.41	0.63	0.18

Table A3 (continued).

Surface Hardness (Shore D Durometer)	45	33	14	34	38	13	30	36	11
Clean-up	9.5	9.5	10.0	10.0	9.5	10.0	9.5	10.0	9.5
Application	6.9	5.6	8.9	7.6	6.6	8.5	7.3	5.5	9.5

* Volume Shrinkage performed according to volume shrinkage determination via ASTM D 2697-03

Table A4.

Data from Paper Presented at 40th Waterborne Symposium, New Orleans, LA, 4 – 8 February 2013, samples 10 – 18

	10	**11**	**12**	**13**	**14**	**15**	**16**	**17**	**18**
Grout PVC	85	85	85	85	85	85	85	85	85
Polymer T_g (K)	287	287	287	287	287	287	287	287	287
Filler OA Value	8	11	6	8	11	6	8	11	6
Filler Particle Size (µm)	6	6	21	6	6	21	6	6	21
Fiber Concentration (%)	3	6	0	3	6	0	3	6	0
Water Absorption (%)	11.5	10.7	28.1	10.1	10.7	23.1	10.2	11.6	22.8
UTS (MPa)	2.54	2.95	0.83	3.38	1.32	1.47	4.33	2.09	1.28

Table A4 (continued).

Young's Modulus (MPa)	0.2	0.9	0.4	0.5	0.4	0.4	0.6	0.4	0.8
Elongation	5.8	4.5	11.2	4.4	6.7	4.4	4.0	5.7	5.2
Total Stain Repellency	19.0	21.0	14.0	18.0	20.5	14.0	21.0	25.0	18.0
Volume Shrinkage (%)*	21.5	17.6	9.6	20.0	25.6	6.7	20.7	26.5	5.5
Cracking	7.0	7.0	9.3	6.0	7.0	9.3	6.8	4.5	9.3
Lap Shear Adhesion (MPa)	0.64	0.57	0.23	0.78	0.41	0.35	0.29	0.38	0.12
Surface Hardness (Shore D Durometer)	21	42	11	30	32	16	39	37	16
Clean-up	10.0	10.0	9.5	9.5	9.5	10.0	10.0	10.0	9.0
Application	8.5	6.9	8.6	7.5	8.1	6.1	6.5	8.2	6.5

* Volume Shrinkage performed according to volume shrinkage determination via ASTM D 2697-03

Table A5.

Data from Paper Presented at 40th Waterborne Symposium, New Orleans, LA, 4 – 8 February 2013, samples 19 – 2

Property / Sample	**19**	**20**	**21**	**22**	**23**	**24**	**25**	**26**	**27**
Grout PVC	80	80	80	80	80	80	80	80	80
Polymer T_g (K)	336	336	336	336	336	336	336	336	336
Filler OA Value	8	11	6	8	11	6	8	11	6
Filler Particle Size (μm)	6	6	21	6	6	21	6	6	21
Fiber Concentration (%)	6	0	3	6	0	3	6	0	3
Water Absorption (%)	3.3	1.8	8.5	2.0	1.7	8.0	1.5	2.4	6.7
UTS (MPa)	4.94	5.18	2.75	5.01	4.78	2.33	6.01	3.56	1.99
Young's Modulus (MPa)	1.1	0.9	0.7	0.3	0.2	0.8	0.8	0.8	1.7
Elongation	1.5	1.7	1.0	1.3	1.6	1.2	1.0	1.6	1.0
Total Stain Repellency	8.0	11.5	16.5	12.0	11.5	10.5	6.0	11.0	16.5

Table A5. (continued).

Volume Shrinkage (%)*	29.5	21.4	13.5	31.1	21.3	13.2	32.1	23.7	13.4
Cracking	6.8	4.5	7.5	6.3	4.5	8.5	4.5	3.8	7.8
Lap Shear Adhesion (MPa)	0.44	0.20	1.28	0.85	0.23	1.15	0.17	0.71	0.98
Surface Hardness (Shore D Durometer)	69	67	53	65	61	55	63	63	62
Clean-up	3.0	3.5	4.0	4.0	3.5	3.0	4.0	4.0	4.5
Application	6.4	8.8	4.1	6.3	7.5	5.4	8.3	8.5	6.0

*Volume Shrinkage performed according to volume shrinkage determination via ASTM D 2697-03

Table A6.

Data from Paper Presented at 40th Waterborne Symposium, New Orleans, LA, 4 – 8 February 2013, samples 28 – 36.

Property / Sample	**28**	**29**	**30**	**31**	**32**	**33**	**34**	**35**	**36**
Grout PVC	85	85	85	85	85	85	85	85	85
Polymer T_g (K)	336	336	336	336	336	336	336	336	336
Filler OA Value	8	11	6	8	11	6	8	11	6
Filler Particle Size (µm)	6	6	21	6	6	21	6	6	21
Fiber Concentration (%)	0	3	6	0	3	6	0	3	6
Water Absorption (%)	1.5	7.0	8.9	1.7	5.7	9.3	1.3	5.5	7.5
UTS (MPa)	5.10	4.28	1.59	2.52	5.74	3.72	8.23	5.59	3.21
Young's Modulus (MPa)	0.1	0.9	0.8	0.7	1.2	1.0	0.9	1.1	1.0
Elongation	1.0	1.0	1.0	1.0	1.2	1.2	1.5	1.0	1.0
Total Stain Repellency	9.5	9.5	8.5	11.0	8.5	11.5	11.0	13.0	11.0

Table A6 (continued).

Volume Shrinkage (%)*	29.5	21.3	11.2	29.5	19.8	6.6	28.9	18.8	10.0
Cracking	4.5	5.0	9.0	3.8	5.3	8.0	6.3	7.0	8.8
Lap Shear Adhesion (MPa)	0.23	0.55	1.60	0.43	1.14	1.03	0.48	0.84	0.72
Surface Hardness (Shore D Durometer)	68	66	70	59	68	60	70	68	68
Clean-up	7.0	7.5	8.0	8.0	7.5	7.0	8.5	8.5	8.5
Application	6.8	7.9	3.6	7.6	8.3	5.1	7.6	7.8	5.3

*Volume Shrinkage performed according to volume shrinkage determination via ASTM D 2697-03

Table A7.

Data from Paper Presented at 41st Waterborne Symposium, New Orleans, LA, 24 – 28 February 2014, samples 1 – 8.

Property / Sample	**T1**	**T2**	**T3**	**T4**	**T5**	**T6**	**T7**	**T8**
Adhesion (psi)	73	97	106	255	214	108	232	161
Water Absorption (%)	10.58	11.42	10.84	17.70	1.74	7.16	1.65	3.87
Dry Surface Hardness (Shore D Durometer)	35	41	15	17	38	39	15	17
Wet Surface Hardness (Shore D Durometer)	10	8	8	6	32	31	14	10
UTS (MPa)	1.03	1.46	1.14	0.92	2.14	2.72	0.86	0.82
Elongation (%)	5.2	13.3	55.1	87.5	4.4	10.1	53.3	29.2
Young's Modulus (MPa)	0.56	0.67	0.17	0.18	1.90	1.95	0.22	0.25
Volume Shrinkage (%)*	21.4	21.3	32.5	33.3	19.7	13.1	15.6	32.2
Cracking	7.0	6.0	2.0	2.0	6.0	8.0	4.0	3.0
Stain Repellency	13.0	11.0	0.5	0.0	4.0	5.0	1.0	4.0
Clean-up	1.0	2.0	4.0	4.0	2.0	2.0	7.0	7.0
Application	8.5	7.0	2.0	2.5	7.5	3.5	6.5	6.5
Polymer T_g (K)	288	288	288	288	291	291	291	291
Grout PVC (%)	80	85	80	80	80	85	80	85
Filler OA Value	8	8	28	28	8.5	8.5	26.6	26.6
Filler Particle Size (µm)	6	6	12	12	12	12	7	7
Fiber Type	PE	Nylon	Cellulose	None	PE	Nylon	Cellulose	None

*Volume Shrinkage performed according to volume shrinkage determination via ASTM D 2697-03

Table A8.

Data from Paper Presented at 41st Waterborne Symposium, New Orleans, LA, 24 – 28 February 2014, samples 9 –16

Property / Sample	**T9**	**T10**	**T11**	**T12**	**T13**	**T14**	**T15**	**T16**
Adhesion (psi)	214	249	149	114	84	111	76	144
Water Absorption (%)	11.71	16.02	19.48	23.64	10.14	12.47	2.96	2.04
Dry Surface Hardness (Shore D Durometer)	29	26	44	49	54	59	63	58
Wet Surface Hardness (Shore D Durometer)	13	18	10	13	21	21	40	42
UTS (MPa)	2.58	2.38	1.26	1.36	2.73	2.68	0.42	2.04
Elongation (%)	10.1	22.0	2.7	3.0	2.4	2.5	0.6	1.5
Young's Modulus (MPa)	1.97	1.16	1.97	1.99	3.59	3.27	2.10	3.33
Volume Shrinkage (%)*	29.3	29.9	6.7	9.2	22.9	28.0	28.5	30.0
Cracking	3.0	4.0	9.0	9.0	2.0	1.0	1.0	5.0
Stain Repellency	5.0	7.0	15.0	10.0	9.5	7.5	8.5	7.0
Clean-up	4.0	5.0	5.0	5.0	2.0	2.0	3.0	1.0
Application	4.5	5.5	1.0	1.0	5.0	6.5	1.0	9.0
Polymer T_g (K)	306	306	306	306	336	336	336	336
Grout PVC (%)	85	80	85	80	85	80	85	80
Filler OA Value	29	29	6.5	6.5	22.5	22.5	11	11
Filler Particle Size (µm)	4	4	21	21	14	14	6	6
Fiber Type	PE	Nylon	Cellulose	None	PE	Nylon	Cellulose	None

*Volume Shrinkage performed according to volume shrinkage determination via ASTM D 2697-03

Table A9.

Data for Polymer T_g and HSP Study used as Main Focus of this Research Thesis

Property / Grout Polymer	**A**	**B**	**C**	**D**	**E**	**F**	**H**	**I**	**J**	**L**
Polymer T_g (K)	336	312	313	290	283	296	268	274	305	274
Dry UTS (MPa)	8.07	7.43	8.18	7.77	3.32	1.81	4.28	1.66	9.23	3.30
Wet UST (MPa)	1.97	1.39	0.46	1.12	0.28	0.06	0.32	0.09	0.25	0.14
Dry Elongation (%)	1.8	1.7	3.6	7.8	13.6	10.6	19.4	16.1	4.5	21.7
Wet Elongation (%)	3.6	2.8	19.6	25.6	64.2	42.2	40.8	134.4	30.3	29.5
Young's Modulus (MPa)	9.0	10.6	9.4	9.7	1.7	2.2	2.5	0.7	9.9	2.6
Dry Surface Hardness (Shore D Durometer)	57	38	43	41	19	19	26	12	49	19

Table A9. (continued).

Wet Surface Hardness (Shore D Durometer)	38	16	43	20	6	3	4	2	10	2
Water Absorption (%)	5.12	7.66	17.02	6.32	17.78	21.85	9.29	25.77	8.81	26.28
Dry Lap Shear Adhesion (psi)	220	166	223	297	107	106	100	84	209	103
Wet Lap Shear Adhesion (psi)	23	36	16	92	14	19	25	14	14	23
Oil Based Stain Repellency	7.5	6.5	8.5	4.5	5.5	3.0	2.0	3.5	0.0	2.0
Water Based Stain Repellency	12.5	5.0	16.0	6.0	13.5	11.0	11.5	17.0	10.0	16.5
Total Stain Repellency	20.0	11.5	24.5	10.5	19.0	14.0	13.5	20.5	10.0	18.5
Flexural Strength (MPa)	14.44	8.31	9.05	7.12	1.95	1.94	2.52	1.58	8.37	1.57
Volume Shrinkage (%)*	5.6	3.0	3.1	4.5	9.0	4.6	7.0	17.6	6.0	20.3

*Volume Shrinkage performed according to volume shrinkage determination via ASTM D 2697-03

APPENDIX D - Formulation

Table A10.

Generalized example starting point RTU grout formulation.

Ingredient	**Mass (%)**	**Volume (%)**	**Description**
Emulsion Polymer Polymer D	25.3	44.6	Main binder – assuming 50% solids
Tamol 851	0.6	0.9	Dispersant – Dow Chemical (formerly Rohm and Haas)
Snowhite 21 PT	61.5	42.5	Filler of largest particle size in formulation – Omya
Minex 3	9.0	6.5	Filler of middle particle size in formulation – Unimin
Omyacarb 6 FL	1.4	1.0	Filler of smallest particle size in formulation – Omya
Nylon Fibers (3mm)	0.5	1.0	Improve physical properties – MiniFibers
Mineral Spirits	0.1	0.1	Defoamer
Walocel MW 15000 PFV	0.1	0.1	Thickener that also aids in water retention and workability – DowWolf
Rozone 2000	0.1	0.1	Mildewcide – Dow Chemical (form Rohm and Haas)
Kathon LX 1.5%	0.1	0.1	In can preservative – Dow Chemical (former Rohm and Haas)
Ammonium Hydroxide	0.1	0.1	pH adjustment
Dowanol PPh	1.0	1.0	Coalescing agent – Dow Chemical
Acrysol RM 825	0.1	1.0	Rheology modifier – Dow Chemical (former Rohm and Haas)
Water	0.1	1.0	As needed to adjust viscosity
Total	100.0	100.0	

REFERENCES

1 – Warner J, *Practical Handbook of Grouting: Soil, Rock, and Structures*, John Wiley & Sons, Inc. Hoboken, New Jersey, 2004, 3 - 14.

2 – O'Halloran S, Grouting a Ceramic Tile Floor, web article at: www.doityourself.com (home/interiorhomeimprovement/flooring/ceramicflooring) (accessed 12 September 2012).

3 – Technical Data Sheet for Grout Boost, www.groutboost.com, no author, HB Fuller Construction Products

4 – Hollerbach, Evie – Internal marketing report for Wacker Chemical Corporation 2011.

5 – Paid Market Report: North American Ceramic Tile Grout and Adhesive Market Analysis: by Frost & Sullivan, July 2007.

6 – Marvin, Dan, Presentation given at Coverings Show 2015 in Orlando Florida (Mapei Corporation)

7 – Mania D, "Investigation of Key Raw Materials and Their Impact Upon Ready-to-Use (RTU) Grout Properties," from the 40th Annual Waterborne, High-Solids and Powder Coating Conference (2012), New Orleans, LA, University of Southern Mississippi, Hattiesburg, MS.

8 – Fowlkes WY, Creveling CM, Engineering Methods for Robust Product Desing: Using Taguchi Methods in Technology and Product Development, Addison-Wesley Publishing Company, Reading, MS, USA, 1995, 125 – 145.

9 – D. J. Mania, Polymer, Fiber and Filler Formulation Effects Upon Ready-to-Use (RTU) Grout, Proceedings of the 41st Annual Waterborne, High-Solids and Powder Coating Symposium, New Orleans, LA, 2014.

10 – Shakhmenko, G. and J. Birsh, Concrete Mix Design and Optimization, Proceedings from 2nd International PhD. Symposium in Civil Engineering, Budapest, Hungary, 1998.

11 – ASTM D 2369 – 10: Standard Test Method for Volatile Content of Coatings, Volume 6.01.

12 – ASTM D 2697 – 03 (Reapproved 2008): Standard Test Method for Volume Non-volatile Matter in Clear or Pigmented Coatings, Volume 6.01.

13 – ASTM D 4017 – 02 (Reapproved 2008): Standard Test Method for Water in Paints and Paint Materials by Karl Fischer Method, Volume 6.01.

14 – ASTM D 3723 – 05 (Reapproved 2011): Standard Test Method for Pigment Content of Water-Emulsion Paints by Low-Temperature Ashing, Volume 6.01.

15 – ASTM D 1475 – 98 (Reapproved 2008): Standard Test Method for Density of Liquid Coatings, Inks and Related Products, Volume 6.01.

16 – CTIOA Field Report T-72 (R-02), Stain Repellency Test Method, http://www.ctioa.org, Ceramic Tile Institute of America.

17 – ASTM D 2240 – 05 (Reapproved 2010): Standard Test Method for Rubber Property – Durometer Hardness, Volume 9.01.

18 – ASTM C 531 – 00 (Reapproved 2012): Standard Test Method for Linear Shrinkage and Coefficient of Thermal Expansion of Chemical-Resistant Mortars, Grouts, Monolithic Surfacings, and Polymer Concretes, Volume 6.02.

19 – Kinloch AJ, *Adhesion and Adhesives: Science and Technology*, Chapman and Hall, New York, NY, USA, 1990.

20 – Koleske JV, *Paint and Coating Testing Manual: 15th Edition of the Gardner-Sward Handbook*, ASTM International, Conshohocken, PA, USA, 2012.

21 – ASTM C 307 – 03 (Reapproved 2012): Standard Test Method for Tensile Strength of Chemical Resistant Mortar, Grouts and Monolithic Surfaces, Volume 6.02.

22 – ASTM D 412 – 06: Standard Test Methods for Vulcanized Rubber and Thermoplastic Elastomers – Tension, Volume 9.01.

23 – ASTM D 2370 – 98 (Reapproved 2010): Standard Test Method for Tensile Properties of Organic Coatings, Volume 6.01.

24 – ASTM D 3182 – 07 (Reapproved 2012): Standard Practice for Rubber – Materials, Equipment and Procedures for Mixing Standard Compounds and Preparing Standard Vulcanized Sheets, Volume 9.01.

25 – ASTM D 4708 – 12: Standard Practice for Preparation of Uniform Free Films of Organic Coatings, Volume 6.01.

26 – ASTM D 1002 – 10: Standard Test Method for Apparent Shear Strength of Single-Lap-Joint Adhesively Bonded Metal Specimens by Tension Loading (Metal-to-Metal), Volume 15.06.

27 – ASTM D 3163 – 01 (2008): Standard Test Method for Determining Strength of Adhesively Bonded Rigid Plastic Lap-Shear Joints in Shear by Tension Loading, Volume 15.06.

28 – ASTM D 3983 – 98 (2011): Standard Test Method for Measuring Strength and Shear Modulus of Nonrigid Adhesives by Thick-Adherend Tensile-Lap Specimen, Volume 15.06.

29 – American National Standard Institute (ANSI), American National Standard Specifications for the Installation of Ceramic Tile, ANSI A108, A118 & A136 Version 2011.1, 82 – 110.

30 – Mania, D.J. “Stain Repellency Testing of Cementitious Grouts,” from the 5th Annual American Drymix Mortar Council, Drymix Mortar Yearbook (2014), pages 54 – 65.

31 – ASTM C 580 – 02 (2012): Standard Test Method for Flexural Strength and Modulus of Elasticity of Chemical-Resistant Mortars, Grouts, Monolithic Surfacings, and Polymer Concretes, Volume 6.02

32 – ASTM D 4476 / D 4476 M – 14: Standard Test Method for Flexural Properties of Fiber Reinforced Pultruded Plastic Rods, Volume 8.02.

33 – Technical Data Sheet for Tamol 851 from Dow Chemical (Rohm and Haas) (2008).

34 – Technical Data Sheet for Minex Functional Fillers and Extenders, Nephton, Ontario, Canada (2001).

35 – Technical Data Sheet for Filler (Snowhite 21 PT), www.omya-na.com, Omya Inc.

36 – Technical Data Sheet for Filler (Omyacarb 6 FL), www.omya-na.com, Omya Inc.

37 – Technical Data Sheet for Polyethylene Fibers, www.minifibers.com, no author, Minifibers Inc.

38 – Technical Data Sheet for Walocel from Dow Chemical (Dow-Wolf) (2010).

39 – Technical Data Sheet for Rozone 2000 from Dow Chemical (Rohm and Haas) (2007).

40 – Technical Data Sheet for Kathon LX 1.5 % from Dow Chemical (Rohm and Haas) (2007).

41 – Technical Data Sheet for 3M FC 4432 from www.3M.com/paintsandcoatings (2016).

42 – Technical Data Sheet for Dowano PPh from www.dow.com (2012)

43 – Technical Data Sheet for Acrysol RM 8W from Dow Chemical (Rohm and Haas) (2007).

44 – C.E. Roland Jones and C.A. Cramers "Analytical Pyrolysis: Proceedings from the Third International Symposium on Analytical Pyrolysis – Held in Amsterdam, September 7 – 9, 1976" Elsevier Science, New York, 1977

45 – Lee W.P. and A.F. Routh, "Time Evolution of Transition Points in Drying Latex Films," *JCT Research,* Volume 3, Number 4, October 2006, pages 301 – 306.

46 – ASTM E 178-08: Standard Practice for Dealing with Outlying Observations, Volume, 14.05.

47 – Cesarone, J. Taguchi or DOE, *IIE Solutions,* November 2001.

48 – Patton, TC, Paint Flow and Pigment Dispersion: A Rheological Approach to Coating and Ink Technology, 2nd Edition, John Wiley & Sons, New York, NY, USA, 1979, 170 – 204.

49 – Sudduth, R.D., "Characterizing the Mechanical Properties of Coatings as Influenced by CPVC and Zero Limit Considerations," Proceedings of the 40th Annual Waterborne, High-Solids and Powder Coating Symposium, New Orleans, LA, 2013.

50 – Toussaint, A. and L. D'Hont, "Ultimate Strength of Paint Films," *Journal of the Oil and Colour Chemists Association,* Volume 64, Issue 8, (1981) pages 302-307. et. al.

51 – Mischke P, Film Formation, Vincentz Network, Hannover, Germany, 2010.

52 – Curtzwiler, G., M. Early, D. Gottschalk, C. Konecki, R. Peterson, S. Wand and J.W. Rawlins, The World of Surface Coatings is Centered around the Glass Transition Temperature, But Which One? – Part 2, *Coatings Tech,* September 2014.

53 – Kempe, Michael D., G.J. Jorgensen, K.M. Terwilliger, T.J. McMahon, C.E. Kennedy, T.T. Borek, "Acetic acid production and glass transition concerns with ethylene-vinyl acetate used in photovoltaic devices," *Solar Energy Materials and Solar Cells (91), 2007, pages 315-329.*

54 – Kim, Seong-Soo, J.B. Lee, T.J. Cho, R.D. Hooton, "Determination of optimum glass transition temperature of acrylic acid ester copolymer to improve performance of cement matrixes," *ACI Materials Journal,* Volume 111, Issue 5, (2014), pages 521-529.

55 – Toledo C and Mania D, In *The Effect of Polymer Structure upon the Performance of Polymer Modified Cementitious Tile Adhesives*, Proceedings from the American Drymix Mortar Council: admmc one Drymix Mortar Yearbook 2008, Charlotte, NC, USA, 4 June 2008, Editor: Ferdinand Leopolder.

56 – Hansen, C. M., The Three Dimensional Solubility Parameter and Solvent Diffusion Coefficient – Their Importance in Surface Coating Formulation, Doctoral Dissertation – Technical University of Denmark, Copenhagen Technical Press, Copenhagen, Denmark, 1967.

57 – Hansen, C. M., Hansen Solubility Parameters – A User's Handbook, CRC Press – Taylor & Francis Group, Boca Raton, FL, 2007.

58 – Software – HSPiP, available at www.hansen-solubility.com/HSPiPPurchase.html.

59 – Teas, Jean P., "Graphic Analysis of Resin Solubilities," *Journal of Paint Technology,* Volume 40, No. 516, pages 19 – 25, January 1968.

60 – Burrell, Harry, "The Challenge of the Solubility Parameter Concept," *Journal of Paint Technology,* Volume 40, No. 520, pages 197 – 208, May 1968.

61 – Hansen, Charles M. and K. Skaarup, "III. Independent Calculation Of the Parameter Components," *Journal of Paint Technology,* Volume 39, No. 511, pages 511 – 514, August 1967.

62 – Koenhen, D. M. and C. A. Smolders, "The Determination of Solubility Parameters of Solvents and Polymers by Means of Correlation with other Physical Properties," *Journal of Applied Polymer Science,* Volume 19, page 1163, 1975.

63 – van Krevelen, D. W. and P. J. Hoftyzer, Properties of Polymers: Their Estimation and Correlation with Chemical Structure, 2nd. Edition, Elsevier, Amsterdam, 1976.

64 – Hansen, C. M. and A. Beerbower, Solubility Parameters in, Kirk-Othmer Encyclopedia of Chemical Technology, Supplemental Volume, 2nd. Edition, Standen, A., Editor, Interscience, New York, 1971.

65 – Barton, A. F. M. (Editor), CRC Handbook of Solubility Parameters and Other Cohesion Parameters, CRC Press, New York, 1983.

66 – Barton, A. F. M. (Editor), CRC Handbook of Polymer-Liquid Interaction Parameters and Solubility Parameters, CRC Press, New York, 1990.

67 – Mark, James E., (Editor), Physical Properties of Polymers Handbook, American Institute of Physics Press, Woodbury, New York, (1996).

68 – Brandrup, J., E.H. Immergut and E.A. Grulke, Polymer Handbook, 4th Edition, John Wiley and Sons, New York, NY, (1999)

69 – van Krevelen, D.W., K. teNijenhuis, Properties of Polymers: Their Correlation with Chemical Structure; Their Numerical Estimation and Prediction from Additive Group Contributions – 4th Edition, Elsevier Science, Boston, MA, (2009)

70 – Yakout, S.M., “Effect of Molecular Structure on the adsorption of soluble aromatic hydrocarbons by activated carbon,” *Asian Journal of Chemistry*, Volume 26, Issue 20, (2014) pages 6891 – 6894.